2018

Investigation of Gold(III) Complexes with HIV-NCp7 and Models

James Beaton
Virginia Commonwealth University

Interactions of Gold(III) Complexes With HIV-NCp7 and Models

A dissertation submitted in partial fulfillment of the requirements for the degree of Doctor of Philosophy

by

James Beaton

B.Sc. in Chemistry with Specialization in Biochemistry, University of Virginia, 2013

Advisor: Dr. Nicholas P. Farrell

Professor, Department of Chemistry, College of Humanities and Sciences

Virginia Commonwealth University

Virginia Commonwealth University

Richmond, Virginia

November 2018

Acknowledgements

The work in this dissertation would not have been possible without the support of a large group of people. First, I would like to thank my parents, who have given me their unwavering support in every endeavor I have ever undertaken. I would also like to thank Dr. Farrell for giving me the opportunity to investigate some truly interesting projects in his lab. My graduate committee provided invaluable insight and thought provoking feedback. Dr. Qu, Dr. Nelson, and Dr. Turner provided invaluable assistance in successfully executing a number of projects, and were always a wealth of advice when it was needed. Members of the Farrell group, both past and present: Daniel Lee, Sarah Spell, Samantha Tsotsoros, Wyatt Johnson, Eric Ginsburg, Samantha Katner, Thomas Wells, David Hampton, Zhifeng Du, and Erica Peterson. Visiting students, Raphael de Paiva, Victor Bernardes, and Douglas Nakahata. Last but certainly not least, Morgan, who I cannot imagine I would have been able to complete this process without.

Table of Contents

List of Figures

List of Tables

List of Schemes

List of Abbreviations

1-MeCyt	1-Methylcytosine
4-pic	4-Picoline
9-EtGua	9-Ethylguanine
ADA	Azodicarbonamide
AIDS	Acquired Immunodeficiency Syndrome
Au	Gold
AuF/Au_2F/Au_4F	Gold finger (1, 2, or 4 gold ions bound to peptide)
AZT	Azidothymidine
Bipy, bpy	2,2-bipyridine
Bnpy	2-benzylpyridine
BPMA	Di-(2-picolyl)amine, bis(2-pyridylmethyl)amine
Cyt	Cytosine
CD	Circular dichroism
CD4	Cluster of differentiation 4
cDDP	Cisplatin
Cl	Chloride
CQ	Chloroquine
CV	Cyclic voltammetry
Cyclam	1,4,8,11-tetraazacyclotetradecane
Cys, C	Cysteine
$d_2$pypp	1,3-bis(di-2-pyridyphosphino)propane

Dampa	2’[(dimethylamino)methyl]phenyl
DAPTA	3,7-diacetyl-1,3,7-triaza-5-phosphabicyclo[3.3.1]nonane
DIBA	2,2-dithiobis(benzamide) disulfide
Dien	diethylenetriamine
DMAP	4-dimethylaminopyridine
DMDT	N,N-dimethylthiocarbamate
DMF	N,N-dimethlyformamide
DMSO	dimethylsulfoxide
DNA	Deoxyribonucleic acid
Dppe	1,2-Bis(diphenylphosphino)ethane
En	Ethylenediamine
ESDT	Ethylsarcosinedithiocarbamate
ESI	Electrospray ionization
EXAFS	Extended X-ray absorption fine structure
F2	HIV-nucleocapsid C-terminal zinc finger
FDA	U.S. Food and Drug Administration
FT	Fourier transform
GR	Glutathione reductase
GSH	Glutathione
HAART	Highly active antiretroviral therapy
His, H	Histidine
HIV	Human immunodeficiency virus
HOMO	Highest occupied molecular orbital

HSQC	Heteronuclear single quantum coherence
IC_{50}	Half maximal inhibitory concentration
IR	Infrared spectroscopy
K_a	Association constant
K_d	Dissociation constant
L	Ligand
LC-MS	Liquid chromatography-mass spectrometry
LUMO	Lowest unoccupied molecular orbital
M	Metal
MDM2	Mouse double minute 2 homolog
Met	Methionine
MS	Mass spectrometry
MS/MS	Tandem mass spectrometry
N-AcCys	N-acetylcysteine
N-AcMet	N-acetylmethionine
N-AcTrp	N-acetyltryptophan
NAD^+	Nicotinamide adenine dinucleotide
NADPH	Nicotinamide adenine dinucleotide phosphate
Nap	Naphthalene
NCp7	HIV-Nucleocapsid protein
NHC	N-heterocyclic carbene
N-Medien	2,2'-diamino-*N*-methyldiethylamine
NMR	Nuclear magnetic resonance

NOBA	3-nitrosobenzamide
NOESY	Nuclear Overhauser effect spectroscopy
NTP	Nucleoside triphosphate
OTf	Triflate
PAR	Poly(ADP-ribose)
PARP	Poly(adenosine diphosphate (ADP)-ribose)polymerase
Pd	Palladium
Phe, F	Phenylalanine
Phen	1,10-phenanthroline
pK_a	Acid dissociation constant
ROS	Reactive oxygen species
PCy_3	Tricyclohexylphosphine
PPh_3	Triphenylphosphine
PR_3	Trialkylphosphine
Pt	Platinum
Py, pyr	Pyridine
Quin	Quinolone
RNA	Ribonucleic acid
RT	Reverse transcriptase
SL2	Stem loop 2
Sp	Specificity protein
Sp1	Specificity protein transcription factor 1
Terpy	2,2',2''-terpyridine

tDDP	Transplatin
TFIIIA	Transcription factor for polymerase IIIA
TMS	Tetramethylsilane
TPP	Tetraphenylporphyrin
Trp, W	Tryptophan
UV/VIS	Ultraviolet/visible spectroscopy
XANES	X-ray absorption near edge structure
XPA	Xeroderma pigmentosum group A
ZF	Zinc finger
Zn	Zinc

Interactions of Gold(III) Complexes With HIV-NCp7 and Models

by

James Beaton

A dissertation submitted in partial fulfillment of the requirements for the degree of Doctor of Philosophy

Virginia Commonwealth University, 2018

Advisor: Dr. Nicholas P. Farrell

Professor, Department of Chemistry

Abstract

The medicinal uses of gold date as far back as 2500 B.C. in China. In modern times, gold has been used in the treatment of a number of different human diseases including rheumatoid arthritis, cancer, and viral infections. This dissertation will focus on the development of gold complexes for the purpose of selective inhibition of HIV NCp7, a 55 amino acid zinc finger protein with two Cys_3His zinc binding domains.

NCp7 is involved in a number of viral life cycle processes including activation of reverse transcription, integration, DNA recognition, RNA packaging, and formation of the viral envelope. The diversity in the roles of NCp7 across the viral life cycle make it a highly attractive target for chemical intervention. Ejection of the tetrahedrally coordinated zinc atoms, modification or deletion of the zinc coordinating amino acids, or modification or deletion of the "essential" tryptophan residue can result in the loss of viral infectivity. This is due to the inability of NCp7 to recognize its "natural" substrate – polynucleic acids. Previous studies have investigated the differences in the manner in which platinum(II), gold(I), and gold(III) complexes interact with

NCp7. The platinum(II) complex $[Pt(dien)(9\text{-}EtGua)]^{2+}$ interacts with the C-terminal zinc finger of NCp7 in a non-covalent manner, through a π-π stacking interaction between the platinated 9-EtGua and the "essential" tryptophan residue. The isostructural and isoelectronic complex $[Au(dien)(9\text{-}EtGua)]^{3+}$ ejects the tetrahedrally coordinated zinc atom and replaces it with a gold atom, forming "gold fingers". This result is consistent with the interactions of the gold(I) complex $[(PPh_3)Au(9\text{-}EtGua)]^{+}$.

In order to complete the series of isoelectronic and isostructural platinum(II), palladium(II), and gold(III) complexes with N-heterocyclic ligands and diethylenetriamine chelates, the complexes $[Au(dien)(1\text{-}MeCyt)]^{3+}$ and $[Au(N\text{-}Medien)(1\text{-}MeCyt)]^{3+}$ were synthesized. These complexes were found to dimerize the C-terminal zinc finger once the central zinc atom is ejected. This is likely the result of a charge transfer from the 1-methylcytosine ligand to the tryptophan residue, and is a product that was not seen as a result of interaction with the previously published 4-dimethylaminopyridine and 9-ethylguanine analogs. The 1-methylcytosine complexes also stabilize the gold(III) oxidation state and associate with N-acetyltryptophan in a manner consistent with the previously studied gold(III) analogs. Finally, in order to address concerns arising from the inner filter effect, a proof of concept study using ^{1}H-NMR spectroscopy was utilized to show that the complex $[Au(dien)(1\text{-}MeCyt)]^{3+}$ likely has a lower association constant with N-acetyltryptophan than the value determined by fluorescence quenching.

The impact of the incorporation of additional steric hindrance on the gold(III) chelate was studied using the di-(2-picolyl)amine ligand. The gold(III) chlorides incorporating this ligand and the centrally methylated analog were found to eject zinc from the C-terminal zinc finger of NCp7, and the electronegativity differences between the gold(III) and platinum(II) metal centers were

highlighted. The attempts to incorporate an N-heterocyclic ligand into these complexes were unsuccessful due to the steric and electronic demands of the chelate.

The use of an organometallic chelating ligand led to the investigation of the ability of gold(III) complexes to catalyze the arylation of zinc-coordinating cysteine residues. The complex [$AuCl_2$(dampa)], which had been formerly investigated as a chemotherapeutic agent due to its structural similarities to cisplatin, was found to arylate N-acetylcysteine, glutathione, and NCp7. The arylation was not found to be dependent on the *cis*- chloride ligand, as blocking that site with the ligand triphenylphosphine did not prevent the arylation of NCp7. The X-Ray crystal structure of the complex [AuCl(dampa)(PPh_3)](PF_6) was also solved. Using the advancement of the knowledge of how the electronic and structural properties of gold(III) complexes described herein impact interactions with NCp7, it is possible that a coordination complex that is a selective inhibitor of NCp7 may eventually be developed.

Chapter 1: Introduction

1.1 Medicinal Uses of Gold Complexes

The earliest known use of gold in a medicinal capacity dates back as far as 2500 B.C. in China, where gold was ingested in order to promote longevity and to cure a number of ailments such as fainting and delirium.[1,2] These treatments generally took the form of ingestion of elemental gold, although the modern scientific community has been unable to confirm a medicinal value for this type of treatment.[3] Modern chemical development of gold-based medicine began in earnest with the discovery that gold-cyanide inhibits the growth of *Tubercule bacillus*, which occurred in 1890.[1,2] This discovery led to the development of gold complexes with the hope of treating tuberculosis.[3] Despite poor results in the treatment of tuberculosis in animal models, researchers ignored these findings and carried out human trials of gold based tuberculosis treatments.[4] While these trials proved to be unsuccessful in preventing the progression of tuberculosis, trial participants noticed an improvement in joint pain, leading to the development of gold complexes for the treatment of rheumatoid arthritis.[2,3] Two of the complexes developed for the treatment of rheumatoid arthritis during this time, aurothiomalate and aurothioglucose (Figure 1.1), are still in use in the clinic.[2,3] In addition to clinical use for the treatment of rheumatoid arthritis, aurothiomalate and aurothioglucose are still being investigated for new applications as medicinal treatments. For example, aurothioglucose is being investigated as an inhibitor of thioredoxin reductase (TrxR), and aurothiomalate is being investigated as an inhibitor of zinc finger proteins.[5–7] The development of auranofin (Figure 1.1) in the 1970s was a significant advancement in the timeline of gold-based medicine, as it was the first orally active gold complex to be introduced into the clinic.[8] While auranofin is clinically approved for the treatment of rheumatoid arthritis, it

continues to be investigated for a wide range of clinical applications including inhibition of TrxR, inhibition of angiogenesis, and antiviral applications.[9–11]

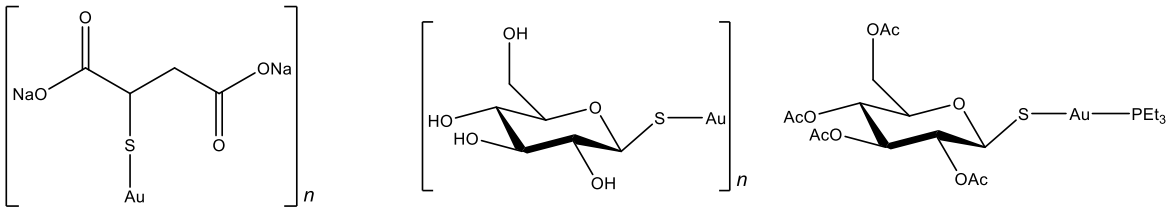

Figure 1.1. The structure of sodium aurothiomalate (left), aurothioglucose (middle), and Auranofin (right).

The widespread clinical acceptance of these gold-based rheumatoid arthritis treatments, and the discovery that auranofin was capable of inhibiting tumor cell growth both *in vitro* and *in vivo*, led to the development of a number of gold complexes for investigation of their potential as pharmaceuticals.[2] In general, some trends in the development of these complexes can be observed, leading most of the complexes developed to fall into two classes: analogs of the antiarthritic agents, which are generally Au(I) complexes, and analogs of cisplatin, which make use of the isoelectronic nature of the Pt(II) and Au(III) oxidation states.[2,3,12]

Many of the Au(I) complexes that have been developed were synthesized with the goal of inhibiting tumor growth contain a gold-sulfur bond and act as inhibitors of TrxR. Many, like auranofin, also contained phosphine ligands.[2,12,13] One such example is Au-napth-1, which is an auranofin analog containing a napthalimide ligand in place of the carbohydrate ligand. This ligand was chosen because of the anticancer properties shown by other complexes containing napthalimide, and likely also targets TrxR.[12] More recently, the design of Au(I) complexes has taken the complexes farther from direct analogs of auranofin. A wide variety of Au(I) complexes containing N-heterocyclic carbene (NHC) ligands, cyclodiphosphazene ligands, phosphole ligands, and cyclic thiourea ligands have been developed and examined for their ability to prevent

tumor growth and proliferation, largely through the targeting of TrxR or glutathione reductase (GR), which causes the generation of reactive oxygen species (ROS).[2,12–14] The use of NHC as a ligand was inspired by the similarities in the donor properties of NHCs and phosphines and by the ease with which NHCs can be modified in order to tune the lipophilic properties of the complex.[15] The ease of modification of NHCs was also leveraged in the creation of [Au(NHC^{Nap})Cl], which contains a naphthalene ligand capable of intercalating DNA, creating a synergistic reaction mechanism.[14]

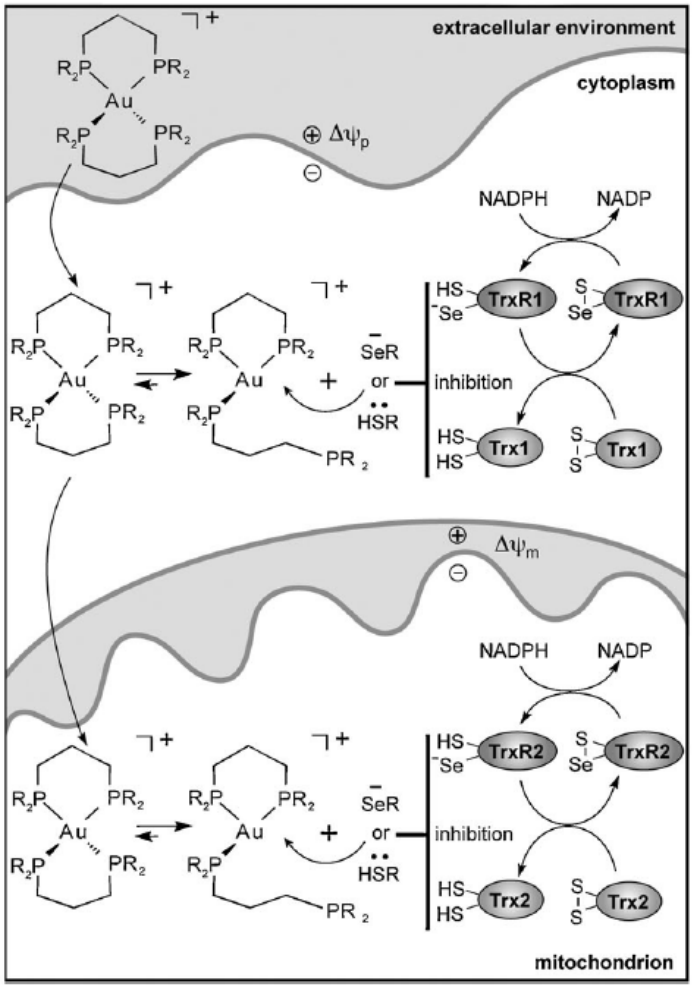

Figure 1.2. Mechanism of inhibition of Thioredoxin or Thioredoxin reductase by a gold complex.[2]

The phosphine ligand in auranofin was, at least at one time, considered critical to its function[2]. This led to the development of Au(I) complexes with multiple phosphine ligands. Two such complexes are $[Au(dppe)_2]^+$ and $[Au(d\textit{n}pype)_2]^+$, which are both tetracoordinate Au(I) complexes. $[Au(dppe)_2]^+$ was developed with the hope that the AuP_4 coordination sphere would display reduced reactivity towards thiol containing biomolecules.[2,16] Additionally, the AuP_4 coordination sphere was found in $[Au(dppe)_2]^+$ was found to have increased stability relative to the two-coordinate Au(I) complexes that had been previously investigated.[14] This complex showed stability in the presence of high concentrations of glutathione (GSH) and *in vivo* antitumor activity in animal models, but research on the complex as a chemotherapeutic agent was discontinued due to high toxicity, which was thought to be caused by general membrane permeability caused by accumulation of the complex in mitochondria.[2,12,14,16] In order to reduce this toxicity, complexes analogous to $[Au(d\textit{n}pype)_2]^+$ were developed, which showed increased efficacy as a TrxR inhibitor and decreased toxicity towards healthy cells.[2,12,14,17] Other analogs of $[Au(dppe)_2]^+$ were designed, including $[Au(dppp)(PPh_3)Cl]$, $[Au(P(CH_2OH)_3)_4]^+$, and the dinuclear complex $[\{AuCl(PPh_3)\}_2(\mu_2\text{-DIPHOS})]$, both of which showed antitumor activity to some extent, including $[Au(P(CH_2OH)_3)_4]^+$, which advanced to clinical trials.[2]

Despite the breadth of research that resulted from the discovery that auranofin and its analogs were active as antitumor agents, the most commonly used inorganic anticancer agents in the clinic continue to be cisplatin and cisplatin analogs such as carboplatin and oxaliplatin.[18,19] While development of platinum based chemotherapies continues, the isoelectronic and isostructural relationship between Pt(II) and Au(III) has led to the investigation of Au(III) complexes as antitumor agents.[2,12,14,20] One of the first such complexes was $[AuCl_2(dampa)]$ (dampa = N,N-dimethylbenzylamine), which, like cisplatin, contains two *cis* chloride ligands.[21] Further

experimentation led to the development of the complexes [Au(acetato)$_2$(dampa)] and [Au(malonato)(dampa)], both of which showed *in vivo* tumor activity.[22]

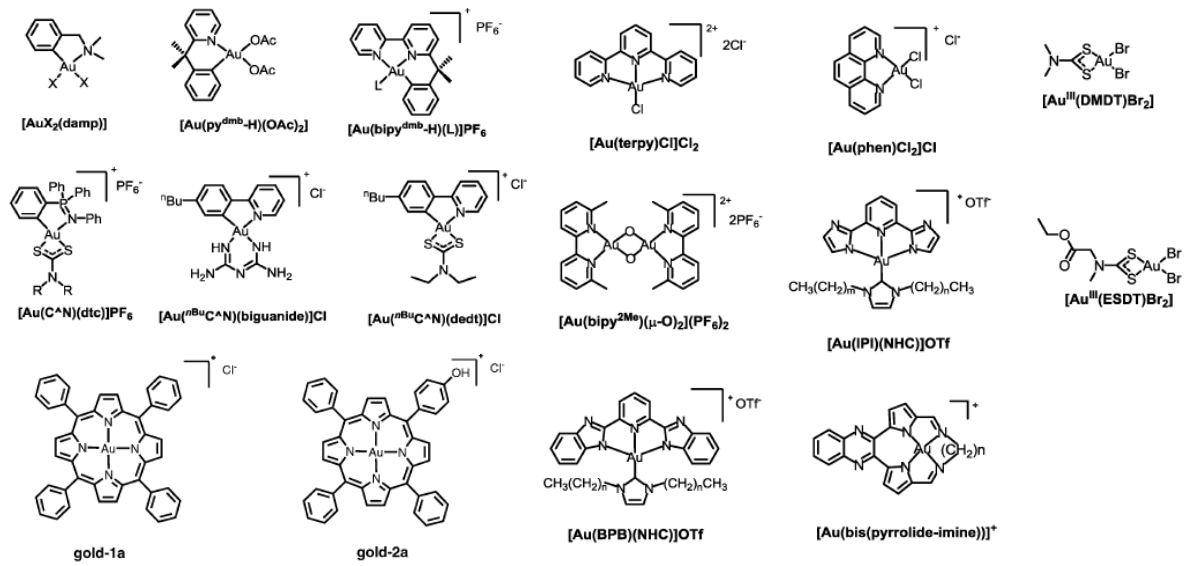

Figure 1. 3. The structures of some gold(III) complexes investigated as anti-cancer compounds.[14]

Only three other types of gold complexes have been reported to show *in vivo* tumor activity: the Au(III) dithiocarbamate complexes such as [Au(DMDT)X_2] and [Au(ESDT)X_2](DMDT = N,N-dimethylthiocarbamate, ESDT = ethylsarcosinedithiocarbamate, X = Cl, Br), the Au(III) porphyrins such as [Au(III)(TPP)]$^+$, and the Au(III) NHC complex [Au(C^N^C)(NHC)]$^+$ (C^N^C = 2,6-diphenylpyridine).[2,12,14] Analysis of a number of dithiocarbamate complexes revealed that the previously mentioned complexes [Au(DMDT)X_2] and [Au(ESDT)X_2] were the most effective complexes in the series, and were more cytotoxic than cisplatin in both sensitive and resistant cell lines. Activity in cell lines both sensitive and resistant towards cisplatin also proves a unique mechanism of antitumor activity relative to cisplatin.[23] A number of mono-, di-, and even trinuclear complexes containing the tridentate chelating ligand 2,6-diphenylpyridine were also tested for their efficacy as chemotherapeutic agents. These complexes were rationally designed due to the

structural similarity they share with the metallointercalator $[Pt(terpy)Cl]^+$, and the ligands that were investigated included N-donors, phosphines, and bridging phosphines. While the complexes did not exhibit remarkably high cytotoxicity, the phosphine ligands improved solubility, and it was concluded that their use could serve as a vehicle for the delivery of a cytotoxic analog.[24] The moderate success of these complexes as cytotoxic agents led to the development of the mono- and polynuclear NHC analogs. These complexes were found to poison Topoisomerase I by stabilizing the enzyme-DNA complex, resulting in the lead compound, $[Au(C^N^C)(NHC)]^+$, displaying a cytotoxic profile up to 28 times more effective than cisplatin.[25] The complex is also significantly more effective than cisplatin against cisplatin resistant cell lines, which shows the difference in mechanism of action from cisplatin, which targets DNA forming crosslinks preventing normal DNA transcription and replication.[26] Finally, porphyrin containing complexes such as $[Au(TPP)]^+$ were synthesized in order to improve the stability of the Au(III) oxidation state in the presence of biologically relevant reducing agents such as glutathione.[2,12,14] The *meso*-tetraarylporphyrin complexes investigated exhibited both stability towards reduction and significant cytotoxicity towards both cisplatin sensitive and resistant cell lines through dose-dependent induction of apoptosis as determined by confocal microscopy and flow cytometry.[27]

Additional investigation of Au(III) complexes as isoelectronic and isostructural analogs of cisplatin were developed in the form of Au(III) complexes with one or more Au-N bonds.[12,14,28] Generally, these complexes contain a multidentate N-donor chelating ligand, and the structures of the chelating ligands that have been investigated are diverse. One of the most important developments from the research into the multidentate N-donor ligands is the stabilization of the Au(III) oxidation state under physiological (reducing) conditions that was observed for complexes such as $[Au(phen)Cl_2]^+$, $[Au(terpy)Cl]^{2+}$, $[AuCl(dien)]^{2+}$, $[Au(cyclam)]^{3+}$, and $[Au(en)_2]^{2+}$ (phen =

phenanthroline, terpy = 2,2':6',2''-Terpyridine, dien = diethylenetriamine, cyclam = 1,4,8,11-tetraazacyclotetradecane, en = ethylenediamine).[12] The cytotoxicities of these complexes were found to be comparable across cisplatin resistant and sensitive cell lines, and it was found by circular dichroism and DNA melting point assays that the dien and the phen complexes caused direct DNA damage.[29]

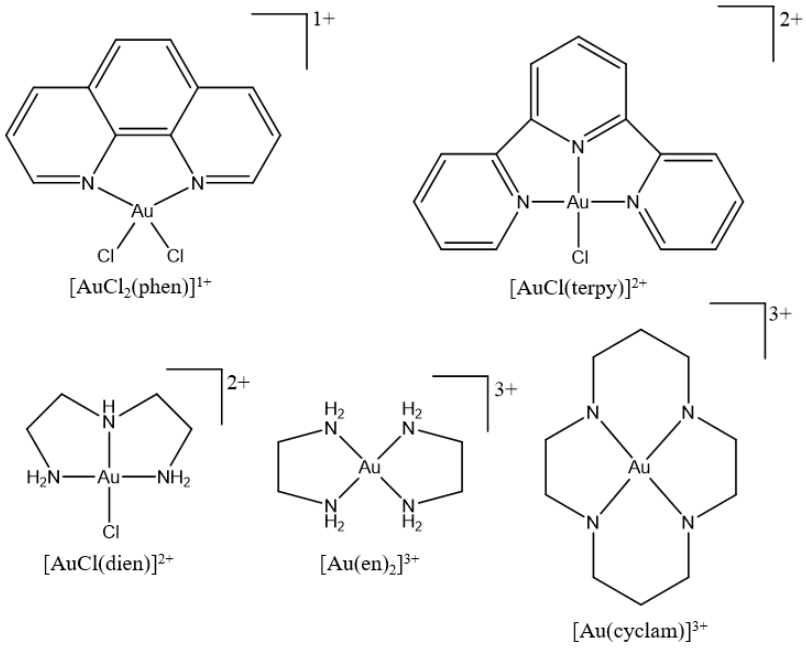

Figure 1.4. The structure of gold(III) complexes investigated for their ability to cause direct DNA damage.[29]

In addition to the uses of gold complexes as treatments for rheumatoid arthritis, as in the case of auranofin and its analogs, and as chemotherapeutic agents, such as the complexes that arose from the investigation of Au(III) analogs of cisplatin, gold complexes have been investigated as potential treatments for parasitic diseases and HIV/AIDS.[2] The parasitic diseases for which gold complexes have been investigated as potential treatments include malaria, leishmaniasis, trypanomiasis, and schitsomiasis.[30]

Traditionally, chloroquine has been used to treat malaria, but the rise of chloroquine resistant parasites has necessitated development of new treatments.[31] The parasite that causes malaria in humans, *Plasmodium falciparum*, possesses a thioredoxin reductase enzyme that have been identified as a target for antimalarial intervention.[32] Initial studies of gold complexes as antimalarial agents used auranofin to target this enzyme. The other gold complexes investigated alongside auranofin were [Au(PEt_3)Cl], aurothiomalate, and [Au(Cyclam)]$^{3+}$. Auranofin was the most successful complex of the four, and the ability of auranofin to inhibit *P. falciparum* growth *in vitro* was used to illustrate the efficacy of gold complexes as antiparasitic agents and show that further investigation was warranted.[33] One of the most successful gold-based complexes investigated as an antimalarial agent was [Au(PPh_3)(CQ)]$^{1+}$, which was developed to study the effect of modulating the electronic properties of chloroquine by binding it to gold as a ligand. Binding chloroquine to gold was a successful strategy, as the complex showed a significant enhancement of activity against chloroquine resistant malaria strains.[34] This positive result led to the synthesis of a series of aurated chloroquine complexes. The most effective Au(I)-chloroquine complex against resistant parasite strains was [Au(PEt_3)(CQ)]$^{1+}$, but the Au(III)-chloroquine complexes generally showed stronger activity than the Au(I) complexes.[30]

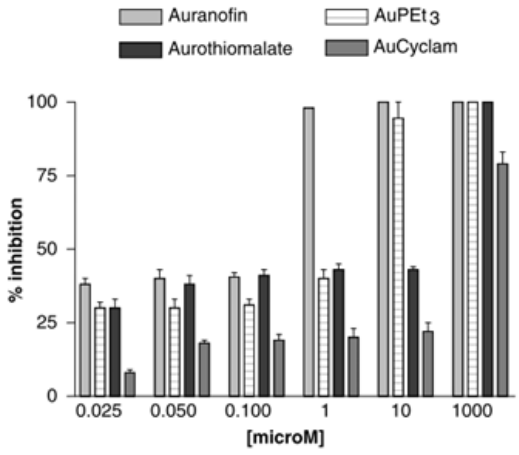

Figure 1.5. Inhibition of *P. falciparum* growth by gold complexes.[33]

1.2 Zinc Finger Proteins

It has been estimated that as much as half of the total proteome is made up of proteins that bind a metal cofactor in some capacity.[35] One of the most abundant metals found in the proteome is zinc. In humans, zinc binding proteins are encoded for by up to 10% of the total genome.[36–38] The functions of zinc as a cofactor are diverse, and include zinc in catalytic, cocatalytic, structural, and inhibitory roles.[39,40] In proteins that incorporate zinc in a structural role, a zinc(II) atom is generally tetrahedrally coordinated to a combination of cysteine and histidine residues.[39] This structural motif was first observed in the DNA binding domain of the *Xenopus laevis* transcription factor TFIIIA, where it was described as "an unusually small, self-folding domain in which Zn is a crucial component of its tertiary structure". This small domain was described as a "zinc finger".[41] Since the discovery of the zinc finger structural motif, zinc fingers have been shown to be involved in a number of biological processes. These processes include DNA recognition, RNA packaging, transcriptional activation, apoptotic regulation, and protein assembly.[36]

Zinc fingers are generally divided into classes based on the zinc coordination sphere. The most common types of zinc fingers fall into three distinct coordination spheres: Cys_2His_2, $Cys_2HisCys$ (Cys_3His), and Cys_4.[36,37,39,42,43] However, recently some additional classifications have been discovered.[37] The rationale for dividing zinc finger proteins by their zinc coordination sphere rather than by the function of the protein or some other metric is that the reactivity of the zinc finger protein is intimately tied to the zinc coordination sphere. Therefore, even though zinc finger proteins are divided by the zinc coordination sphere rather than protein function, many zinc finger proteins with similar functions have the same zinc coordination sphere.[42] In addition to differences in reactivity between the classes of zinc finger proteins, there is also a significant difference in their abundance. One study concluded that while the human genome encodes for 4500 Cys_2His_2

zinc finger domains across 564 proteins, only 17 domains across 9 proteins are encoded.[44] The inert nature of d^{10} zinc means that the reactivity of zinc fingers is proportional to the number of cysteine residues – the greater the number of nucleophilic cysteine residues, the greater the reactivity.[45]

Due to the large number of zinc finger proteins observed in nature and their diverse functions, many have been studied as potential targets for chemical intervention.

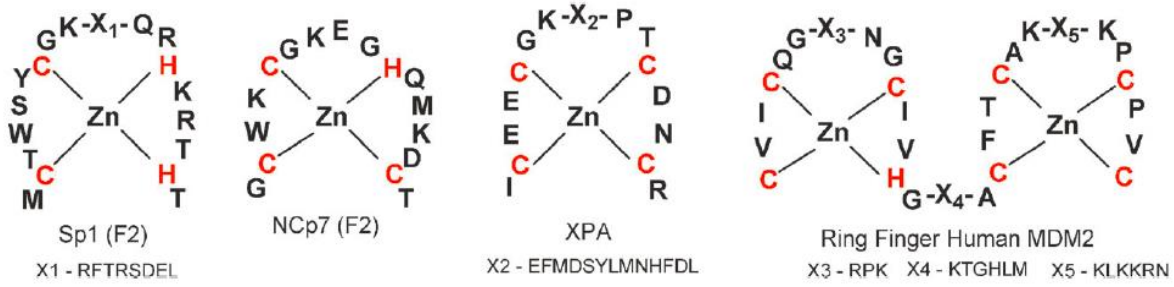

Figure 1.6. Representative zinc finger motifs from each class of zinc finger protein: Cys_2His_2 (left), Cys_3His (left center), Cys_4 (right center), and mixed (right).[36]

Cys_2His_2 Zinc fingers

One of the most commonly recognized roles of Cys_2His_2 zinc finger proteins is that of transcription factors.[39] In fact, the first eukaryotic zinc finger to have its structure elucidated was TFIIIA, a transcription factor in *Xenopus laevis*.[46] TFIIIA was found to contain a repeating zinc-containing structural motif, which bound to DNA and gave rise to the term "zinc finger".[46] TFIIIA was found to bind to both the RNA and the DNA gene that encodes for the RNA. This binding interaction is only possible because of the specificity imparted by the zinc finger domains.[47]

Human transcription factor specificity protein 1 (Sp1) is another zinc finger protein containing three Cys_2His_2 zinc finger domains.[36,39] Sp1 was found to enhance transcription by RNA polymerase II as much as 50 fold, and is present in quantities up to 10,000 molecules per cell.[48]

Additionally, the structure of Sp1 together with its DNA binding domain was determined by NMR, and it was found that all three zinc finger domains recognize DNA, working together to impart selectivity for the GC box binding domain.[49] Sp1 expression levels are abnormal in many types of cancer, and higher Sp1 expression has been associated with decreased patient survival times in some cases.[50] This has led to Sp1 becoming the most widely characterized transcription factor in mammalian cells, and makes it a highly studied target for chemotherapy development.[39]

Cys_3His Zinc fingers

One example of a Cys_3His zinc finger that has been widely studied as a chemotherapeutic agent is poly(ADP-ribose) polymerase (PARP-1). PARP-1 catalyzes the transfer of ADP-ribose to nuclear proteins from NAD.[51] PARP-1 was found to contribute to repair of damaged DNA when it was shown that cellular NAD content was lowered after treatment with alkylating agents or γ-radiation. The drop in NAD content is accompanied by an increase in PARP-1 activity.[52,53]

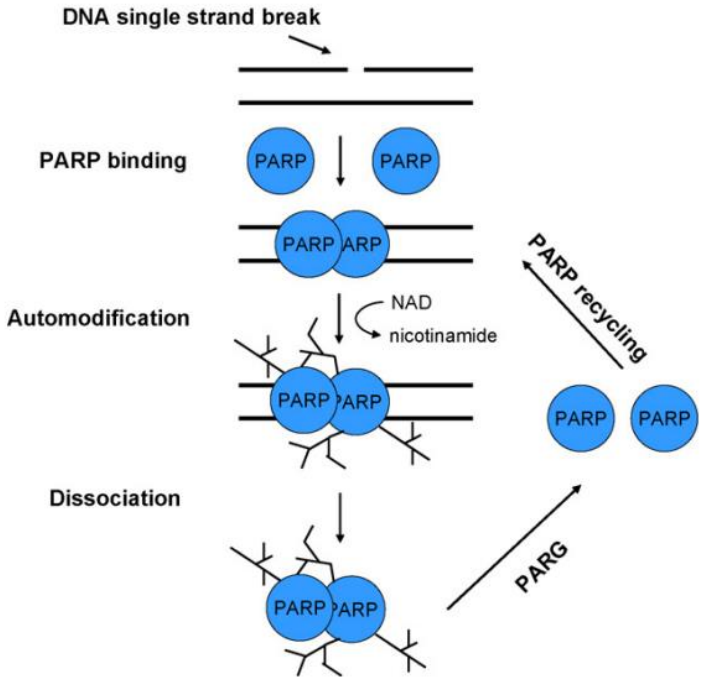

Figure 1.7. The mechanism of single-strand DNA break repair by PARP. Gold complexes have been extensively investigated as PARP inhibitors for the purpose of treating cancer.[53]

PARP-1 localizes to DNA single and double strand breaks and facilitates the assembly of repair factors. The zinc finger domains of PARP-1 do not bind specific DNA sequences. Instead, the structure imparted by the tetrahedral coordination of zinc recognizes damaged DNA, highlighting the diverse set of structure-activity relationships that can be achieved using the zinc finger motif. While the N-terminal zinc binding domain is essential to the function of PARP-1, the C-terminal zinc binding domain was found to be less important to the function of the protein despite having a higher affinity for DNA than the C-terminal domain, and was therefore assumed simply to assist in the specificity for certain types of DNA strand breaks. PARP-1 does not bind to the DNA strand breaks. Instead, the protein binds to exposed nucleobases that are present in DNA with strand breaks, but are also present in other abnormal DNA structures, allowing PARP-1 to interact with multiple types of damaged DNA. PARP-1 binds DNA through an interaction that has been termed the "phosphate backbone grip" with 3-nucleotide DNA segments, allowing it to interact with damaged DNA regardless of the DNA sequence.[54] Interestingly, the repair of platinated DNA damage by PARP-1 has also been investigated.[55]

Cys_4 Zinc fingers

The Cys_4 zinc binding motif is the most reactive traditional zinc finger structure due to the highly electrophilic nature of the four zinc-coordinating cysteine residues. One example of the Cys_4 zinc binding motif is the human xeroderma pigmentosum group A (XPA) protein.[56] XPA has a single Cys_4 zinc finger motif that acts as a recognition site for damaged DNA, and the mutation or deletion of the zinc-coordinating cysteine residues has been shown to reduce activity. XPA is a part of the nucleotide excision repair process, and functions by recognizing DNA damage and recruiting other proteins in order to repair the damaged DNA.[57] The increased reactivity of the

Cys_4 zinc binding motif may aid in the recognition of a number of structurally diverse patterns of DNA damage.

Mixed Zinc Fingers

In some cases, a single protein may contain more than one type of zinc finger motif.[36,37,39] One such example is the E3 ubiquitin-protein ligase Mdm2, which contains one Cys_3His zinc finger and one Cys_4 zinc finger.[36] The function of an E3 is to catalyze the formation of a linkage between Ubiquitin and its substrate, and in the case of Mdm2 this function is dependent on the C-terminal zinc finger.[58] Zinc coordination is essential for the E3 function of Mdm2, but has been found to be non-essential in the RNA binding function.[58,59]

HIV-NCp7

Cys_3His zinc fingers are significantly less common than Cys_2His_2 zinc fingers, and the incorporation of an additional sulfur-containing cysteine into the zinc coordination sphere causes them to be more reactive than Cys_2His_2 zinc fingers as well. One of the most well studied Cys_3His zinc finger proteins is the HIV nucleocapsid protein (NCp7).[60,61] NCp7 has two Cys_3His zinc finger motifs, and these two zinc fingers are linked by a region of high basicity.[61] The zinc in NCp7 is bound with very high affinity ($K_a = 10^{12} - 10^{14}$ M^{-1}), as determined by spectrophotometric monitoring of cobalt(II) displacement by zinc(II).[62] The zinc bound protein was found to have a high degree of flexibility, and the zinc finger motifs were found to interact weakly by ^1H-NOESY.[63]

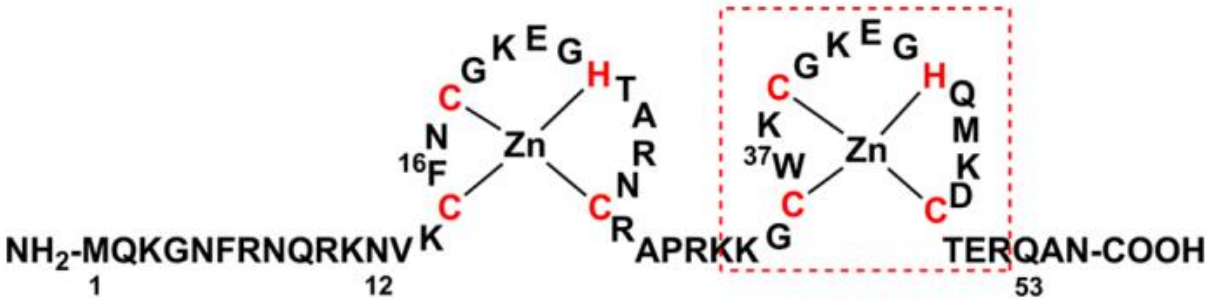

Figure 1.8. The structure of HIV NCp7. The C-terminal zinc finger is highlighted in red.

Like many zinc finger proteins, the primary natural substrate of NCp7 is nucleic acids. The structure imparted by zinc coordination forms a "hydrophobic plateau", which has a strong influence on the binding properties of the protein.[64] NCp7 binds nucleic acids in both sequence-specific and nonspecific interactions.[65] In particular, NCp7 has a high affinity for guanine residues.[66] As determined by NMR, this association occurs through a π-π stacking interaction between the nucleobases and the aromatic residues on the zinc finger motifs, F16 and W37.[44,65,67] There is a very high degree of conservation, especially among the zinc-coordinating residues, and mutations that prevent the binding of zinc result in noninfectious virions.[68]

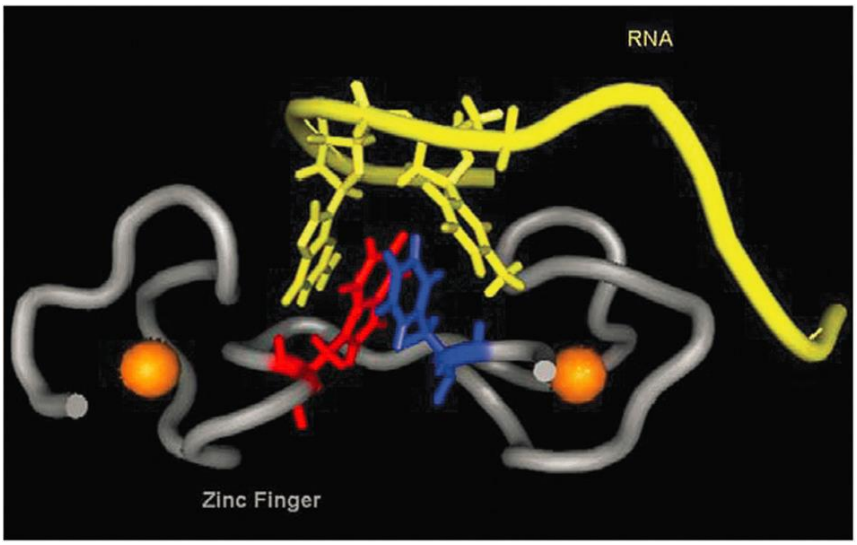

Figure 1.9. The structure of NCp7 bound to an RNA substrate.[36]

NCp7 is involved in a number of processes at nearly every point in the viral life cycle.[69,70] These processes include reverse transcription, integration, selective packaging of viral RNA, formation of the new viral particle, packaging RNA into a stable dimer, and protection of viral RNA against nucleases.[69] Primarily, NCp7 is a nucleic acid chaperone, meaning that it helps nucleic acid structures to obtain their most thermodynamically stable conformations.[70] As previously mentioned, the interactions between NCp7 and its substrates can be both specific and non-specific. This allows NCp7 to interact with virtually any oligonucleotide substrate between 5 and 8 nucleobases in length.[70] This low-affinity electrostatic binding motif allows for the protection of the viral RNA from cellular nucleases by coating the gRNA in a large number of molecules (1500-2000) of NCp7.[70] In contrast, NCp7 binds strongly and selectively to the SL3 stem-loop recognition element of the genomic Ψ-RNA, which is highly conserved across HIV-1 strains.[68]

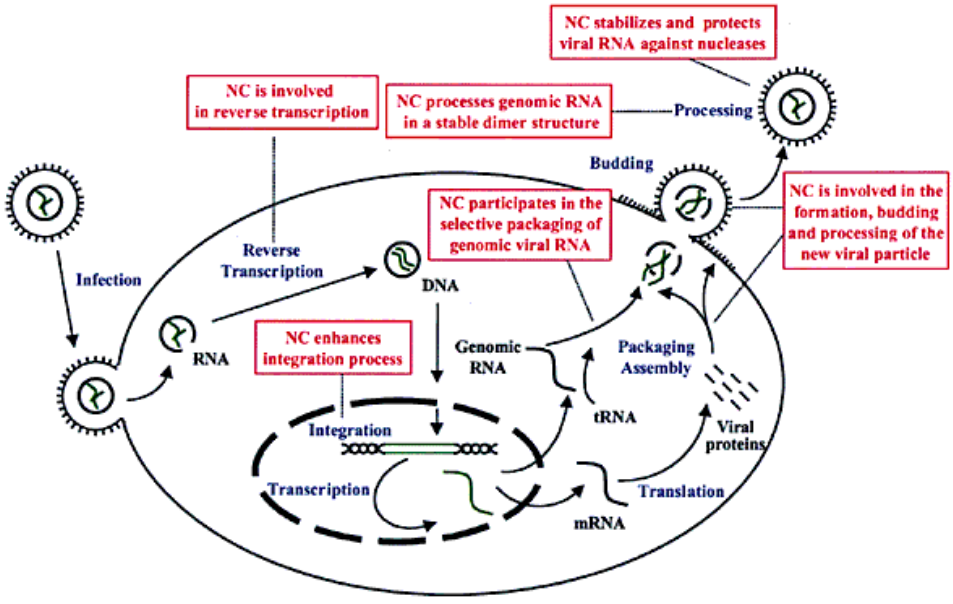

Figure 1.10. NCp7 plays a part in numerous viral life cycle processes.[69]

1.3 Current Treatments in HIV

There are six distinct classes of drugs currently prescribed for the treatment of HIV. These classes are nucleoside reverse transcriptase inhibitors, non-nucleoside reverse transcriptase inhibitors, protease inhibitors, integrase inhibitors, and fusion inhibitors.[71]

Reverse transcription is the process by which double-stranded DNA is synthesized from the viral single-stranded RNA genome. The protein that carries out reverse transcription is reverse transcriptase (RT), which was the target of the first approved anti-AIDS drug, azidothymidine (AZT). AZT is a nucleoside reverse transcriptase inhibitor. This class of complexes functions by acting as a prodrug, which is converted to a dNTP analog and catalytically incorporated at the 3'-end of the DNA primer synthesized by RT. Generally, this inhibits the addition of more nucleotides. Conversely, non-nucleoside reverse transcriptase inhibitors inhibit RT by binding to an allosteric inhibitory site on RT. Both classes of RT inhibitors suffer from drug-resistance mechanisms. In the case of nucleoside RT inhibitors, the enzyme can also work in reverse, acting to remove the inhibitor from the DNA strand being synthesized.[72]

HIV-1 protease is an enzyme that cleaves Gag and Gag-Pol polyprotein precursors in order to produce functioning viral enzymes. Protease is a vital enzyme in the viral life cycle, and its involvement in the production of essential enzymes makes it an attractive target for chemical intervention. Ten protease inhibitors have been approved by the FDA, and all ten share structural and binding similarities. All of the approved protease inhibitors bind in the active site of protease, preventing the enzyme from binding its natural substrates by mimicking the substrate transition state. However, the protease inhibitors suffer from high toxicity and cause significant adverse side effects.[73]

Integrase catalyzes the integration of retroviral genetic material into the DNA of the host cell. The integrase enzyme does not have a human homolog, making it an attractive target for chemical intervention. Many different classes of compounds have been investigated as integrase inhibitors, including hydroxylated aromatics, diketo acids, naphthyridine carboxamides, pyrrolloquinolones, dihydroxypyrimidine carbpxamides, and others. This research led to the development of three FDA approved integrase inhibitors: Raltegravir, Elvitegravir, and Dolutegravir. All three of these complexes function as integrase strand transfer inhibitors, and target the active site of integrase.[74]

Fusion is the process in which the virus fuses with the human cell membrane in order to gain access to the intracellular human machinery. During fusion, a viral surface protein, HIV-1 surface protein 120 (gp120), binds to CD4 receptors on human cells. The interaction between gp120 and CD4, the conformation of gp120 is changed, allowing the viral glycoprotein 41 (gp41) to breach the cell membrane, forming a pore through which the virus can enter the cell. This process is required for viral replication, making it an attractive target for chemical intervention. The representative fusion inhibitor is enfuvirtide, a synthetic peptide analog that binds gp41 and disrupts its function, preventing the formation of the pore through which the virus enters the cell. However, some patients do not tolerate the drug well, and resistance due to amino acid mutations on gp41 that prevent drug binding has been observed.[75]

1.4 NCp7 as a Drug Target

The high conservation and large number of viral life cycle processes in which NCp7 is involved make it an attractive target for chemical intervention.[36,39,42,60,61,76] In fact, all known retroviruses, with the exception of spumaretroviruses, contain at least one Cys_3His zinc finger.[76] The first complexes developed to target the zinc finger motifs of viral nucleocapsid proteins were the C-nitroso complexes. The complex 3-nitrosobenzamide (NOBA) was found, using ^{1}H-NMR, to eject

zinc stoichiometrically from the N-terminal zinc finger of NCp7, and was found to significantly reduce both propagation and infectivity of HIV.[77] Mechanistically, NOBA acts as an electrophile. A nucleophilic zinc-coordinating cysteine residue donates electrons to the C-nitroso group of NOBA, resulting in the covalent modification of the cysteine thiolate, preventing zinc coordination.[78] Other organic complexes investigated for their ability to eject zinc from NCp7 include the disulfide benzamides, such as 2,2'-dithiobisbenzamide (DIBA), dithiaheterocyclic complexes, such as 1,1-dioxide-*cis*-1,2-dithiane-4,5-diol (Dithiane), and α-carbonyl azoic complexes, such as azodicarbonamide (ADA), which were all shown to inhibit NCp7 while avoiding unwanted interactions with other zinc finger proteins.[79] In general, the mechanisms by which the organic zinc ejecting complexes react with NCp7 are thought to be the same.[80] These complexes were somewhat successful in targeting NCp7, however they suffered from inadequate selectivity and poor effective half-life *in vivo*.[81]

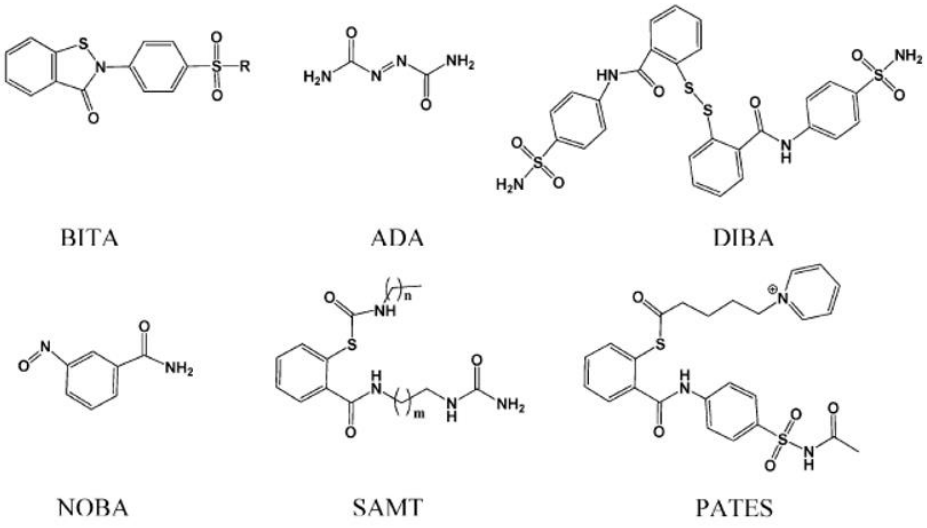

Figure 1.11. Organic electrophiles that have been investigated for their ability to eject zinc from NCp7.[36]

A high throughput screening method was used in order to identify a reversible antagonist of the NCp7-polynucleotide interaction, and fluorescein and gallein analogs were found to inhibit oligonucleotide recognition of the protein. These complexes were shown to inhibit the activity of NCp7 proportionally to their ability to π-π stack with the tryptophan residue on the C-terminal zinc finger, as monitored by fluorescence quenching of tryptophan. However, these complexes also inhibited unrelated targets. The promiscuity of these complexes was attributed to aggregate formation, and disqualified them from significant further investigation as selective inhibitors of NCp7.[82]

In order to improve on the selectivity of the electrophilic agents and develop complexes that are capable of targeting NCp7 selectively, inorganic coordination complexes have been investigated for their ability to act as selective agents against both NCp7 and other zinc finger proteins. A variety of metal centers have been investigated including nickel, lead, chromium, mercury, selenium, palladium, platinum, and gold.[36,39]

The current investigation of platinum, palladium, and gold complexes as zinc finger inhibitors grew out of the success of cisplatin (*cis*-$[PtCl_2(NH_3)_2]$) as a chemotherapeutic agent, and the investigation of a diverse number of cisplatin analogs as treatments for both cancer and other human diseases has been undertaken. In fact, cisplatin was found to eject zinc from a zinc finger protein, DNA polymerase α.[83] The interactions of cisplatin and transplatin with the C-terminal zinc finger of NCp7 were investigated, and it was found that both isomers caused the ejection of the central zinc atom as a result of a replacement of a chloride ligand by a nucleophilic cysteine thiol.[84] Clearly, however, it would be impossible for a chemotherapeutic complex that functions as a DNA damaging agent to selectively target a zinc finger protein, but this discovery offered a starting point for further investigation.[36] Generally, three methods have been proposed for targeting zinc finger

proteins in order to treat human diseases: chelation of the central zinc atom, electrophilic attack on the zinc-coordinating residues, and interference with the recognition of the protein's natural substrate – generally polynucleic acids.[36]

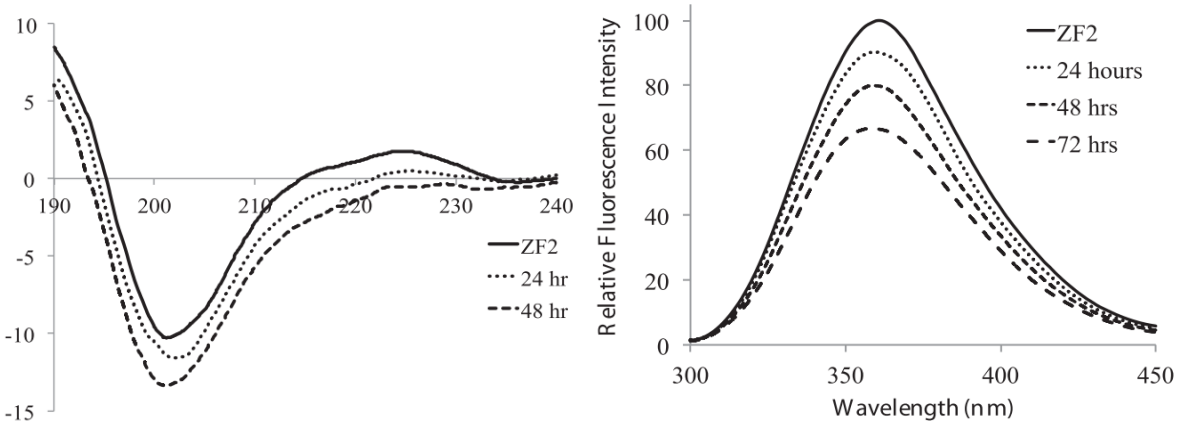

Figure 1.12. Interactions of cisplatin with the C-terminal zinc finger of NCp7 as monitored by CD (left) and Fluorescence quenching (right).[84]

The π-π stacking interactions between nucleobases and the aromatic amino acids of proteins has been extensively studied and characterized.[85,86] Additionally, the realization that N-quaternization (via protonation or methylation) of a nucleobase increases the π-π stacking ability of the nucleobase with an aromatic amino acid provided an excellent starting point for the development of a selective NCp7 inhibitor.[85,87] The enhancement of π-π stacking ability of nucleobases was expanded to N-quaternization via metalation. The first system examined was the $[Pt(dien)(Nucleobase)]^{2+}$ system.[88] The nucleobase analogs initially investigated were 9-ethylguanine, 1-methylcytosine, 5'-guanosine monophosphate, and 5'-cytosine monophosphate, and the diethylenetriamine chelate was selected in order to eliminate a labile leaving group and ensure that only non-covalent hydrogen bonding interactions were possible. Fluorescence quenching of tryptophan showed a significant enhancement of the association constant for the platinated nucleobases over the free analogs, and upfield shifts of the ^{1}H-NMR signals of N-

acetyltryptophan upon interaction with the platinated nucleobases were indicative of a π-π stacking interaction.[88]

The faster hydration kinetics of palladium complexes (relative to their platinum counterparts) led to the investigation of the Pd(II) analogs of the $[Pt(dien)(Nucleobase)]^{2+}$ complexes.[89] In contrast to their Pt(II) analogs, the Pd(II) complexes formed covalent analogs with N-acetyltryptophan as shown by NMR and mass spectrometry, highlighting the increased kinetic lability of the Pd(II) metal center.[89] Theoretical studies comparing these complexes to the free nucleobases and alkylated nucleobases showed a significant increase in the overlap between the N-acetyltryptophan HOMO and the nucleobase LUMO upon metalation relative to the free and alkylated nucleobases.[90] The enhancement of the orbital overlap is the source of the increased association for the metallated nucleobases over the free ligands.[88–90] It was also postulated that steric interactions with the metal center, which is relatively bulky, and rotation around the metal-nucleobase bond also have an impact on the π-π stacking ability of complexes of this nature.[90] Evidence for the presence of rotamers found in the platinum complexes and the great deal of steric modification that is possible around a metal center led to the further investigation of complexes of this form as potential selective inhibitors of NCp7.[88]

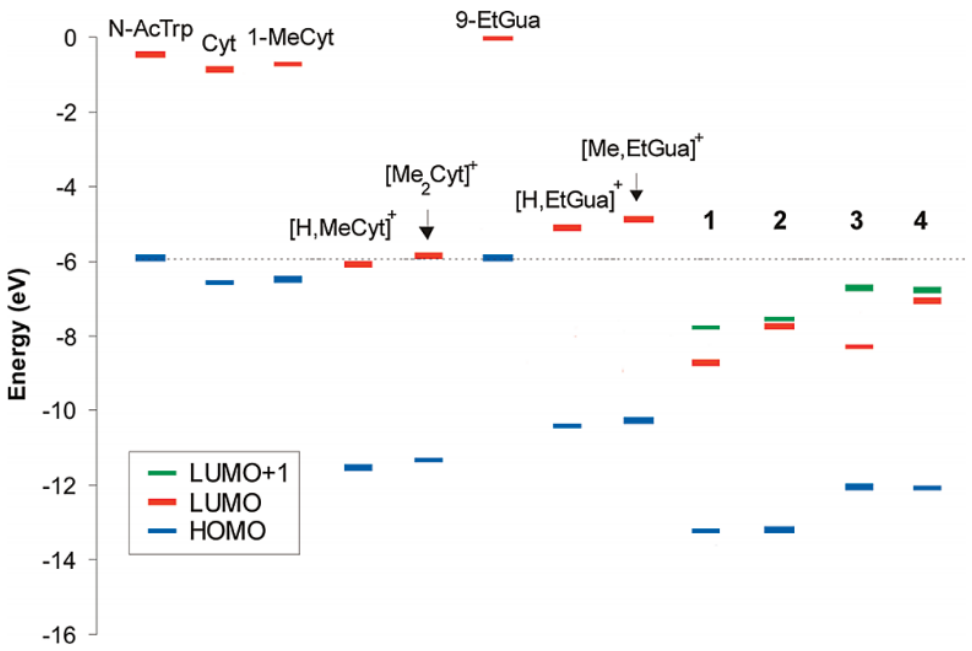

Figure 1.13. N-Quaternization improves the overlap of the N-acetyltryptophan HOMO and nucleobase LUMOs.[90] 1 – $[Pd(dien)(1\text{-MeCyt})]^{2+}$, 2 – $[Pt(dien)(1\text{-MeCyt})]^{2+}$, 3 – $[Pd(dien)(9\text{-EtGua})]^{2+}$, 4 – $[Pt(dien)(9\text{-EtGua})]^{2+}$.

A series of *trans*-planar amine platinum complexes showed a strong preference for the sulfur containing amino acid cysteine over methionine. This result is expected due to the high lability of the chloride ligands and the high nucleophilicity of the cysteine thiol.[91] The lead complex, *trans*-$[PtCl(9\text{-EtGua})(py)_2]^{2+}$, was also found to eject zinc small molecule models for the NCp7 zinc finger.[92] This complex was later found to eject zinc from the C-terminal zinc finger of NCp7. This was determined through the use of circular dichroism, where a loss of tertiary structure indicative of zinc ejection was observed, and by mass spectrometry, where it was shown that the complex ejected zinc and bound 2:1 in the form $[Pt(py)_2]_2$-peptide. It was proposed that the ejection of zinc occurred by a three step mechanism: non-covalent recognition of the protein by a π-π stacking interaction between the tryptophan and the platinated 9-ethylguanine, displacement of the chloride and covalent binding to a cysteine thiol, and zinc ejection concomitant with displacement of the

platinated nucleobase and coordination to a second cysteine thiol.[93] The complex [Pt(dien)(9-EtGua)]$^{2+}$ was also investigated, and was found to interact noncovalently with the C-terminal zinc finger of NCp7 – zinc ejection and covalent adduct formation were not observed.[93] The 9-EtGua and DMAP analogs were found to quench tryptophan fluorescence more effectively than a number of other N-heterocycles, leading to the use of these N-heterocycles in many of the further investigations into complexes containing N-heterocycles.[94]

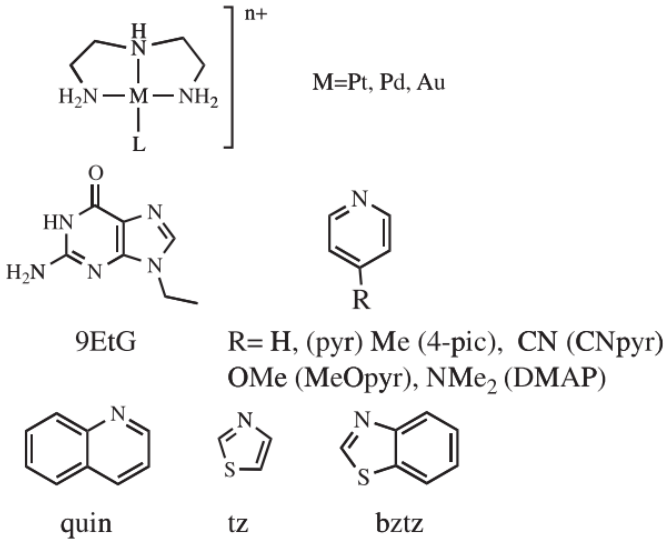

Figure 1.14 The structures of platinum(II), palladium(II), and gold(III) complexes containing a diethylenetriamine chelating ligand that were investigated as NCp7 inhibitors.[94]

The [Pt(dien)(9-EtGua)]$^{3+}$ system was further investigated to show that DNA could be metallated in order to disrupt the interaction between DNA and NCp7 by inhibiting the recognition of the polynucleotide by the protein.[95] The differences in the substitution kinetics between [MCl(dien)]$^{n+}$ and [MCl(terpy)]$^{n+}$ (M = Pt(II), Pd(II), Au(III); terpy = 2,2':6',2''-terpyridine) were also investigated. In all cases, the labile chloride ligand resulted in covalent adduct formation with the peptide, but it was proven that the modulation of the metal center and the chelate were a viable platform for further investigation.[96]

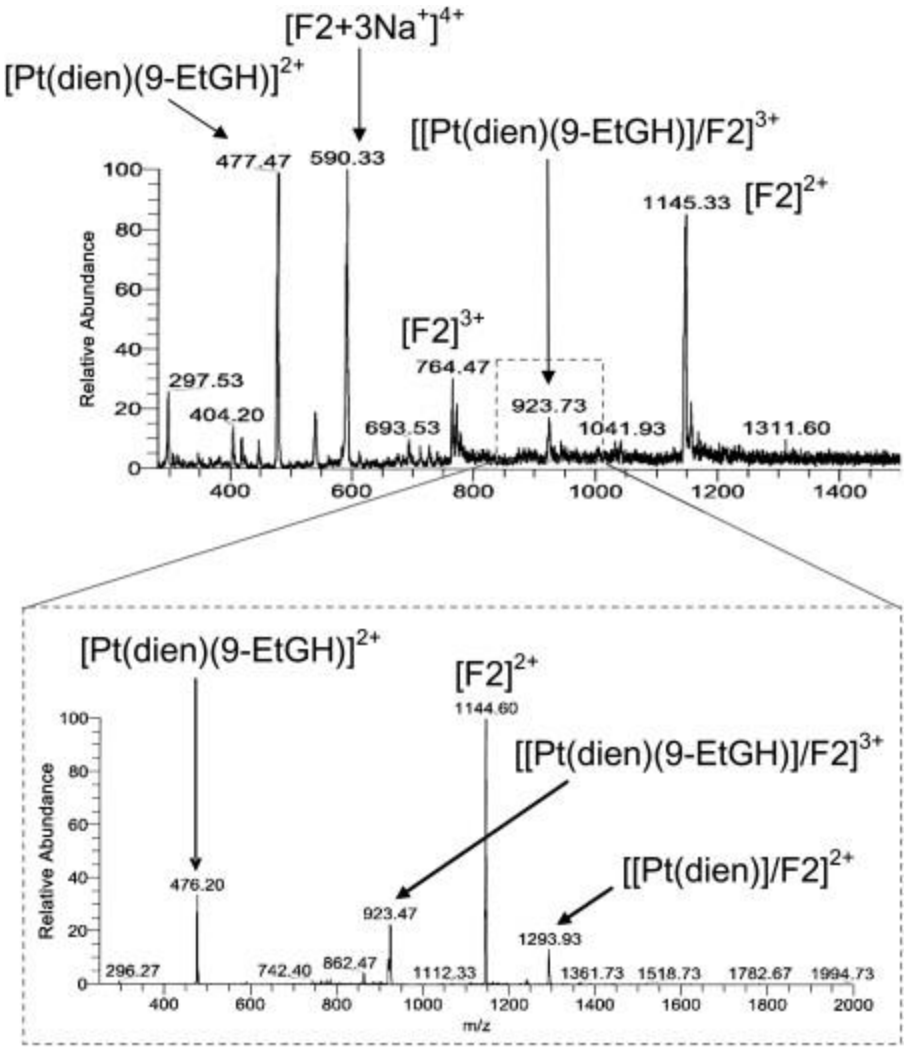

Figure 1.15. Interaction of $[Pt(dien)(9\text{-}EtGua)]^{2+}$ with the C-terminal zinc finger of NCp7 (top). Noncovalent adducts are not formed until MS/MS is performed (bottom).[93]

The noncovalent analogs formed by the complex $[Pt(dien)(9\text{-}EtGua)]^{2+}$ led to the study of analogs using the more reactive gold(III). The complexes $[Au(dien)(DMAP)]^{3+}$ and $[Au(dien)(9\text{-}EtGua)]^{3+}$ were found to exhibit ^{1}H-NMR spectral differences over a range of pH values. These spectral changes were attributed to the deprotonation of the central amine, assigned a pK_a value of 3.3 for the 9-ethylguanine complex, the deprotonation of the 9-ethylguanine N_1, assigned a pK_a value of 5.3, and finally dissociation of the 9-ethylguanine ligand, assigned a pK_a value of 7.5. Tryptophan fluorescence quenching was used in order to show that these complexes had a stronger

association constant with N-acetyltryptophan than their platinum(II) and palladium(II) counterparts. The use of the AuN_4 coordination sphere was also found to stabilize the gold(III) oxidation state relative to the $AuClN_3$ coordination sphere, and the stabilization was found to be proportional to the basicity of the N-heterocyclic ligand. This stabilization indicates that AuN_4 complexes of this nature would be less likely to interact with sulfur-containing biomolecules, and warranted their further investigation as selective inhibitors of NCp7.[97]

Complex	E_p (V)
$[AuCl(dien)]^{2+}$	-0.280
$[Au(dien)(9\text{-EtGua})]^{3+}$	-0.349
$[Au(dien)(DMAP)]^{3+}$	-0.328
$[AuCl(N\text{-MeDien})]^{2+}$	-0.232
$[Au(N\text{-MeDien})(9\text{-EtGua})]^{3+}$	-0.263
$[Au(N\text{-MeDien})(DMAP)]^{3+}$	-0.238

Table 1.1. Peak potential values for the reduction of gold(III) complexes. Reduction was determined at a platinum electrode (vs Ag/AgCl), in 50 mM phosphate buffer, 4 mM NaCl, pH 7.4.[97]

In a later work, ^{1}H-NMR studies showed a reduced reactivity with the sulfur containing amino acids N-acetylmethionine and N-acetylcysteine for the AuN_4 complexes with respect to the $AuClN_4$ complexes, with signals representing substitution by N-acetylmethionine appearing after 15 hours. The substitution by the thiol containing N-acetylcysteine is more rapid than the thioether containing N-acetylmethionine. The fluorescent emission of the N-terminal zinc finger was quenched by both the N-heterocycle containing complexes and the chloride containing complex, indicating quenching occurred through loss of the central zinc atom and a change in peptide structure, rather than through a π-π stacking mechanism. This change in structure was confirmed

by circular dichroism and mass spectrometry. Interaction with the complexes caused the circular dichroism spectrum to shift from a spectrum characteristic of zinc finger (positive band at 220 nm and slight negative band at 195 nm) to random coil type structure (decrease in positive band intensity, increase in negative ellipticity, slight blueshift) very rapidly. Mass spectrometric results showed zinc ejection and formation of "gold fingers" immediately upon interaction.[98] Interestingly, however, recent results obtained by EXAFS and XANES have showed that the AuN_4 coordination sphere is maintained longer than previously expected.[99]

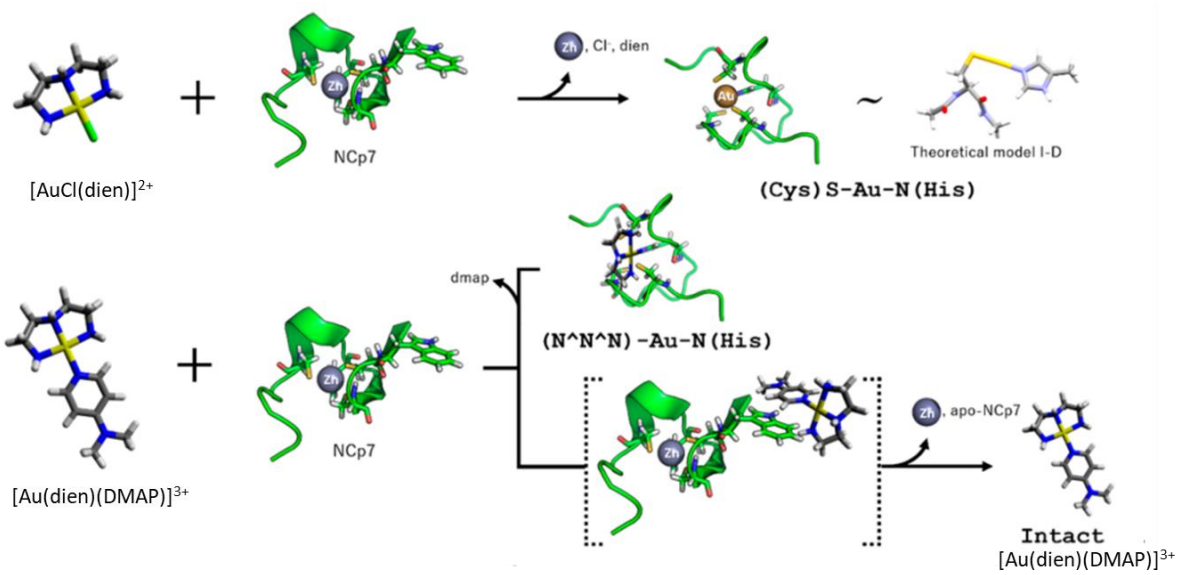

Figure 1.16. Differences in interactions of [AuCl(dien)]2+ and [Au(dien)(DMAP)]3+ with NCp7 as determined by EXAFS.[99]

In further studies were designed to probe the ability of these complexes to prevent NCp7-polynucleotide binding. Mass spectrometry of a solution of NCp7 that had been incubated with $[Au(dien)(9\text{-EtGua})]^{3+}$ to which SL2 was added showed only uncomplexed SL2. Additionally, mass spectrometry of a solution of complexed NCp7-SL2 to which $[Au(dien)(9\text{-EtGua})]^{3+}$ was added showed a significant amount of free SL2, indicating that $[Au(dien)(9\text{-EtGua})]^{3+}$ was capable of both preventing NCp7 from recognizing its natural substrate, and that the complex could disrupt

the complex of NCp7 and its natural substrate once the complex had already formed. These mass spectrometry results were also confirmed using an electrophoretic mobility shift assay and a fluorescence polarization assay.[100]

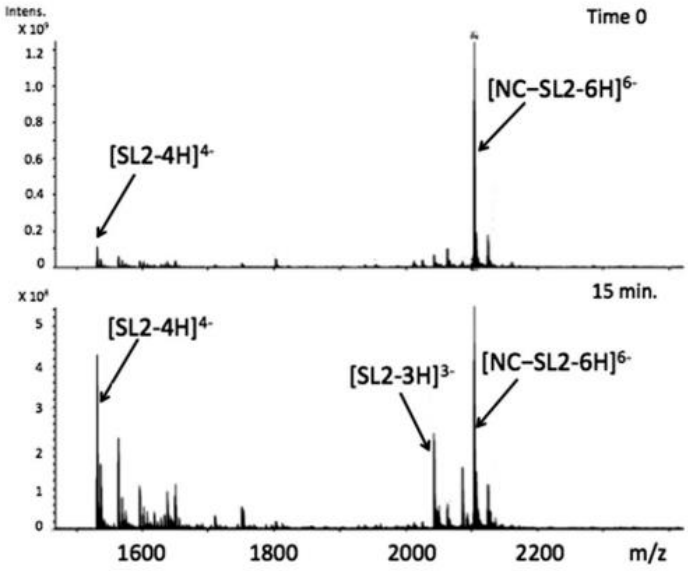

Figure 1.17. [Au(dien)(9-EtGua)]$^{3+}$ causes dissociation of the SL2-NCp7 complex.[100]

A similar strategy was used in the attempt to design a gold(I) complex with the ability to selectively inhibit NCp7 as well. Complexes of this form were developed to leverage the success of auranofin as an arthritis treatment coupled with the incorporation of the N-heterocycle recognition element utilized in the [M(dien)(N-heterocycle)]$^{n+}$ type complexes. Complexes of the form [(PPh_3)Au(N-heterocycle)]$^{+}$ formed a white precipitate immediately upon interaction with N-acetylcysteine, indicating rapid N-heterocycle displacement. Upon interaction with the C-terminal zinc finger motifs of NCp7 and Sp1, the gold was observed bound to the apopeptide with the triphenylphosphine ligand still bound. This was the first example of a gold complex bound to these zinc finger proteins without total ligand dissociation. Formation of gold fingers was also observed. These results further illustrate that tuning the electronic and steric properties around the

metal center can have dramatic effects on the reactivity of coordination complexes with zinc finger protein targets.[101] Additional evidence that reactions with zinc finger proteins are modulated by the metal coordination sphere was found in the complexes in which 2-mercaptothiazole and cyanide were used as ligands in place of the N-heterocycle. In one such complex, it was found that the phosphine ligand may dissociate first, due to the high trans effect of the 2-mercaptothiazole ligand.[102]

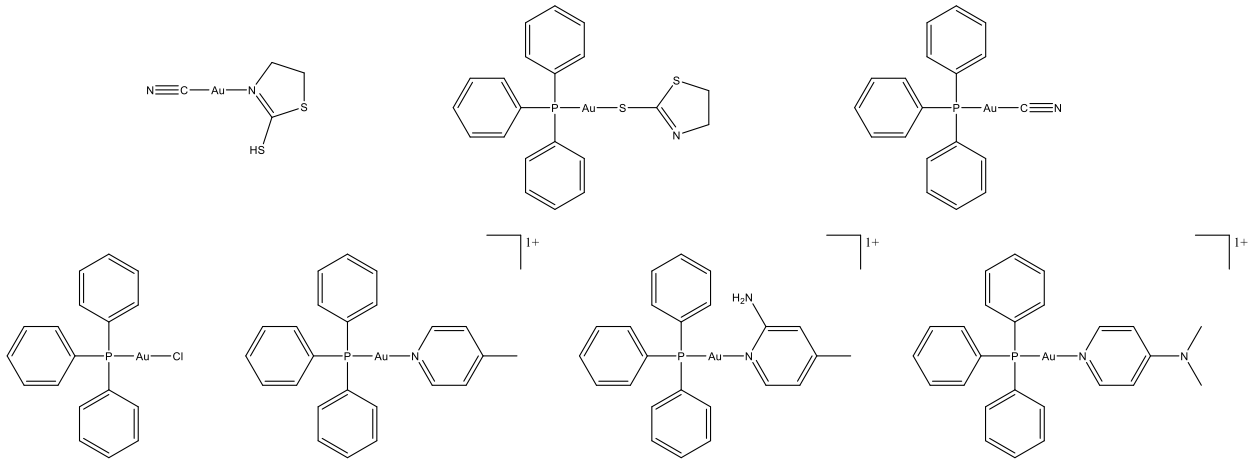

Figure 1.18. The structures of gold(I) complexes investigated as NCp7 inhibitors.[101,102]

1.5 The Use of Gold Complexes to Target Zinc Finger Proteins

In addition to the study of gold complexes as selective inhibitors of NCp7, gold complexes have also been investigated as selective inhibitors of other zinc finger proteins.[103] Auranofin, $[Au(bpy)Cl_2]^{1+}$, and $[Au(phen)Cl_2]^{1+}$ (bpy = bipyridine, phen = 1,10-phenanthroline) were investigated for their ability to inhibit PARP-1, and were found to inhibit the protein more effectively than the "benchmark" inhibitor, the organic complex 3-aminobenzamide. The gold(III) complexes rapidly lost all ligands and formed "gold-finger" type structures more quickly than auranofin, a gold(I) complex, highlighting the enhanced reactivity of the gold(III) oxidation state.

Additionally, both the gold(I) and the gold(III) complexes formed adducts with the protein more rapidly than the representative platinum(II) (cisplatin), ruthenium(III) (NAMI-A), and ruthenium(II) (RAPTA-T) complexes.[104]

The ability of gold complexes to inhibit PARP-1 was further investigated through the synthesis of a library of gold complexes that contained multidentate N-donor chelating ligands. It was found that the gold complexes that displayed cytotoxic effects, such as the dinuclear $[Au_2\{2\text{-}(2\text{-pyridyl})imidazolate\}(PPh_3)_2]^{1+}$ also displayed the ability to inhibit PARP-1 activity in cisplatin sensitive cells, while the complex [Au(2-phenylimidazole)(DAPTA)] (DAPTA = 3,7-diacetyl-1,3,7-triaza-5-phosphabicyclo[3.3.1]nonane), which did not display cytotoxicity was also unable to inhibit PARP-1.[105] Additionally, the analog of $[Au(bpy)Cl_2]^{1+}$ containing the bidentate chelating ligand 2-((2,2'-bipyridin)-5-yl)-1*H*-benzimidazol-4-carboxamide was found to preferentially target PARP-1 over the traditional target for complexes of this nature, thioredoxin reductase.[106] Gold(I) complexes containing N-heterocyclic carbene ligands were also investigated for their cytotoxic properties. These complexes were thought to interact with PARP-1 in a non-covalent manner without loss of the gold-bound ligands.[107]

1.6 Gold Complexes Containing a C-Donor Ligand

Research into methods by which to further stabilize the gold(III) oxidation state has evolved into investigation of complexes containing one or more gold-carbon bonds.[14,108] While many of the complexes containing gold-carbon bonds have been developed as chemotherapeutic agents, with the thioredoxin/thioredoxin reductase system as the main target, some interesting protein interactions have been discovered. A reductive elimination mechanism by which the C-donor ligand of complexes containing 2-arylpyridine or an analog as a chelating ligand is transferred to a cysteine thiol forming a thioether was discovered. The proof of cysteine arylation was obtained

using a number of short cysteine-containing peptide sequences, and it was found that the reaction proceeded over a wide range of pH and temperature. Cysteine arylation by these complexes was also achieved on the larger proteins bovine serum albumin and human serum albumin, proving that bioconjugation on a full protein was possible.[109] This mechanism is of particular importance, as it parallels the mechanism by which the *E. coli* N-Ada protein repairs DNA which has been damaged by alkylation.[110,111] While a great deal of investigation has been conducted on palladium-catalyzed cysteine bioconjugation, the analogous gold-catalyzed reactions have been studied to a significantly lesser extent.[112–115] A recent example of a gold complex, $[(\text{Me-DalPhos})\text{Au}(\text{R})\text{Cl}]^{1+}$ (Me-DalPhos = $\text{Ad}_2\text{P}(o\text{-}\text{C}_6\text{H}_4)\text{NMe}_2$, R = aryl), showed that bioconjugation of a number of different arylating ligands is possible, including an chemotherapy drug, an affinity tag, and a fluorescent dye. Cysteine arylation was confirmed on a short peptide sequence and on glutathione, a target of biological relevance, by LC-MS.[116]

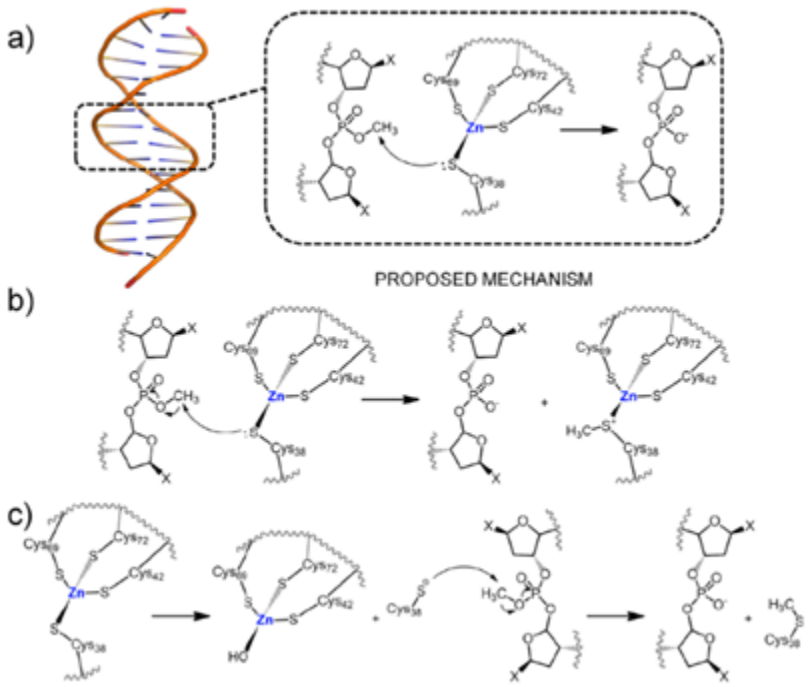

Figure 1.19. Proposed mechanism of DNA repair by the N-Ada enzyme. Alkylated DNA is repaired by alkylation of a zinc-coordinating cysteine residue.[37]

In order to probe the reactivity of complexes with a gold-carbon bond in zinc finger proteins, the complex $[Au(bnpy)Cl_2]$ (bnpy = 2-benzylpyridine) was synthesized. The interactions of $[Au(bnpy)Cl_2]$ were compared to the analogous N^N complexes $[Au(bpy)Cl_2]^{1+}$, $[Au(4,4'\text{-}Me_2bpy)Cl_2]^{1+}$, and $[Au(phen)Cl_2]^{1+}$. The interaction between the small molecule model N-acetylcysteine and $[Au(bnpy)Cl_2]^{1+}$, the cysteine arylation product was observed. It was proposed that this arylation mechanism requires a *cis* orientation between the coupling partners in order for the reductive elimination to proceed.[117]

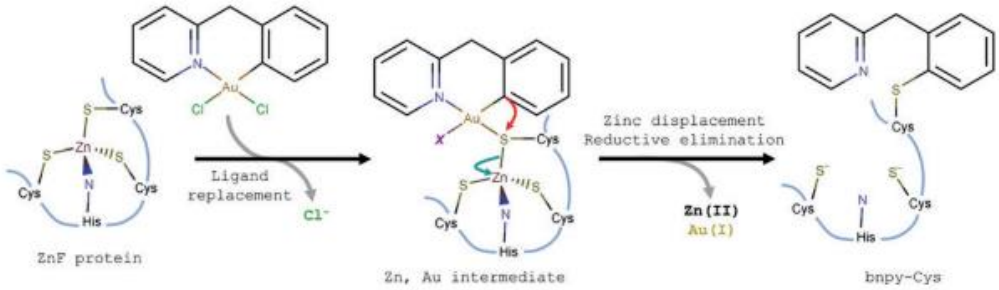

Figure 1.20. General scheme of zinc finger arylation by [Au(bnpy)Cl2]. X represents an N-donor, likely from the peptide.[117]

The reaction of $[Au(bnpy)Cl_2]^{1+}$ with the C-terminal zinc finger motif of NCp7 showed the production of the cysteine arylation product after 48 hours, while the N^N complexes showed products typical of interaction with a gold complex containing a labile chloride ligand. In contrast, reaction with glutathione did not produce the cysteine arylation product, showing that the microenvironment of the cysteine residue is important to the ability of the cysteine to be arylated. The ability of the C-terminal zinc finger to be covalently modified by a gold complex shows the potential for the development for a selective complex to covalently modify NCp7.[117]

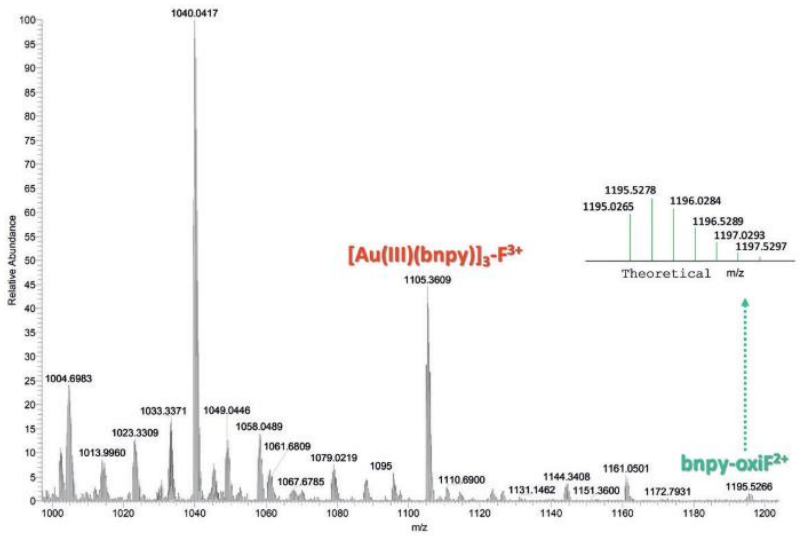

Figure 1.21. Interaction of [Au(bnpy)Cl2] with the C-terminal zinc finger of NCp7 after 48 hours of incubation.[117]

1.7 Dissertation Outline

It is the goal of this dissertation to expand on the chemistry of gold(III) complexes and their potential uses as inhibitors of HIV NCp7 so that they might be competitive with the lead platinum(II) complex $[Pt(dien)(xanthosine)]^{2+}$ and the lead organic compounds that were discovered to interact with NCp7 through a high throughput screening process.[118,119] The promiscuity of the previously reported $[Au(dien)(N\text{-heterocycle})]^{3+}$ complexes necessitates further tuning of the electronic and steric environment of the AuN_4 coordination sphere if a selective inhibitor of NCp7 is to be developed. Chapter 2 discusses the attempt to develop an AuN_4 complex using the more sterically hindered chelating ligand di-(2-picolyl)amine in order to slow the reaction with NCp7 and prevent interactions with undesirable biomolecules such as glutathione, creating selectivity for NCp7. The gold(III) chloride complexes based on this chelate were investigated for their interactions with NCp7 and compared with the platinum(II) analogs.

Given the increased affinity of 1-methylcytosine for N-acetyltryptophan relative to the other previously studied nucleobase analogs, such as 9-ethylguanine and 4-dimethylpyridine, it is natural that the gold(III) analog of the previously studied $[Pt(dien)(1\text{-}MeCyt)]^{2+}$ and $[Pd(dien)(1\text{-}MeCyt)]^{2+}$ be investigated. The synthesis, characterization, and interactions with the C-terminal zinc finger of NCp7 are discussed in detail in Chapter 3.

The emergence of organometallic gold complexes has shown their potential for use in a variety of applications. Chapter 4 aims to investigate the interactions between the organometallic complex $[AuCl_2(dampa)]$ and biologically relevant molecules, including NCp7. The comparison of the interactions between this complex and the similar $[Au(bnpy)Cl_2]$ are compared and contrasted. In addition, the novel triphenylphosphine-containing complex $[AuCl(dampa)(PPh_3)]^{1+}$ was investigated. The synthesis, characterization, X-ray crystal structure, and interactions of this complex with biologically relevant molecules, including NCp7, are detailed.

Additional data, including the attempted synthesis of sterically hindered analogs of $[Au(dien)(N\text{-heterocycle})]^{3+}$ complexes and the investigation of the binding differences between gold(I) and gold(III) complexes with polypeptides are described in Chapter 5. Chapter 6 will detail the recovery of residual platinum from laboratory waste. Submitted and published works are in a format as close to the submitted format as possible.

1.8 References

1. Huaizhi, Z. and Yuantao, N. China's ancient gold drugs. *Gold Bull.* **34,** 24–29, 2001.

2. Berners-Price, S. J. and Filipovska, A. Gold compounds as therapeutic agents for human diseases. *Metallomics* **3,** 863, 2011.

3. Shaw, C. F. Gold-Based Therapeutic Agents. *Chem. Rev.* **99,** 2589–2600, 1999.

4. Benedek, T. G. The History of Gold Therapy for Tuberculosis. *J. Hist. Med. Allied Sci.* **59,** 50–89, 2004.

5. Wall, S. *et al.* The Thioredoxin Reductase-1 Inhibitor Aurothioglucose Enhances Glutathione-dependent Antioxidant Responses in a Murine Model of Bronchopulmonary Dysplasia. *Free Radic. Biol. Med.* **112,** 37–38, 2017.

6. Larabee, J. L., Hocker, J. R. & Hanas, J. S. Mechanisms of aurothiomalate-Cys2His2 zinc finger interactions. *Chem. Res. Toxicol.* **18,** 1943–1954, 2005.

7. Bindoli, A. *et al.* Thioredoxin reductase: A target for gold compounds acting as potential anticancer drugs. *Coord. Chem. Rev.* **253,** 1692–1707, 2009.

8. Kean, W. F., Hart, L. & Buchanan, W. W. Auranofin. *Rheumatology* **36,** 560–572, 1997.

9. Gromer, S., Arscott, L. D., Williams, C. H., Schirmer, R. H. & Becker, K. Human placenta thioredoxin reductase. Isolation of the selenoenzyme, steady state kinetics, and inhibition by therapeutic gold compounds. *J. Biol. Chem.* **273,** 20096–101, 1998.

10. Pavic, A. *et al.* Mononuclear gold(III) complexes with phenanthroline ligands as efficient inhibitors of angiogenesis: A comparative study with auranofin and sunitinib. *J. Inorg. Biochem.* **174,** 156–168, 2017.

11. De Paiva, R. E. F., Du, Z., Peterson, E. J., Corbi, P. P. & Farrell, N. P. Probing the HIV-1 NCp7 Nucleocapsid Protein with Site-Specific Gold(I)−Phosphine Complexes. *Inorg. Chem.*, **56,** 12308-12318, 2017.

12. Ott, I. On the medicinal chemistry of gold complexes as anticancer drugs. *Coord. Chem. Rev.* **253,** 1670–1681, 2009.

13. Tiekink, E. R. T. Gold derivatives for the treatment of cancer. *Crit. Rev. Oncol. Hematol.* **42,** 225–48, 2002.

14. Zou, T., Lum, C. T., Lok, C.-N., Zhang, J.-J. & Che, C.-M. Chemical biology of anticancer gold(iii) and gold(i) complexes. *Chem. Soc. Rev.* **44,** 8786–8801, 2015.

15. Hickey, J. L. *et al.* Mitochondria-Targeted Chemotherapeutics: The Rational Design of Gold(I) *N* -Heterocyclic Carbene Complexes That Are Selectively Toxic to Cancer Cells and Target Protein Selenols in Preference to Thiols. *J. Am. Chem. Soc.* **130,** 12570–12571, 2008.

16. Berners-Price, S. J. *et al.* In vivo antitumor activity and in vitro cytotoxic properties of bis[1,2-bis(diphenylphosphino)ethane]gold(I) chloride. *Cancer Res.* **46,** 5486–93, 1986.

17. Humphreys, A. S. *et al.* Gold(i) chloride adducts of 1,3-bis(di-2-pyridylphosphino)propane: synthesis, structural studies and antitumour activity. *Dalt. Trans.* **0,** 4943, 2007.

18. Farrell, N. P. Multi-platinum anti-cancer agents. Substitution-inert compounds for tumor selectivity and new targets. *Chem. Soc. Rev.* **44,** 8773–8785, 2015.

19. Kelland, L. The resurgence of platinum-based cancer chemotherapy. *Nat. Rev. Cancer* **7,** 573–584, 2007.

20. Gabbiani, C., Casini, A. & Messori, L. Gold(III) compounds as anticancer drugs. *Gold Bull.* **40,** 73–81, 2007.

21. Parish, R. V. *et al.* Chemical and Biological Studies of Dichloro(2-((dimethylamino)methyl)phenyl)gold(III). *Inorg. Chem.* **35,** 1659–1666, 1996.

22. Buckley, R. G. *et al.* Antitumor properties of some 2-[(dimethylamino)methyl]phenylgold(III) complexes. *J. Med. Chem.* **39,** 5208–5214, 1996.

23. Luca Ronconi *et al.* Gold Dithiocarbamate Derivatives as Potential Antineoplastic Agents: Design, Spectroscopic Properties, and in Vitro Antitumor Activity. **44,** 1867-1881, 2005.

24. Li, C. K.-L., Sun, R. W.-Y., Kui, S. C.-F., Zhu, N. & Che, C.-M. Anticancer Cyclometalated [AuIIIm(C∧N∧C)mL]n+ Compounds: Synthesis and Cytotoxic Properties. *Chem. - A Eur. J.* **12,** 5253–5266, 2006.

25. Yan, J. J. *et al.* Cyclometalated gold(iii) complexes with N-heterocyclic carbene ligands as topoisomerase I poisons. *Chem. Commun.* **46,** 3893, 2010.

26. Fuertes, M. A., Castilla, J., Alonso, C. & Pérez, J. M. Cisplatin Biochemical Mechanism of Action: From Cytotoxicity to Induction of Cell Death Through Interconnections Between Apoptotic and Necrotic Pathways. *Current Medicinal Chemistry,* **10,** 2003.

27. Che, C. M. *et al.* Gold(iii) porphyrins as a new class of anticancer drugs: cytotoxicity, DNA binding and induction of apoptosis in human cervix epitheloid cancer cells. *Chem. Commun.*, **0,** 1718, 2003.

28. Casini, A. *et al.* Chemistry, antiproliferative properties, tumor selectivity, and molecular mechanisms of novel gold(III) compounds for cancer treatment: A systematic study. *J. Biol. Inorg. Chem.* **14,** 1139–1149, 2009.

29. Messori, L. *et al.* Gold(III) complexes as potential antitumor agents: Solution chemistry and cytotoxic properties of some selected gold(III) compounds. *J. Med. Chem.* **43,** 3541–

3548, 2000.

30. Navarro, M. Gold complexes as potential anti-parasitic agents. *Coord. Chem. Rev.* **253,** 1619–1626, 2009.

31. Bloland, P. B. *WHO/CDS/CSR/DRS/2001.4 Drug resistance in malaria*. (2001).

32. Kanzok, S. M., Schirmer, R. H., Turbachova, I., Iozef, R. and Becker, K. The thioredoxin system of the malaria parasite Plasmodium falciparum. Glutathione reduction revisited. *J. Biol. Chem.* **275,** 40180–40186, 2000.

33. Sannella, A. R. *et al.* New uses for old drugs. Auranofin, a clinically established antiarthritic metallodrug, exhibits potent antimalarial effects *in vitro* : Mechanistic and pharmacological implications. *FEBS Lett.* **582,** 844–847, 2008.

34. Navarro, M., Perez, H. & Sanchez-Delgado, R. A. Toward a novel metal-based chemotherapy against tropical diseases. 3. Synthesis and antimalarial activity in vitro and in vivo of the new gold- chloroquine complex [Au(PPh3)(CQ)]PF6. *J. Med. Chem.* **40,** 1937–1939, 1997.

35. Thomson, A. J. & Gray, H. B. Bioinorganic chemistry Editorial overview. *Curr. Opin. Chem. Biol.* **2,** 155–158, 1998.

36. Quintal, S. M., Depaula, Q. A. & Farrell, N. P. Zinc finger proteins as templates for metal ion exchange and ligand reactivity. Chemical and biological consequences. *Metallomics* **3,** 121–139, 2011.

37. Kluska, K., Adamczyk, J. & Krężel, A. Metal binding properties, stability and reactivity of zinc fingers. *Coord. Chem. Rev.* **367,** 18–64, 2018.

38. Andreini, C., Banci, L., Bertini, I. & Rosato, A. Counting the zinc-proteins encoded in the human genome. *J. Proteome Res.* **5,** 196–201, 2006.

39. Anzellotti, A. I. & Farrell, N. P. Zinc metalloproteins as medicinal targets. *Chem. Soc. Rev.* **37,** 1629, 2008.

40. Daniel, A. G., Peterson, E. J. & Farrell, N. P. The Bioinorganic Chemistry of Apoptosis: Potential Inhibitory Zinc Binding Sites in Caspase-3. *Angew. Chemie* **126,** 4182–4185, 2014.

41. Klug, A. & Rhodes, D. Zinc fingers: a novel protein fold for nucleic acid recognition. *Cold Spring Harb. Symp. Quant. Biol.* **52,** 473–482, 1987.

42. Abbehausen, C. Zinc finger domains as therapeutic targets for metal-based compounds – an update. *Metallomics*, 2018.

43. Krishna, S. S., Majumdar, I. & Grishin, N. V. Structural classification of zinc fingers: survey and summary. *Nucleic Acids Res.* **31,** 532–550, 2003.

44. Morellet, N. *et al.* Structure of the complex between the HIV-1 nucleocapsid protein NCp7 and the single-stranded pentanucleotide d(ACGCC). *J. Mol. Biol.* **283,** 419–434, 1998.

45. Maynard, A. T. & Covell, D. G. Reactivity of zinc finger cores: Analysis of protein packing and electrostatic screening. *J. Am. Chem. Soc.* **123,** 1047–1058, 2001.

46. Klug, A. The discovery of zinc fingers and their development for practical applications in gene regulation and genome manipulation. *Q. Rev. Biophys.* **43,** 1–21, 2010.

47. Miller, J., McLachlan, A. D. & Klug, A. Repetitive zinc-binding domains in the protein

transcription factor IIIA from Xenopus oocytes. *EMBO J.* **4,** 1609–1614, 1985.

48. Kadonaga, J. T., Jones, K. A. & Tjian, R. *Promoter-specific activation of RNA polymerase II transcription by Sp1*. *Trends in Biochemical Sciences* **11,** 1986.

49. Oka, S. *et al.* NMR structure of transcription factor Sp1 DNA binding domain. *Biochemistry* **43,** 16027–16035, 2004.

50. Safe, S. & Abdelrahim, M. Sp transcription factor family and its role in cancer. *Eur. J. Cancer* **41,** 2438–2448, 2005.

51. Yamanaka, H., Penning, C. A., Willis, E. H., Wasson, D. B. & Carson, D. A. Characterization of human poly(ADP-ribose) polymerase with autoantibodies. *J. Biol. Chem.* **263,** 3879–3883, 1988.

52. Durkacz, B. W., Omidiji, O., Gray, D. A. & Shall, S. (ADP-Ribose)nparticipates in DNA excision repair. *Nature* **283,** 593–596, 1980.

53. Woodhouse, B. C. & Dianov, G. L. Poly ADP-ribose polymerase-1: An international molecule of mystery. *DNA Repair*, **7,** 1077-1086, 2008.

54. Langelier, M.-F., Planck, J. L., Roy, S. & Pascal, J. M. Crystal structures of poly(ADP-ribose) polymerase-1 (PARP-1) zinc fingers bound to DNA: structural and functional insights into DNA-dependent PARP-1 activity. *J. Biol. Chem.* **286,** 10690–10701, 2011.

55. Zhu, G., Chang, P. & Lippard, S. J. Recognition of platinum-DNA damage by Poly(ADP-ribose) polymerase-1. *Biochemistry* **49,** 6177–6183, 2010.

56. Asahina, H. *et al.* The XPA protein is a zinc metalloprotein with an ability to recognize various kinds of DNA damage. *Mutat. Res. Repair* **315,** 229–237, 1994.

57. Hess, N. J. *et al.* Human nucleotide excision repair protein XPA: Extended X-ray absorption fine-structure evidence for a metal-binding domain. *Protein Science,* **7,** 1970-1975, 1998.

58. Fang, S., Jensen, J. P., Ludwig, R. L., Vousden, K. H. & Weissman, A. M. Mdm2 is a RING finger-dependent ubiquitin protein ligase for itself and p53. *J. Biol. Chem.* **275,** 8945–51, 2000.

59. Lai, Z., Freedman, D. A., Levine, A. J. & McLendon, G. L. Metal and RNA binding properties of the hdm2 RING finger domain. *Biochemistry* **37,** 17005–17015, 1998.

60. Iraci, N., Tabarrini, O., Santi, C. & Sancineto, L. NCp7: targeting a multitask protein for next-generation anti-HIV drug development part 2. Noncovalent inhibitors and nucleic acid binders. *Drug Discov. Today* **23,** 687–695, 2018.

61. Sancineto, L., Iraci, N., Tabarrini, O. & Santi, C. NCp7: targeting a multitasking protein for next-generation anti-HIV drug development part 1: covalent inhibitors. *Drug Discov. Today* **23,** 260–271, 2018.

62. Mclendon, G., Hull, H., Larkin, K. & Chang, W. Metal binding to the HIV nucleocapsid peptide, *J. Biol. Inorg. Chem.*, **4,** 171-174, 1999.

63. Lee, B. M., De Guzman, R. N., Turner, B. G., Tjandra, N. & Summers, M. F. Dynamical behavior of the HIV-1 nucleocapsid protein. *J. Mol. Biol.* **279,** 633–649, 1998.

64. Godet, J. & Mély, Y. Biophysical studies of the nucleic acid chaperone properties of the HIV-1 nucleocapsid protein. *RNA Biol.*, **7,** 687–699, 2010.

65. Bourbigot, S. *et al.* How the HIV-1 Nucleocapsid Protein Binds and Destabilises the

(−)Primer Binding Site During Reverse Transcription. *J. Mol. Biol.*, **383,** 1112–1128, 2008.

66. South, T. L. & Summers, M. F. Zinc- and sequence-dependent binding to nucleic acids by the N-terminal zinc finger of the HIV-1 nucleocapsid protein: NMR structure of the complex with the Psi-site analog, dACGCC. *Protein Sci.* **2,** 3–19, 1993.

67. Morellet, N. *et al.* Determination of the structure of the nucleocapsid protein NCp7 from the human immunodeficiency virus type 1 by 1H NMR. *EMBO J.* **11,** 3059–3065, 1992.

68. De Guzman, R. N. *et al.* Structure of the HIV-1 nucleocapsid protein bound to the SL3 ψ-RNA recognition element. *Science*, **279,** 384–388, 1998.

69. Levin, J. G., Guo, J., Rouzina, I. & Musier-Forsyth, K. Nucleic Acid Chaperone Activity of HIV-1 Nucleocapsid Protein: Critical Role in Reverse Transcription and Molecular Mechanism. *Prog. Nucleic Acid Res. Mol. Biol.* **80,** 217–286, 2005.

70. Darlix, J. L. *et al.* Flexible nature and specific functions of the HIV-1 nucleocapsid protein. *Journal of Molecular Biology* **410,** 565–581, 2011.

71. Panel on Clinical Practices for Treatment of HIV infection. Guidelines for the use of antiretroviral agents in HIN-infected adults and adolescents. *Pan American journal of public health*, **10,** (2001).

72. Das, K. & Arnold, E. HIV-1 reverse transcriptase and antiviral drug resistance. Part 2. *Curr. Opin. Virol.* **3,** 119–128, 2013.

73. Lv, Z., Chu, Y. & Wang, Y. HIV protease inhibitors: A review of molecular selectivity and toxicity. *HIV/AIDS - Res. Palliat. Care*, **7,** 95–104, 2015.

74. Hajimahdi, Z. & Zarghi, A. Progress in HIV-1 Integrase Inhibitors: A Review of their Chemical Structure Diversity. *Iranian Journal of Pharmaceutical Research* **15,** 595-628, 2016.

75. Boyd, M. & Pett, S. Experimental and clinical pharmacology: HIV fusion inhibitors: a review. *Aust. Prescr.* **31,** 66–69, 2008.

76. de Rocquigny, H. *et al.* Targeting the viral nucleocapsid protein in anti-HIV-1 therapy. *Mini Rev. Med. Chem.* **8,** 24–35, 2008.

77. Rice, W. G. *et al.* Inhibition of HIV-1 infectivity by zinc-ejecting aromatic C-nitroso compounds. *Nature*, **361,** 473–475, 1993.

78. Rice, W. G. *et al.* Inhibitors of HIV nucleocapsid protein zinc fingers as candidates for the treatment of AIDS. *Science*, **270,** 1194–1197, 1995.

79. Huang, M. *et al.* Anti-HIV agents that selectively target retroviral nucleocapsid protein zinc fingers without affecting cellular zinc finger proteins. *Journal of Medicinal Chemistry* **41,** 1371-1381, 1998.

80. Maynard, A. T., Huang, M., Rice, W. G. & Covell, D. G. Reactivity of the HIV-1 nucleocapsid protein p7 zinc finger domains from the perspective of density-functional theory. *Proc. Natl. Acad. Sci. U. S. A.* **95,** 11578–11583, 1998.

81. Jenkins, L. M. M. *et al.* Studies on the mechanism of inactivation of the HIV-1 nucleocapsid protein NCp7 with 2-mercaptobenzamide thioesters. *J. Med. Chem.* **48,** 2847–2858, 2005.

82. Stephen, A. G. *et al.* Identification of HIV-1 nucleocapsid protein: nucleic acid

antagonists with cellular anti-HIV activity. *Biochem. and Biophys. Res. Comm.*, **296,** 1228-1237, 2002.

83. Kelley, T. J., Moghaddas, S., Bose, R. & Basu, S. Inhibition of immunopurified DNA polymerase-alpha from PA-3 prostate tumor cells by platinum (II) antitumor drugs. *Cancer Biochem. Biophys.* **13,** 135–146, 1993.

84. Tsotsoros, S. D., Qu, Y. & Farrell, N. P. The reaction of dichlorodiammineplatinum(II), [PtCl2(NH3)2], isomers with zinc fingers. *J. Inorg. Biochem.* **143,** 117–122, 2015.

85. Ishida, T., Ueda, H., Segawa, K., Doi, M. & Inoue, M. Prominent stacking interaction with aromatic amino acid by N-quarternization of nucleic acid base: X-ray crystallographic characteristics and biological implications. *Arch. Biochem. Biophys.* **278,** 217–227, 1990.

86. Hamilton, A. D. & Pant, N. Nucleotide base recognition: Ditopic binding of guanine to a macrocyclic receptor containing naphthyridine and naphthalene units. *Journal of the Chemical Society, Chemical Communications*, **0,** 765-766, 1988.

87. Ishida, T. *et al.* Cooperative face-to-face and edge-to-face aromatic interactions of tryptophan indole ring with N7-quarternized guanine and neutral cytosine bases. *FEBS Lett.* **333,** 214–216, 1993.

88. Anzellotti, A. I., Ma, E. S. & Farrell, N. Platination of nucleobases to enhance noncovalent recognition in protein-DNA/RNA complexes. *Inorg. Chem.* **44,** 483–485, 2005.

89. Anzellotti, A. I., Sabat, M. & Farrell, N. Covalent and Noncovalent Interactions for

[Metal(dien)nucleobase]2+ Complexes with L-Tryptophan Derivatives: Formation of Palladium−Tryptophan Species by Nucleobase Substitution under Biologically Relevant Conditions. *Inorg. Chem.*, **45,** 1638-1645, 2006.

90. Anzellotti, A. I., Bayse, C. A. & Farrell, N. P. Effects of nucleobase metalation on frontier molecular orbitals: Potential implications for π-stacking interactions with tryptophan. *Inorg. Chem.* **47,** 10425–10431, 2008.

91. Strukl, J. V., De Paula, Q. A., Yang, X., Qu, Y. & Farrell, N. P. Comparison of cis and trans-platinum mononucleobase compounds with DNA and protein models. *Aust. J. Chem.* **61,** 694–699, 2008.

92. Liu, Q., Golden, M., Darensbourg, M. Y. & Farrell, N. Thiolate-bridged heterodinuclear platinum-zinc chelates as models for ternary platinum-DNA-protein complexes and zinc ejection from zinc fingers. Evidence from studies using ESI-mass spectrometry. *Chem Comm.*, **34,** 4360-4362, 2005.

93. Anzellotti, A. I., Liu, Q., Bloemink, M. J., Scarsdale, J. N. & Farrell, N. Targeting Retroviral Zn Finger-DNA Interactions: A Small-Molecule Approach Using the Electrophilic Nature of trans-Platinum-Nucleobase Compounds. *Chem. Biol.* **13,** 539–548, 2006.

94. Tsotsoros, S. D. *et al.* Modulation of the stacking interaction of MN4 (M = Pt, Pd, Au) complexes with tryptophan through N-heterocyclic ligands. *J. Inorg. Biochem.* **132,** 2–5, 2014.

95. Quintal, S., Viegas, A., Erhardt, S., Cabrita, E. J. & Farrell, N. P. Platinated DNA affects zinc finger conformation. Interaction of a platinated single-stranded oligonucleotide and

the C-terminal zinc finger of nucleocapsid protein HIVNCp7. *Biochemistry*, **51,** 1752–1761, 2012.

96. de Paula, Q. A., Mangrum, J. B. & Farrell, N. P. Zinc finger proteins as templates for metal ion exchange: Substitution effects on the C-finger of HIV nucleocapsid NCp7 using M(chelate) species (M = Pt, Pd, Au). *J. Inorg. Biochem.* **103,** 1347–1354, 2009.

97. Spell, S. R. & Farrell, N. P. Synthesis and properties of the first [Au(dien)(N-heterocycle)] 3+ compounds. *Inorg. Chem.*, **53,** 30–32, 2014.

98. Spell, S. R. & Farrell, N. P. [Au(dien)(N-heterocycle)] 3+ : Reactivity with Biomolecules and Zinc Finger Peptides. *Inorg. Chem.*, **54,** 79-86, 2015.

99. Abbehausen, C. *et al.* X-ray Absorption Spectroscopy Combined with Time-Dependent Density Functional Theory Elucidates Differential Substitution Pathways of Au(I) and Au(III) with Zinc Fingers. *Inorg. Chem.*, **57,** 218-230, 2018.

100. Spell, S. R. *et al.* Au(iii) compounds as HIV nucleocapsid protein (NCp7)-nucleic acid antagonists. *Chem. Commun.*, **53,** 91–94, 2017.

101. Abbehausen, C. *et al.* Gold(I)-Phosphine-N-Heterocycles: Biological Activity and Specific (Ligand) Interactions on the C-Terminal HIVNCp7 Zinc Finger. *Inorg. Chem* **52,** 11280-11287, 2013.

102. Abbehausen, C., Manzano, C. M., Corbi, P. P. & Farrell, N. P. Effects of coordination mode of 2-mercaptothiazoline on reactivity of Au(I) compounds with thiols and sulfur-containing proteins. *J. Inorg. Biochem.*, **165,** 136–145, 2016.

103. de Almeida, A., Oliveira, B. L., Correia, J. D., Soveral, G. & Casini, A. Emerging protein

targets for metal-based pharmaceutical agents: An update. *Coord. Chem. Rev.*, **257,** 2689–2704, 2013.

104. Mendes, F. *et al.* Metal-based inhibition of poly(ADP-ribose) polymerase-the guardian angel of DNA. *J. Med. Chem.* **54,** 2196–2206, 2011.

105. Serratrice, M. *et al.* Cytotoxic gold compounds: Synthesis, biological characterization and investigation of their inhibition properties of the zinc finger protein PARP-1. *Dalt. Trans.* **41,** 3287–3293, 2012.

106. Citta, A. *et al.* Toward anticancer gold-based compounds targeting PARP-1: A new case study. *RSC Adv.* **6,** 79147–79152, 2016.

107. Bertrand, B. *et al.* Caffeine-based gold(I) N-heterocyclic carbenes as possible anticancer agents: Synthesis and biological properties. *Inorg. Chem.* **53,** 2296–2303, 2014.

108. Sophie, J., Fritz, E. K. & Angela, C. Cyclometalated Complexes of Platinum and Gold with Biological Properties: State-of-the-Art and Future Perspectives. *Curr. Med. Chem.* **25,** 437–461, 2018.

109. Kung, K. K. Y. *et al.* Cyclometalated gold(iii) complexes for chemoselective cysteine modification via ligand controlled C—S bond-forming reductive elimination. *Chem. Commun.* **50,** 11899–11902, 2014.

110. Mishina, Y., Duguid, E. M. & He, C. Direct Reversal of DNA Alkylation Damage. *Chem. Rev.*, **106,** 215-232, 2006.

111. He, C. *et al.* A Methylation-Dependent Electrostatic Switch Controls DNA Repair and Transcriptional Activation by E. coli Ada. *Mol. Cell* **20,** 117–129, 2005.

112. Rojas, A. J., Pentelute, B. L. & Buchwald, S. L. Water-Soluble Palladium Reagents for Cysteine S-Arylation under Ambient Aqueous Conditions. *Org. Lett* **19,** 4263-4266, 2017.

113. Rojas, A. J. *et al.* Divergent unprotected peptide macrocyclisation by palladium-mediated cysteine arylation. *Chem. Sci.* **8,** 4257–4263, 2017.

114. Vinogradova, E. V., Zhang, C., Spokoyny, A. M., Pentelute, B. L. & Buchwald, S. L. Organometallic palladium reagents for cysteine bioconjugation. *Nature*, **526,** 687–691, 2015.

115. Kubota, K., Dai, P., Pentelute, B. L. & Buchwald, S. L. Palladium Oxidative Addition Complexes for Peptide and Protein Cross-linking. *J. Am. Chem. Soc.* **140,** 3128–3133, 2018.

116. Messina, M. S. *et al.* Organometallic Gold(III) Reagents for Cysteine Arylation. *J. Am. Chem. Soc.* **140,** 7065–7069, 2018.

117. de Paiva, R. E. F. *et al.* Au-catalyzed C-S aryl group transfer in Zinc Finger Proteins. *Angew. Chemie Int. Ed.* **57,** 9305-9309, 2018.

118. Tsotsoros, S.D. *et al*. Enhancement of the Physiochemical Properties of $[Pt(dien)(nucleobase)]^{2+}$ for HIVNCp7 Targeting. *Chem. Sci.* **2,** 1269-1281, 2017.

119. Shvadchak, V. *et al*. Identification by High Throughput Screening of Small Compounds Inhibiting the Nucleic Acid Destabilization Activity of the HIV-1 Nucleocapsid Protein. *Biochimie*. **91,** 916-923, 2009.

Chapter 2: Interaction of the HIV NCp7 protein with platinum(II) and gold(III) complexes containing tridentate ligands

Victor H. F. Bernardes[a,b], Yun Qu[b], Zhifeng Du[b], James Beaton[b], Maria D. Vargas[a], and Nicholas P. Farrell[b]*

[a] Chemistry Institute, Fluminense Federal University, Campus Valonguinho, Niterói-RJ, Brazil;

[b] Department of Chemistry, Virginia Commonwealth University, Richmond-VA, USA

**As supporting author for the following work, I performed all work pertaining to the synthesis and characterization of the gold(III) complexes described and all investigation into the attempted synthesis of AuN_4 complexes. Additionally, I performed all analyses using the gold(III) complexes and played a significant role in the interpretation of the mass spectrometry data obtained from the interactions of gold(III) complexes with zinc fingers.

2.1 Abstract

Herein, we describe the interactions of $[MCl(N_3)]^{n+}$ complexes [M = Pt^{2+} (n = 1) and Au^{3+} (n = 2); N_3 = tridentate ancillary ligands: bpma (bis(2-pyridylmethyl)amine) or Mebpma (bis(2-pyridylmethyl)methylamine)] with the C-terminal finger of HIV-1 nucleocapsid protein NCp7 (ZF2). Substitution-inert analogs $[Pt(N_3)L]^{2+}$ were prepared with 9-EtGua and substituted pyridines to examine stacking interactions with tryptophan and the tryptophan-containing ZF2 and "full" 2-finger HIVNCp7. The use of the bpma and Mebpma ligands gives slightly higher affinity

than analogous $[Pt(dien)L)]^{2+}$ complexes. The dmap-containing complexes have the greatest affinity for the Trp residue in *N*-AcTrp and ZF2 peptide. Complex **PtL^{1}a** has the greatest K_a when compared with other known Pt^{2+} analogues; $[Pt(dien)(9\text{-EtGua})]^{2+}$ < **PtL^{2}c** <$[Pt(dien)(dmap)]^{2+}$< **PtL^{2}a** < **PtL^{1}a**. The K_a value was also obtained for the full NCp7 peptide with **PtL^{1}a** (*ca.* 40.6±1.0). In addition, the ESI-MS spectrum of the mixture of the ZF2 with this complex confirms formation of a 1:1 **PtL^{1}a**:ZF adduct. The reactivities of the $[MCl(Mebpma)]^{n+}$ (**PtL^1** and **AuL^1**) complexes with NCp7 ZF2 (C-terminal of the NCp7 Zinc finger domain) were investigated by ESI-MS. When compared with the known dien-containing analogs $[MCl(dien)]^{n+}$, the $[MCl(Mebpma)]^{n+}$ complexes are far more reactive. The initial product of reaction of **PtL^1** with ZF2 results in loss of all ligands and release of zinc to give the platinated apopeptide {PtF}. This is in contrast to $[PtCl(dien)]^{+}$ where {Pt(dien)}-peptide adducts are observed. The reaction of the Au^{3+} complex **AuL^1** with ZF2 gives Au_xF^{n+} species (x =1,2,4) with loss of all ligands. The $[Pt(N_3)L]^{2+}$ complexes **PtL^{1}a**, **PtL^{2}a**, and **PtL^{2}c** were inert when incubated with *N*-AcCys, whereas the precursor compounds $[PtCl(N_3)]Cl$ (**PtL^1**, N_3= Mebpma; **PtL^2**, bpma) reacted readily with the sulfur-containing amino acid.

2.2 Introduction

The HIV nucleocapsid (NCp7) protein has an amino acid sequence highly conserved in all HIV retrovirus subtypes. NCp7 has important roles in the viral life cycle, especially in the assembly and reverse transcription stages.[1,2] Its functions are intimately related to the protein structure. The two zinc finger (ZF) domains in the NCp7 sequence, both of the CCHC-type, are responsible for the protein folding that allows non-covalent interactions between amino acid residues and the viral RNA. The π-π stacking between ZF Trp37 and the RNA guanine is one of the most important interactions in the NCp7/RNA adduct.[1,3,4] Deletion of Trp37 can lead to loss

of protein function causing HIV inhibition.[5] Due to these characteristics the NCp7 ZF has been investigated as a target in anti HIV therapies.[1,2,6–10] To enhance selectivity over other zinc fingers, and zinc proteins in general, the aromatic amino acids Phe(ZF1) and Trp(ZF2) can be designated as molecular targets whereby ligands (drugs) capable of π-π stacking interactions, especially with the essential tryptophan, can inhibit DNA/RNA recognition.[11,12]

We are actively engaged in designing metallated-*N*-heterocyclic complexes targeted to tryptophan recognition, to examine eventual interruption of the NCp7-RNA interaction.[12-16] Metallation, along with protonation and alkylation, of purines and pyrimidines can increase the affinity for π-π stacking with tryptophan over the "parent" nucleobase.[13,17] The same trend is seen for other aromatic heterocycles, *e.g.* 4-dimethylaminopyridine (dmap).[18] For the simple amino acid, the complexes $[Pt(dien)(dmap)]^{2+}$, $[Au(dien)(dmap)]^{3+}$ and $[Au(N\text{-}Medien)(dmap)]^{3+}$ showed the highest association constants among other *N*-heterocyclic containing complexes.[18,19] The use of formally substitution-inert MN_4 systems is critical to this design as they enable initial "non-covalent" recognition between the metallated nucleobases and tryptophan, followed by nucleophilic attack of a zinc-finger cysteine at the metal site. The mechanism of action of *trans*-$[PtCl(py)_2(9\text{-}EtGua)]^+$ (which has incipient HIV inhibitory action and ejects Zn^{2+} of the ZF domain) has been proposed to involve the two steps of target recognition (Trp stacking) followed by target "fixation" (Pt-Cys binding).[14] Use of MN_4 systems could allow for greater selectivity where the Pt-N bond is more substitution-inert than its Pt-Cl counterpart.[20]

In this paper we describe and compare the chemistry and biology of Pt^{2+} and Au^{3+} complexes containing tridentate ligands based on bis(2-pyridylmethyl)amine (bpma) and further compare their properties with the previously studied diethylenetriamine (dien) chelates. Pt^{2+}, Pd^{2+} and Au^{3+} complexes containing the bpma ligand have been extensively studied.[21–27] Herein we describe the

reactions of formally isostructural and isoelectronic complexes $[MCl(N_3)]^{n+}$ (M = Pt, n = 1; Au, n = 2; N_3 = Mebpma (bis(2-pyridylmethyl)methylamine)) (Figure 2.1) with the simple amino acid *N*-AcCys and the C-terminal finger NCp7(ZF2) that result in Zn^{2+} ejection and metallation of the apoF2. Furthermore, we show that the stacking interactions of the platinum(II) complexes $[Pt(N_3)L]^{2+}$ (L = *N*-heterocyclic ligand: 4-dimethylaminopyridine (dmap), 9-ethylguanine (9-EtGua) and 4-methylpyridine (4-pic)) with tryptophan and the ZF2 can be tuned by judicious choice of both tridentate ligand carrier, N_3 (Mebpma instead of bpma) and L (Figure 2.1). The properties of the bpma and Mebpma complexes are also compared with previous results using the diethylenetriamine (dien) chelate. These results open new avenues in the search for potential and selective candidates for HIV inhibition.

2.3 Results and Discussion

Synthesis and Characterization of the chloro-complexes $[PtCl(N_3)]Cl$ and $[AuCl(N_3)]X_n$ (N_3 = Mebpma and bpma).

[PtCl(Mebpma)]Cl (**PtL^1**) was synthesized from *cis*-$[PtCl_2(DMSO)_2]$ and Mebpma (bis(2-pyridylmethyl)methylamine), in CH_2Cl_2 in 60% yield. The analogous bpma (bis(2-pyridylmethyl)amine) [PtCl(bpma)]Cl (**PtL^2**) was obtained in similar yields (98%) by the same method. The bpma compound was previously described in the literature through synthesis in water from $[PtCl_2(COD)]$.[23,26] The analogous gold(III) complex $[AuCl(Mebpma)](PF_6)_2$ (**AuL^1**) was synthesized from hydrogen tetrachloroaurate hydrate and Mebpma, as previously described for the analogous Bbpma (bis(2-pyridylmethyl)benzylamine) compound,[25] and isolated in 53.5% yield. In the case of the bpma ligand, the pale yellow $[AuCl(bpma)](OTf)_2$ (**AuL^2**) is thermally unstable with a strong tendency to deprotonation of the "central" N.[25] The red (**AuL^2**) was isolated in the amide form as the $[AuCl(bpma\text{-}H)](PF_6)$ salt as described previously.[25] The related compounds

[PtCl(dien)]Cl and [AuCl(dien)]Cl_2 were also prepared for comparison following literature methods.[29,30,31]

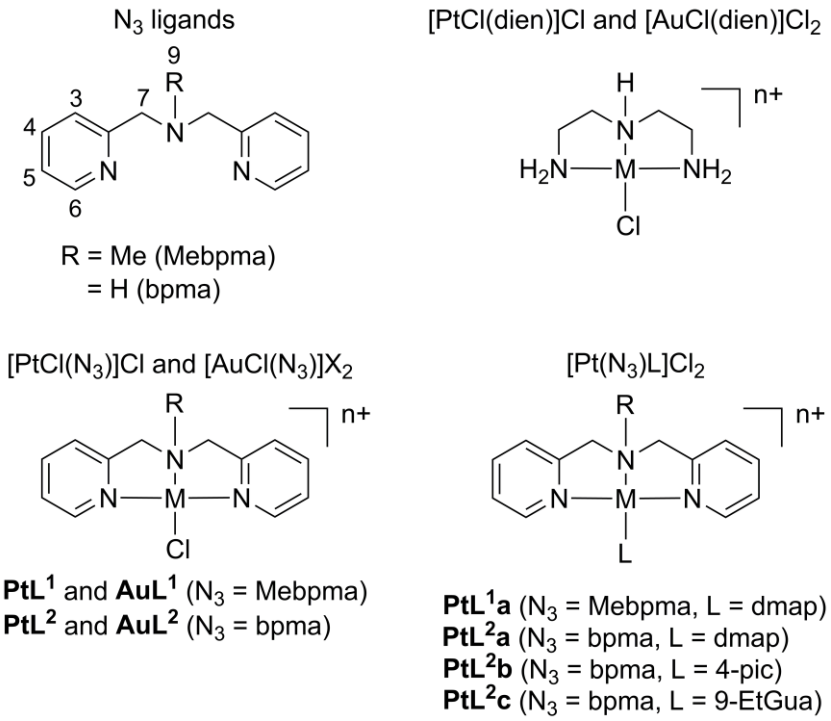

Figure 2.1. Structures of N_3 ligands, the platinum(II) and gold(III) complexes investigated in this study and of [MCl(dien)]Cl_n (M = Pt, n = 1; Au, n = 2).

^{1}H Nuclear Magnetic Resonance spectroscopy.

In the ^{1}H NMR spectra of the two free ligands, obtained in D_2O, the C*H*$_2$ signal (H7) appears as a singlet, at δ 3.55 (Mebpma) and 3.76 (bpma). After coordination, the signals are shifted downfield and due to restricted rotation the C*H*$_2$ signal becomes a doublet of doublets δ 4.60 and 5.17 for **PtL^1** and δ4.65 and 4.96 for **PtL^2**. (Table 2.1, Figure 2.2). The diastereotopic protons are designated as *endo*-CH and *exo*-CH protons (Figure 2.3a).[27] The same trend is observed for the **AuL^1** Mebpma complex (Figure 2.4). The spectrum, obtained in dmf-d_7 due to low solubility of the complex in water, shows a singlet at δ 3.75 (free Mebpma) and the doublet of doublets at δ

5.47 and 6.35 (**AuL^1**). As previously reported, the room temperature ^{1}H NMR spectrum of **AuL^2** does not exhibit the split CH_2 signal due to the amine-amide equilibrium and a broad singlet is observed.[25] Similarly, the amide-form [AuCl(bpma- H)](PF_6) shows a sharp singlet at δ 4.40 ppm (Figure 2.4).

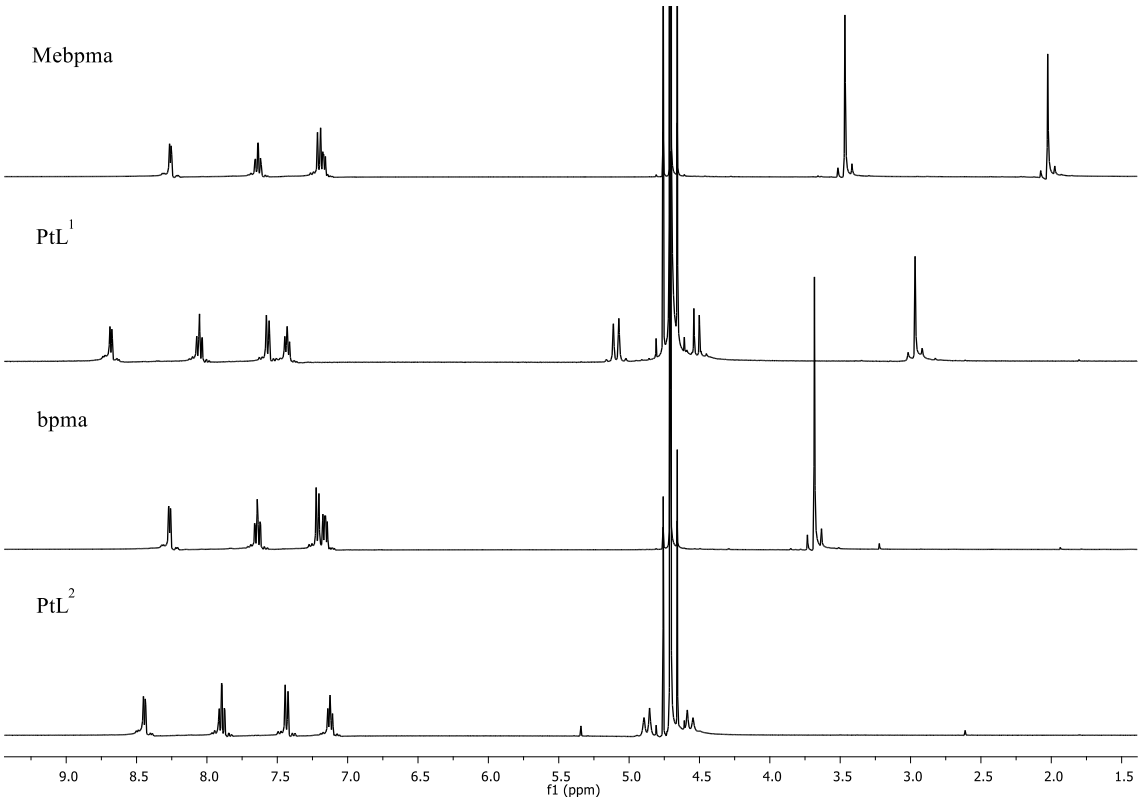

Figure 2.2. ^{1}H NMR spectra of the free ligands Mebpma and bpma and their platinum(II) complexes **PtL^1** and **PtL^2**.

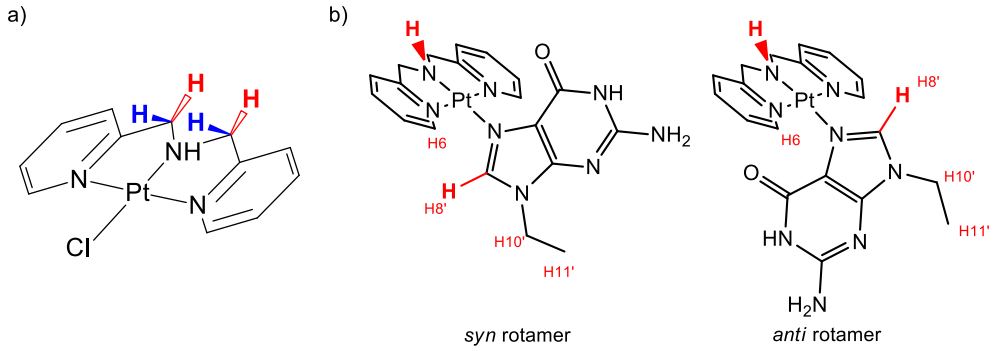

Figure 2.3. a) Designation of the *endo*-CH(blue) and the *exo*-CH(red) protons. **b)** Rotamers for **PtL^{2}c**.[1]

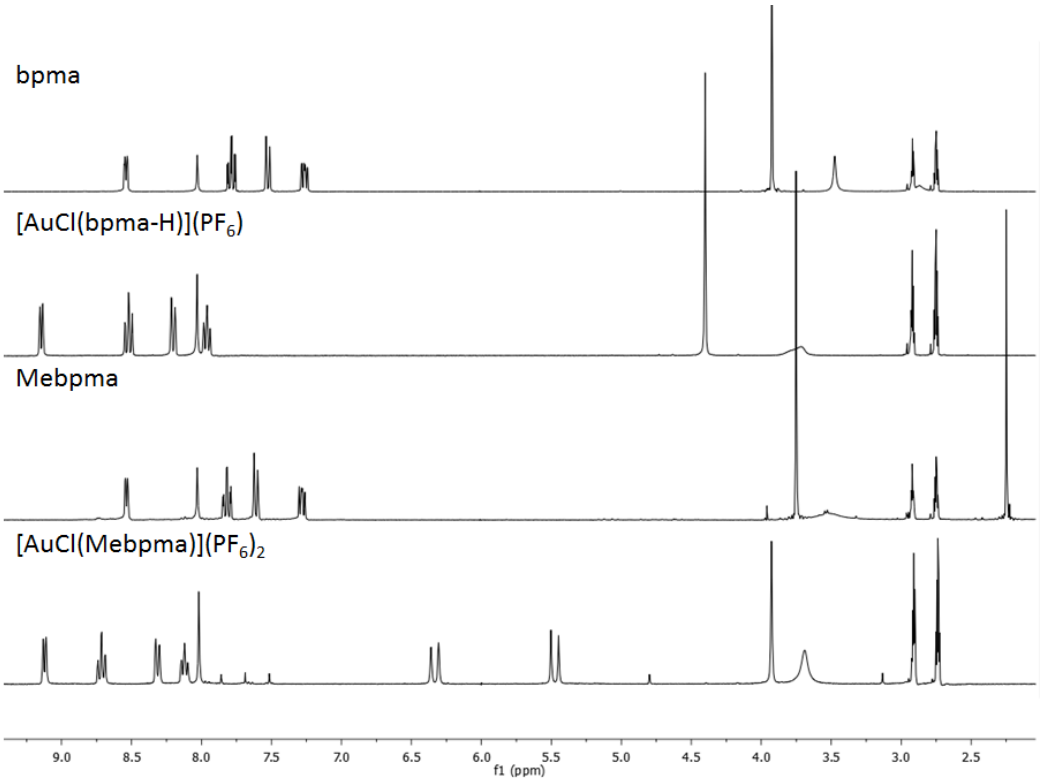

Figure 2.4. ^{1}H NMR spectra for ligands and [AuCl(Mebpma)]$^{2+}$ (**AuL^1)** and [AuCl(bpma-H)]$^+$**Au(L^2-H)**.

Compound[a]	H6	H5	H4	H3	H7	H9
Mebpma	8.34	7.25	7.72	7.29	3.55	2.11
	(d, 8.0)	(d, 8.0)	(td, 8.0)	(d, 8.0)	(s)	(s)
PtL^1	8.76	7.51	8.14	7.65	4.60/5.17	3.05
	(d, 4.0)	(t, 8.0)	(t, 8.0, 4.0)	(d , 8.0)	(dd, 16.0)	(s)
bpma	8.35	7.24	7.72	7.30	3.76	-
	(d, 4.0)	(t, 8.0)	(td, 8.0)	(d, 8.0)	(s)	
PtL^2 [26]	8.53	7.21	7.98	7.52	4.65/4.96	-
	(d, 4.0)	(t, 8.0)	(td, 8.0; 4.0)	(d, 8.0)	(dd, 16.0)	
Mebpma*	8.54	7.29	7.82	7.61	3.75	2.25
	(d, 3.0)	(td, 6.0, >1.0)	(td, 9.0, 3.0)	(d, 6.0)	(s)	(s)
AuL^{1*}	9.13	8.13	8.72	8.32	5.47/6.35	3.94
	(d, 6.0)	(t, 6.0)	(t, 6.0)	(d; 9.0)	(dd, 15.0)	(s)
bpma *	8.54	7.26	7.79	7.52	3.92	-
	(d, 6.0)	(td, 6.0, 3.0)	(td, 6.0, >1.0)	(d, 9.0)	(s)	
Au(L^2-H) [25]*	9.14	7.96	8.55	8.21	4.40	-
	(d, 6.0)	(m, 6.0)	(m, 9.0)	(d, 9.0)	(s)	
AuL^2	9.15	8.00	8.57	8.19	6.00	-
	(dd, 6.0, >1.0)	(td, 9.0, >1.0)	(td, 9.0, >1.0)	(d, 9.0)	(br s)	

a: δ(Pt) for PtL^1 = -2331.9 ppm; for PtL^2 = -2301.8 ppm rel. to Na_2PtCl_6 in D_2O (See Experimental Section). *The spectra of the Pt^{2+} complexes were obtained in D_2O and those of the Au^{3+} complexes in dmf-d_7. Spectra of the free ligands were obtained in both solvents for comparison. See Figs. S1 and S3. br = broad, s = singlet, d = doublet, dd = doublet of doublets, t = triplet, td = triplet of doublets, m = multiplet. The values in parenthesis are multiplicity and coupling constants (Hz).

Table 2.1. ^{1}H NMR shifts (ppm) for the $[MCl(N_3)]^{n+}$ complexes **PtL^1**, **PtL^2**, **AuL^1**, **AuL^2**, **Au(L^2-H**) and for the free N_3 ligands (Mebpma and bpma).

Metal coordination leads to characteristic downfield shifts of the aromatic hydrogens of both ligands, due to the decrease of electron density on the pyridine rings. The same occurs for the C*H*$_3$

hydrogen signal (H9) of the methylated ligand in **PtL^1** and **AuL^1** (Table 2.1). In all cases the relative changes in shift {δ(L) - δ(ML)} are uniformly higher for the Au^{3+} *versus* Pt^{2+} reflecting the greater electronegativity of the Au^{3+} center. The pK_a for the amine-amide equilibrium in the Au(III)-bpma compound has been estimated to be 3.5,[25] comparable to that measured for $[AuCl(dien)]^{2+}$ in the range of 4.0-4.7 depending on conditions.[32,33] In this respect, the behavior of Au^{3+} is in stark contrast to the formally isoelectronic Pt^{2+} where a pK_a of 11.94 has been measured for $[Pt(dien)(DMSO)]^{2+}$.[34]

Synthesis and Characterization of N-heterocycle-complexes $[Pt(N_3)L]Cl_2$ (N_3 = Mebpma, L = dmap; N_3 = bpma, L = dmap, 4-pic or 9-EtGua).

The substitution reactions of the $[MCl(N_3)]^{n+}$ complexes with L = *N*-heterocycles were investigated to prepare formally substitution-inert complexes of the type $[Au(N_3)L]^{3+}$ and $[Pt(N_3)L]^{2+}$ for model studies for recognition and fixation on the zinc finger. The novel anticipated platinum(II) species $[Pt(Mebpma)(dmap)]Cl_2$ (**PtL^{1}a**) $[Pt(bpma)(dmap)]Cl_2$ (**PtL^{2}a**), $[Pt(bpma)(4\text{-pic})]Cl_2$ (**PtL^{2}b**) and $[Pt(bpma)(9\text{-EtGua})]Cl_2$ (**PtL^{2}c**) were obtained in good yields from the reactions with the respective *N*-heterocycles in H_2O, without the necessity for activation of the respective precursors **PtL^1** and **PtL^2** with $AgNO_3$, (Scheme 2.1). The reaction of **PtL^2** with 9-EtGua and Guanosien (Guo) has been previously investigated by ^{1}H NMR spectroscopy in aqueous solution but the products were not isolated.[27]

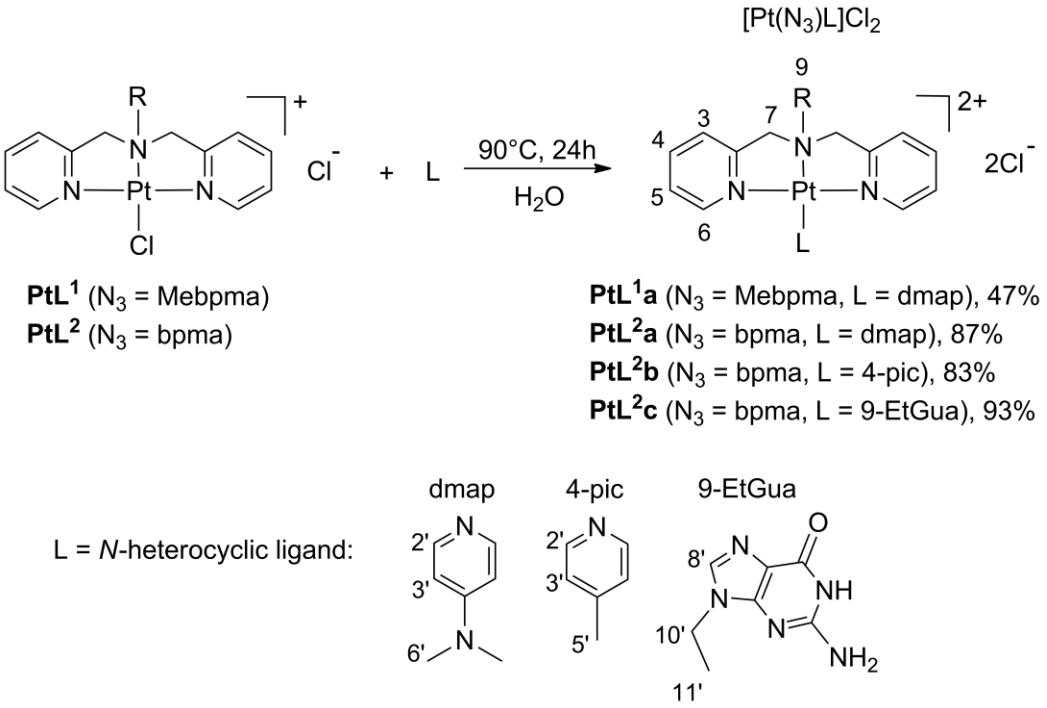

Scheme 2.1. Synthetic route and numbering for the $[Pt(N_3)L]Cl_2$ compounds.

The ^{1}H NMR spectrum of the 9-EtGua-containing complex **PtL^{2}c** (Table 2.2 and Figure 2.5) evidences the presence of *anti* and *syn* rotamers related to two different spatial orientations of the NH group which interconvert by rotation about the Pt–NH bond.[27] In the ^{1}H NMR spectra of the dmap (**PtL^{1}a** and **PtL^{2}a**) and 4-pic-containing complexes (**PtL^{2}b**) the H2' and H3' hydrogen signals of the substituted pyridines appear as broad singlets: at δ 8.92 (H2') and 7.67 (H3') for **PtL^{2}b** and at around δ 8.40 (H2') and 6.85 (H3') for the $[Pt(N_3)(dmap)]^{2+}$ compounds **PtL^{1}a** and **PtL^{2}a** (Table 2.2). This is due to restricted rotation of the coordinated *N*-heterocycle, where different ligand conformations contribute to broaden the signals. The H2' and H3' signals become narrower, more intense and slightly deshielded upon increasing the temperature to 60ºC (Figure 2.6). After cooling to 20°C (starting temperature), the NMR spectra exhibited the same profile as before heating. These results are consistent with the refined crystal structure of the $[Pt(bpma)(py)]^{2+}$ cation where the pyridine ring is almost perpendicular to the PtN_3(bpma) plane,

with the capacity for steric hindrance – indeed broad signals of the pyridine protons were also reported for the similar $[Pt(bpma)(4\text{-pic})]^{2+}$ cation.[26]

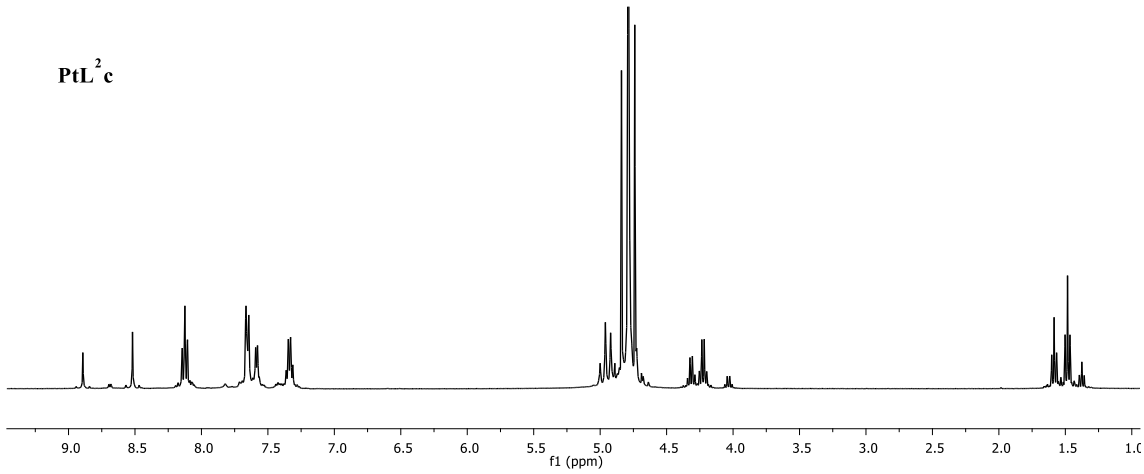

Figure 2.5. ^{1}H NMR spectrum of **PtL^{2}c**.

The ^{195}Pt NMR spectra of all complexes show the signals expected for the $[PtCl(N_3)]^{+}$ and $[Pt(N_3)L]^{2+}$ platinum(II) coordination spheres.[35,36] For the chloride species signals are seen at δ -2331.9 ppm (**PtL^{1}**) and δ -2301.8 ppm (**PtL^{2}**) (See Table 1). Substitution of Pt-Cl by the N-donor results in expected chemical shifts to δ -2413.1 (**PtL^{1}a**), δ -2401.5 (**PtL^{2}a**) and δ -2405.5 (**PtL^{2}b**) while the spectrum of **PtL^{2}c** exhibits two signals at δ -2362.7 and δ -2379.1 ppm in accordance with the presence of *syn* and *anti* rotamers (Table 2.2).[27]

NMR Shifts (ppm), Multiplicity and Coupling Constants (Hz)										
Compound	^{195}Pt NMR	N_3 hydrogens (Mebpma and bpma)						L hydrogens		
		H3	H4	H5	H6	H7	H9	H2’	H3’	H6’ (H5’ for 4-pic)
PtL^{1}a	-2413.1	7.73 (m)	8.18 (td, 8.0, 4.0)	7.43 (t, 8.0)	7.73 (m)	4.66 (d, 16.0) 5,17 (d,16.0)	3.06 (s)	8.38 (br s)	6.84 (br s)	3,15 (s)
PtL^{2}a	-2401.5	7.67 (m)	8.13 (td, 8.0, 4.0)	7.37 (t, 8.0)	7,67 (m)	overlapped	-	8.46 (br s)	6.85 (br s)	3,15 (s)
PtL^{2}b	-2405.5	7.67 (d, 8.0)	8.15 (td, 8.0, 4.0)	7.35 (t, 8.0)	7.56 (d, 4.0)	overlapped	-	8.92 (br s)	7.67 (br s)	2.58 (s)
PtL^{2}c	-2362.7; -2379.0	7.57-7.66 (m)	8.12 (t, 8.0)	7.33 (q, 8.0)	7.57-7.66 (m)	4.95 (m)	-	H8’ 8.51(syn) (s) 8.88 (anti) (s)	H10’ 4.22 (syn) (q, 8.0) 4.31 (anti) (q, 8.0)	H11’ 1.48 (syn) (t, 8.0) 1.58 (anti) (t, 8.0)

Table 2.2. ^{195}Pt and ^{1}H NMR sifts for the $[PtN_3L]^{2+}$ complexes.

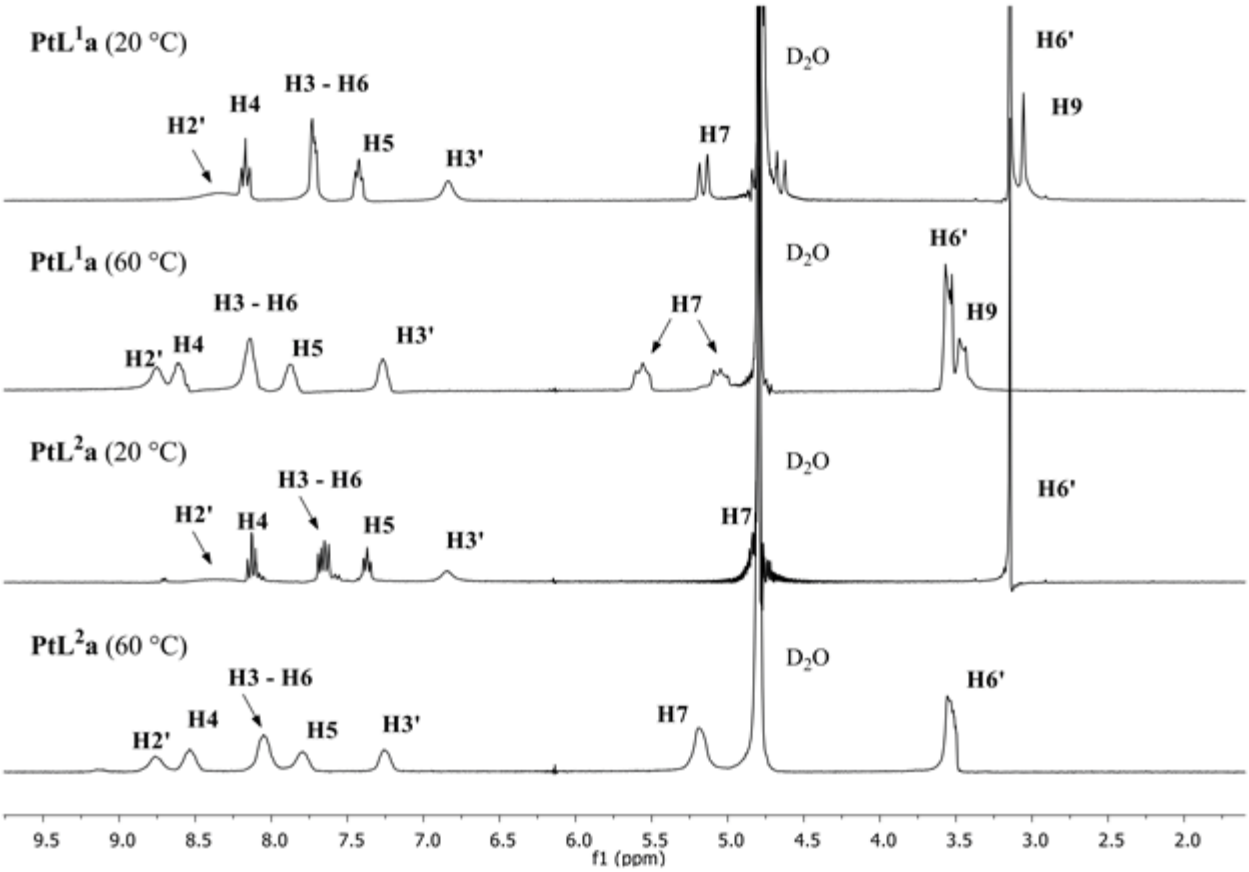

Figure 2.6. ^{1}H NMR (300 MHz) spectra of **PtL^{1}a** and **PtL^{2}a** at 20 and 60°C.

Attempted Synthesis of [Au(N$_3$)L]$^{3+}$ N-heterocycle-complexes.

The analogous [Au(N$_3$)L]$^{3+}$ complexes could not be isolated as stable solids from the reactions of **AuL^{1}** and **AuL^{2}** with the same *N*-heterocycles in DMF as solvent and the black products suggested decomposition. The reactions of **AuL^{1}** and **AuL^{2}** with dmap and 9-EtGua, respectively, were therefore monitored by ^{1}H NMR spectroscopy, in dmf-*d*^{7} solution at room temperature, to probe the formation of the desired products. While chemical shifts indicative of Au-9-EtGua and Au-dmap binding were observed, multiple peaks corresponding to likely decomposition or dissociation of the chelate rings were observed over time. The purine and substituted pyridine ligands do remain bound even in evidence of chelate ring dissociation - the strength of the Au-N(dmap) bond has been noted previously.[31]

Reactivity with Biomolecules.

The structure of the HIV NCp7 peptide is shown in Scheme 2.2. In general, two aspects are important – the recognition interaction with tryptophan and the reactivity of the [MCl(N_3)] and [M(N_3)L] species toward cysteine attack. In both cases, we have used extensively the C-terminal finger (red box) as it contains the essential tryptophan residue and is a good prognosticator of the interaction with the full 2-finger peptide. We also compared reactivity toward the simple amino-acid *N*-AcetylCysteine (*N*-AcCys).

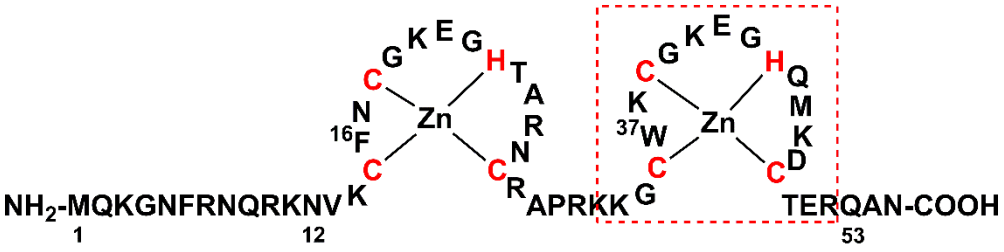

Scheme 2.2. Structure of the HIV NCp7 peptide.

Pt(N_3)L ***π-π*** *stacking interaction - Tryptophan Quenching Assay.*

In earlier studies we have shown that Pt^{2+} and Au^{3+}-dmap containing complexes exhibit good affinity for *N*-AcTrp and the NCp7 ZF2 peptide.[18,19] For the diethylenetriamine (dien) derivatives, $[Au(dien)(dmap)]^{3+}$ and $[Pt(dien)(dmap)]^{2+}$ the K_a values are about 3.6 times larger than those for the 9-EtGua-containing analogue $[Pt(dien)(9\text{-EtGua})]^{2+}$ and almost 8 times larger than the K_a for the free dmap ligand itself. The K_a values for the $[Pt(N_3)L]^{2+}$ complexes described in this study are consistent with previous trends and confirm that the dmap containing compounds (**PtL^1a** and **PtL^2a**) are good tryptophan quenchers (Table 2.3). The K_a values for these complexes are 2 to 3 times larger than those for complexes containing the *N*-heterocycles 4-pic (**PtL^2b**) or 9-EtGua (**PtL^2c**). Tryptophan affinity for **PtL^1a** containing the Mebpma tridentate ligand is somewhat greater than for the bpma containing analogue **PtL^2a** and for the earlier reported Pt(II) and Au(III)-

dien complexes, with the exception of [Au(N-Medien)(dmap)]$^{3+}$.[18,19] Coordination to the platinum(II) ion increases about 10 times the association constant when compared with the results for the free dmap ligands increasing in the following order [Pt(dien)(dmap)]$^{2+}$< **PtL^{2}a** < **PtL^{1}a**. Tryptophan quenching in the zinc finger ZF2 also follows this trend and the complex **PtL^{1}a** represents a significant increase over the first-published [Pt(dien)(9-EtGua)]$^{2+}$.[14] For **PtL^{1}a**, the value for interaction with the full NCp7 (residues 1-55) is slightly higher again, K_a = (40.6 ± 1.0) x 10^3 M^{-1}, validating the use of the C-terminal ZF2 as a general indicator of quenching efficacy. The electronic delocalization of the dmap π electrons and ligand basicity may be responsible for its advantage over 9-EtGua, modifying the HOMO-LUMO gap which has been considered a major predictor of stacking affinity.[17]

Compound	**K_a (x10^3) M^{-1}**	
	***N*-AcTrp**	**ZF2**
PtL^{1}a	32.8 ± 2.0	33.1 ± 3.7 (40.6 ± 1.0)*
PtL^{2}a	28.3 ± 3.4	30.7 ± 4.6
PtL^{2}b	13.4 ± 2.6	17.4 ± 4.7
PtL^{2}c	11.7 ± 0.7	15.9 ± 1.5
[Pt(dien)(dmap)]$^{2+}$	25.0 ± 0.9[a]	28.1 ± 1.8[a]
[Au(dien)(dmap)]$^{3+}$	25.5 ± 0.3[a]	-
[Pt(dien)(9-EtGua)]$^{2+}$	6.88 ± 0.3[a]	7.5[a]
dmap	3.19 ± 0.01[b]	-

References: a[18] and b[15]. *Values in parentheses were obtained with the full NCp7.

Table 2.3. Association constants for N-heterocycle compounds with the *N*-AcTrp and NCp7

Studies of the reactivity of platinum(II) complexes with N-acetylcysteine.

The covalent interaction with zinc fingers is considered to occur through electrophilic attack on the ZF cysteine residues. To examine the reactivity pattern, the reactions of the precursors **PtL^1** and **PtL^2** and of [Pt(N_3)L]Cl_2 (**PtL^{1}a**, **PtL^{2}a** and **PtL^{2}c**) with 4 molar equiv. of *N*-AcCys in D_2O were first monitored by ^{1}H and ^{195}Pt NMR spectroscopy. The reactions of the substitution-labile precursors **PtL^1** and **PtL^2** were complete after 2 h, as shown by the appearance of a new signal in the ^{195}Pt NMR spectra of both reactions. The signal due to starting material **PtL^1**, at δ -2331.9, was replaced by a signal at δ -2903.2, assigned to the reaction product [Pt(Mebpma)Cys]$^{2+}$, whereas the signal due to **PtL^2**, at δ -2301.8, was replaced by that at δ -2848.3, also in agreement with a square planar N_3S coordination sphere, and therefore formation of [Pt(bpma)Cys]$^{2+}$.[35,36] The ^{195}Pt NMR spectra of both the **PtL^1** and **PtL^2** reaction mixtures after 24 h show that the intensity of the signal assigned to the PtN_3S complex has significantly decreased with the rise of broader peaks in the same region suggesting that decomposition or further reaction in the presence of excess *N*-AcCys had taken place. To examine this point further the time course of the reactions were followed by ^{1}H NMR spectroscopy.

The ^{1}H NMR spectra of the two [PtCl(N_3)]Cl compounds **PtL^1** and **PtL^2** show the same profile. The spectral interpretation is complicated somewhat by the presence of excess *N*-AcCys but the aromatic region is informative. The ^{1}H NMR spectra of **PtL^1** and **PtL^2** in the aromatic region in the presence of *N*-AcCys over 2, 6 and 24 h are presented in Figure 2.7. For **PtL^1** at 2 h, the spectrum of the reaction mixture shows signals of coordinated Mebpma, which are shifted to higher frequencies, δ 7.56 (t, 2H, H5), 7.66 (d, 2H, H3), 8.15 (t, 2H, H4), 9.11 (d, 2H, H6) in comparison with those in both the free and coordinated Mebpma thus suggesting formation of the product [Pt(Mebpma)Cys]$^+$. The characteristic "pair" of doublets of the H7 protons is obscured

somewhat by solvent but the downfield doublet diminishes in intensity and appears as a virtual triplet (Figure 2.8). Over time a new set of signals arises with concomitant decrease of the initial product peaks. The bulkier S-thiolate ligand could cause steric hindrance and the multiple signals arising over time, along with the broadening of the PtNMR signals, could arise from the presence of mixtures or isomers of $[PtN_3(Cys)]^+$. The related compound [PtCl(di-6-methyl-2-picolyl)amine]$^+$ (with a Me group in the C6 position of the N_3 ligand , See Scheme 1) undergoes relatively facile chelate ring opening in the presence of excess 9-EtGua to produce bisubstituted bis(9-EtGua) products.[37] Similar ring opening could be expected under the strong *trans* influence of the thiolate ligand. The final product signals and an accompanying singlet at δ 4.31 are most compatible with assignment to free ligand – the shifts are slightly different due to protonation in the more acidic environment created by excess of *N*-AcCys (data not shown). The reaction of **PtL^2** occurs more quickly than for the Mebpma derivative. After 24 h the spectrum of the non-methylated complex **PtL^2** reaction mixture presents signals assigned to only one aromatic species and also attributed to free ligand (Figure 2.7).

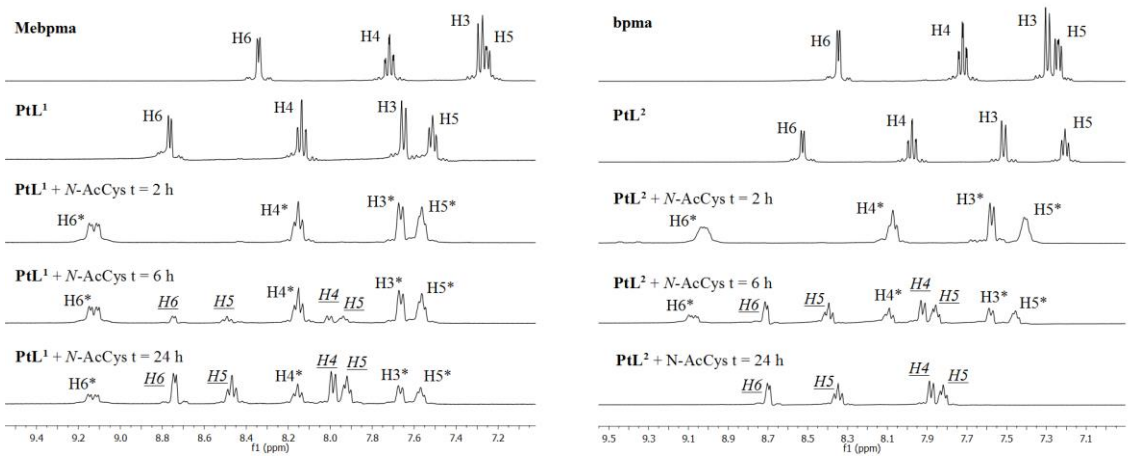

Figure 2.7. ^{1}H NMR (400 MHz) spectra in the aromatic region for reactivity assay of **PtL^1** and **PtL^2** with *N*-AcCys. Hydrogens marked with a * are assigned to $[Pt(N_3)(N\text{-AcCys})]^+$ complex, and underscores assigned to the protonated free ligand.

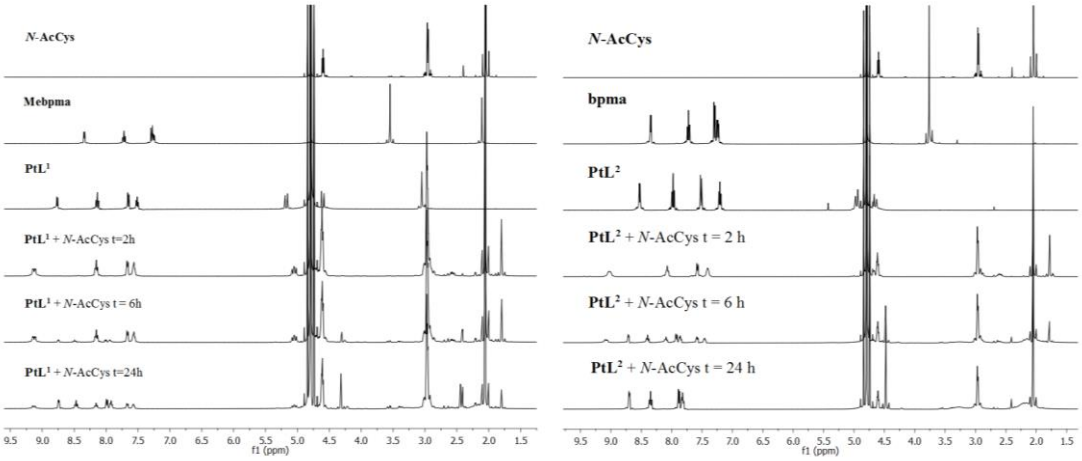

Figure 2.8. Complete ^{1}H NMR spectra: reactivity assay of PtL^{1} and PtL^{2} with *N*-AcCys.

Mass Spectrometry.

The ESI-MS spectra of 1:1 reactions are clean and consistent with the interpretation of the initial NMR spectra. For **PtL^{1}** immediately upon incubation with one equivalent of *N*-AcCys (t = 0) the MS showed the major species of starting material (Figure 2.9B) whereas after 24 h this gives way to a peak at m/z = 570.11 consistent with $[Pt(Mebpma)(N\text{-AcCys})]^{+}$ (Figure 2.9D). The spectrum of **PtL^{2}** immediately upon incubation (Figure 2.9A) shows the presence of starting material and also product $[Pt(bpma)(N\text{-AcCys})]^{+}$ with a very minor peak at m/z = 948.15 indicative of the μ-cysteine dimer $[\{Pt(bpma)_2\}\mu\text{-}N\text{-AcCys}]^{+}$ (not shown). Thus, the MS data confirm the greater reactivity of **PtL^{2}** over **PtL^{1}**, as seen by NMR spectroscopy. After 24 h the dominant peak is that of the mononuclear product (Figure 2.9C). An interesting feature at t = 24 h is the presence of $[\{Pt(bpma)_2\}\mu\text{-}N\text{-AcCys}]^{+}$ and a species at m/z = 1111.18 which corresponds to $[Pt(bpma)(N\text{-AcCys})]_2$ (Figure 2.10). Isotopic distribution patterns of products were consistent with these assignments in all spectra.

The reactions of cysteine and glutathione (GSH) with Pt chelate complexes is usually discussed in relation to the *trans*-labilization induced upon formation of the Pt-SR(thiolate) bond and also the propensity to form bridged diplatinum μ-thiolate(SR) species.[38,39] In the case of cisplatin, binding of biologically relevant thiols such as cysteine and glutathione can result in rapid dissociation of the Pt-NH_3 bond.[36,40] In the case of $[PtCl(dien)]^+$, dissociation of the dien ligand eventually occurs over long periods of time upon reaction with both cysteine and glutathione.[39] The results discussed here suggest that the bpma and Mebpma ligands are more susceptible to ligand dissociation and *trans* labilization than the 'aliphatic" dien ligand. The dinuclear $[\{Pt(dien)\}_2\mu\text{-}GS]^{3+}$ species has been observed in a rapid reaction of $[Pt(dien)(GS)]^+$ with a second $[PtCl(dien)]^+$ unit.[38] However, the peak assignable to formation of the μ-Cys dinuclear species for **PtL^1** is of very minor intensity, suggesting that the increased "in-plane" steric demands of the bpma and Mebpma ligands[27] do not favor the approach of a second Pt unit to the first formed $[Pt(bpma/Mebpma)(N\text{-AcCys})]^+$ species.

Gold Complexes.

The reactions of **AuL^1** and **AuL^2** with *N*-AcCys immediately produce white precipitates (data not shown). This behavior is identical to that observed for $[AuCl(dien)]^{2+}$ and also $[Au(dien)(dmap)]^{3+}$.[31] The thiol-containing amino acid L-cysteine quickly reduces Au^{3+} in aqueous solution, the reaction being complete in the first minute.[22,41,42] The initial rapid substitution reaction results in an unstable Au(III)-S complex that is reduced to Au^{1+}/Au^0 in a slower electron-transfer process.[22,41]

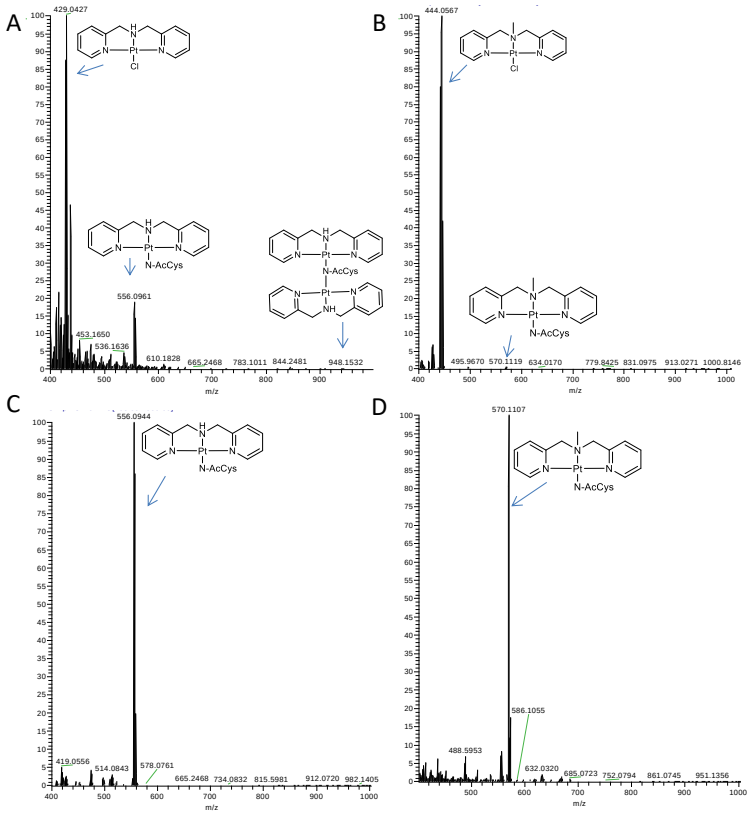

Figure 2.9. MS spectra of 1:1 reaction between *N*-AcCys and (A) **PtL^2** immediately; (B) **PtL^1** immediately; (C) **PtL^2** after 24 h; (D) **PtL^1** after 24 h.

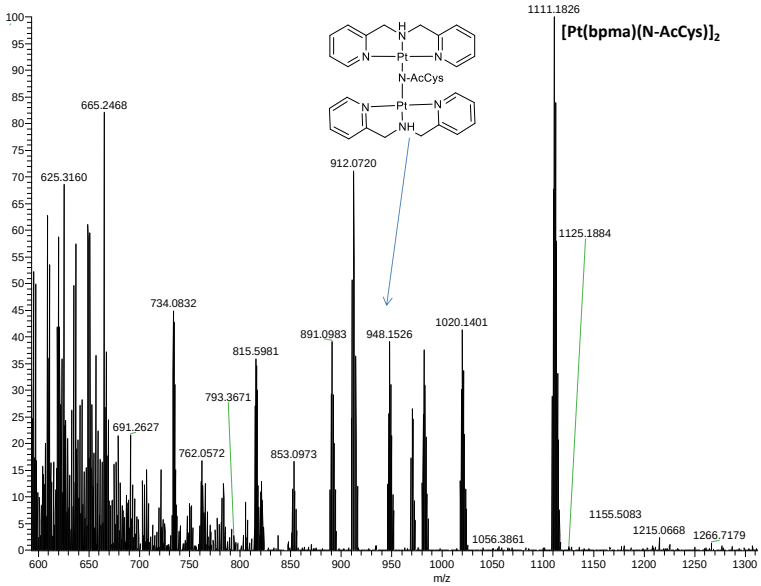

Figure 2.10. Expanded MS spectrum of 1:1 reaction between N-AcCys and [PtCl(bpma)]Cl (**PtL^2**) after 24 h.

Formally substitution-inert $[Pt(N_3)L]^{2+}$ complexes.

In contrast with the results discussed above for the substitution-labile $[PtCl(N_3)]^+$ complexes **PtL^1** and **PtL^2**, the ^{1}H and ^{195}Pt NMR spectra obtained after mixing the $[Pt(N_3)L]Cl_2$ (**PtL^{1}a**, **PtL^{2}a** and **PtL^{2}c**) compounds with *N*-AcCys in 1:1 stoichiometric ratios do not show any change, even after 72 h of incubation (Figure 2.11). When 1:4 {Pt:*N*-AcCys} stoichiometry is used in the reaction of **PtL^{1}a**, peaks of very low intensity appear after 24-72 h at δ = -2850-2900 ppm indicating some formation of PtN_3S species. These results confirm the inertness of the $[Pt(N_3)L]Cl_2$ compounds in the presence of the sulfur-containing amino acid *N*-AcCys. In principle, the advantage of a substitution-inert system, such as $[Pt(N_3)L]^{2+}$ complexes in general, as an *in vivo* NCp7 inhibitors, is that they would not be easily "deactivated" by other sulfur-containing biomolecules. In this context, efforts towards tuning these complexes is essential, so as to favor reactions with strong nucleophiles, such as ZF cysteine residue thiol groups, as suggested previously.[19]

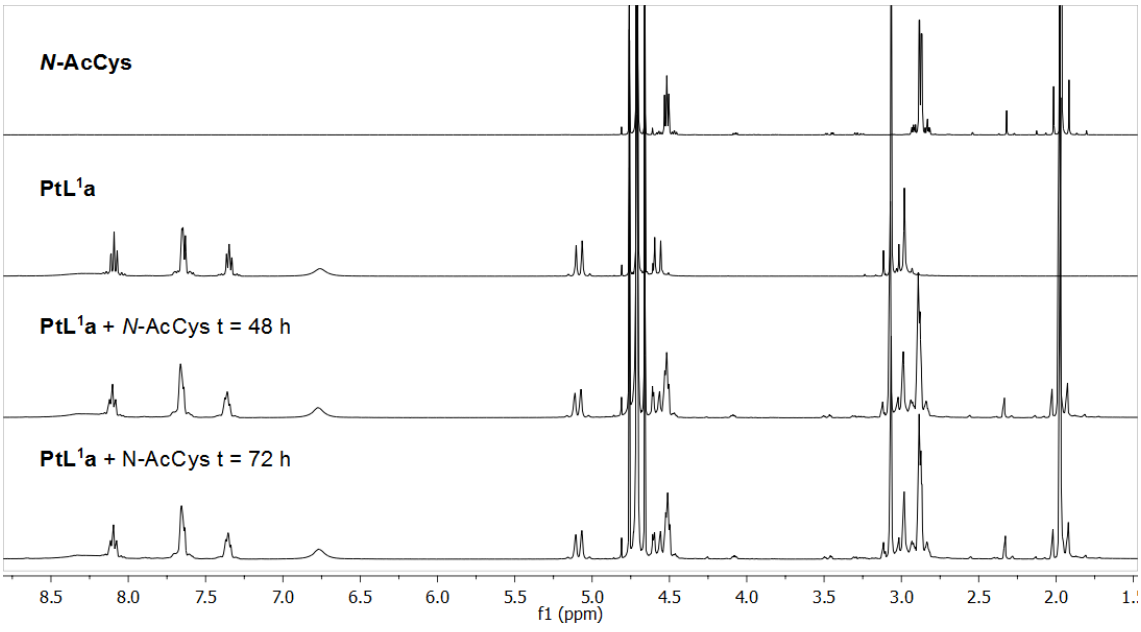

Figure 2.11. ^{1}H NMR spectra: reactivity assay of **PtL^{1}a** with *N*-AcCys.

Studies of the reactivity of complexes PtL[1], AuL[1] and PtL[1]a with the C-terminal finger of HIV NCp7, ZF2.

The interactions between the $[MCl(N_3)]^{n+}$ (**PtL^1** and **AuL^1**) and $[Pt(N_3)L]^{2+}$ (**PtL^{1}a**) complexes with the C-terminal finger of the HIC NCp7 peptide (ZF2) have been monitored by mass spectrometry. Immediate interaction between **PtL^1** and ZF2 results in complete loss of the Zn^{2+} ion and Mebpma ligand (Figure 2.12A). The mass spectrum shows an intense peak at m/z of 371.50 assigned to the apoprotein $[apoF]^{6+}$ and minor peaks at m/z of 445.40 $[apoF]^{5+}$ and 556.49 $[apoF]^{4+}$. The peak at m/z of 484.39 corresponding to $[PtF]^{5+}$ proves that **PtL^1** was able to eject the Zn^{2+} ion of the ZF2 domain, forming a 1:1 [Pt:F] adduct. To our knowledge this is the first observation of the "simple" {PtF} species. After 24 h the spectra show adducts corresponding to species with multiple Pt units $[(PtL)\text{-}PtF]^{n+}$ perhaps from gas-phase interaction of **PtL^1** with the initially pre-formed PtF (Figure 2.12B). The results contrast to those previously shown for $[PtCl(dien)]^+$ where the dien ligand is retained in the initial stages of the reaction producing species such as Pt(dien)-ZF or Pt(dien)-F and no {PtF} species was observed.[14,42] In contrast, the MS spectrum obtained after incubation with [PtCl(dien)]Cl for 15 h (Figure 2.13), still shows the presence of unoxidized ZF as the major product, at m/z of 762.31 (ZF^{3+}) and 1144.46 (ZF^{2+}), and only a small peak corresponding to Pt(dien)-ZF^{3+} is observed at m/z of 862.33, which is very similar to previous MS results for this complex.[43] The results overall are broadly consistent with the model NAcCys case discussed above. The greater reactivity of the Mebpma complex could be related to its electron-withdrawing properties, due to the π-back bonding of the pyridine nitrogens, responsible for its lesser basicity compared with dien.[27] The same trend was observed previously for the $[MCl(dien)]^{n+}$ and $[MCl(terpy)]^{n+}$ complexes.[43]

Indeed, the behavior of {Pt(Mebpma)} species with total loss of ligand in the initial reaction is more reminiscent of the general Au(III) behavior we observed here and previously.[31,43] The MS spectra of the **AuL^1** and ZF2 mixture indicate immediate reaction with peptide oxidation and ejection of the Zn^{2+} ion (Figure 2.12C). As seen before for other gold(III) complexes,[31,43] Zn^{2+} ejection and Au_xF^{n+} formation occurs immediately, with peaks assigned to $[Au_2F]^{5+}$ (m/z = 523.78), $[AuF]^{4+}$ (m/z = 604.98), $[Au_2F]^{4+}$ (m/z = 654.48), $[AuF]^{3+}$ (m/z = 806.64), $[Au_2F]^{3+}$ (m/z = 872.30) and $[Au_4F]^{3+}$ (m/z = 1003.61). Peaks corresponding to the oxidized apoprotein are also seen at m/z of 445.00 [apoF^{5+}], 555.99 [apoF^{4+}] and 741.33 [apoF^{3+}]. Careful examination of the spectra show low intensity companion peaks of, for example, the apoF^{4+} species corresponding to the presence of an extra 1, 2, or 3 oxygen atoms suggesting higher-order oxidized sulfur species (Figure 2.14). The rapid reaction of **AuL^1** (and also $[AuCl(dien)]^{2+}$) to form "gold fingers" is in accordance with the greater reactivity of gold(III) compared with platinum(II) complexes.

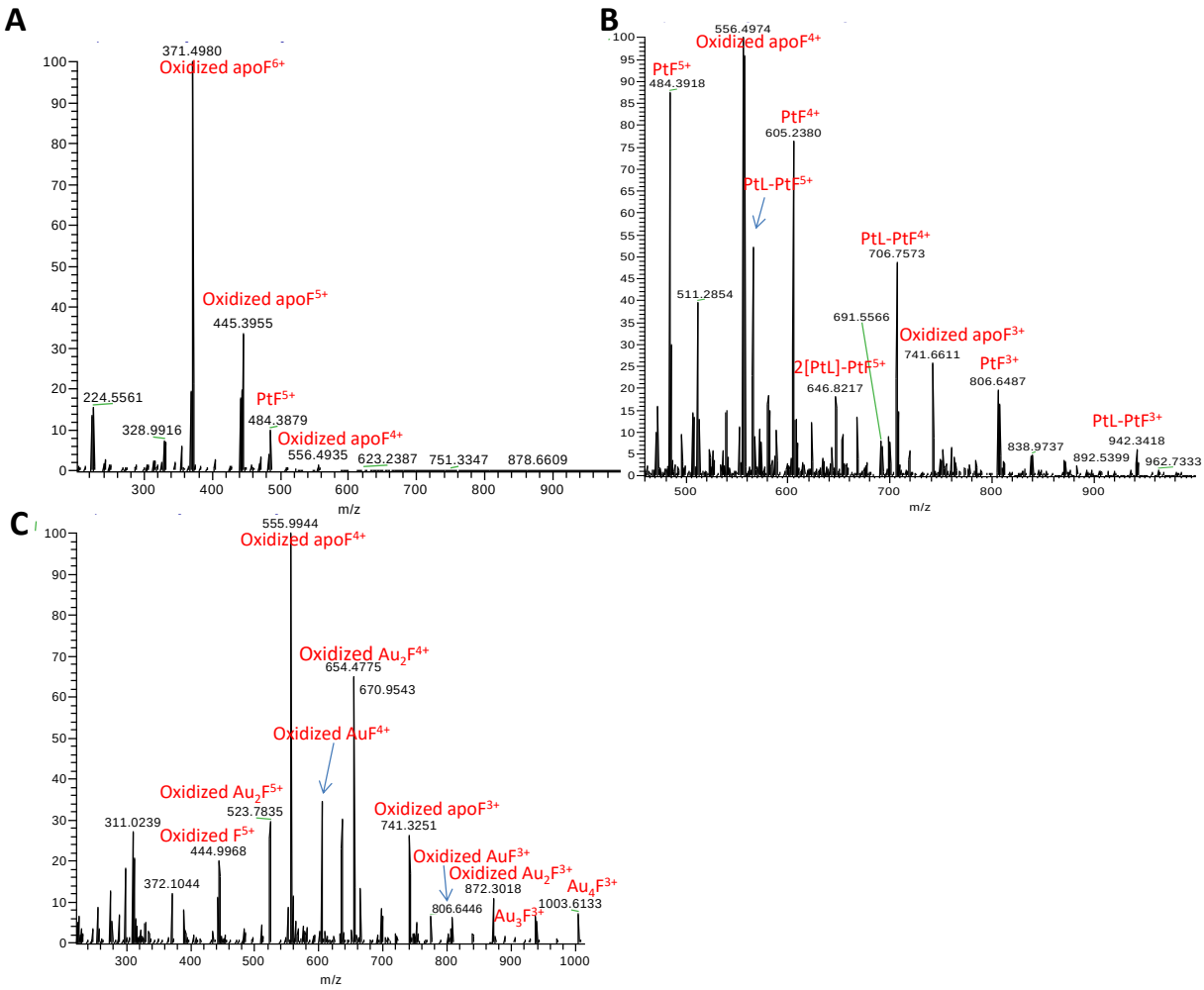

Figure 2.12. MS spectra of 1:1 reaction between NCp7 ZF2 of (A) **PtL^1** immediately; (B) **PtL^1** after 24 h; (C) **AuL^1** immediately.

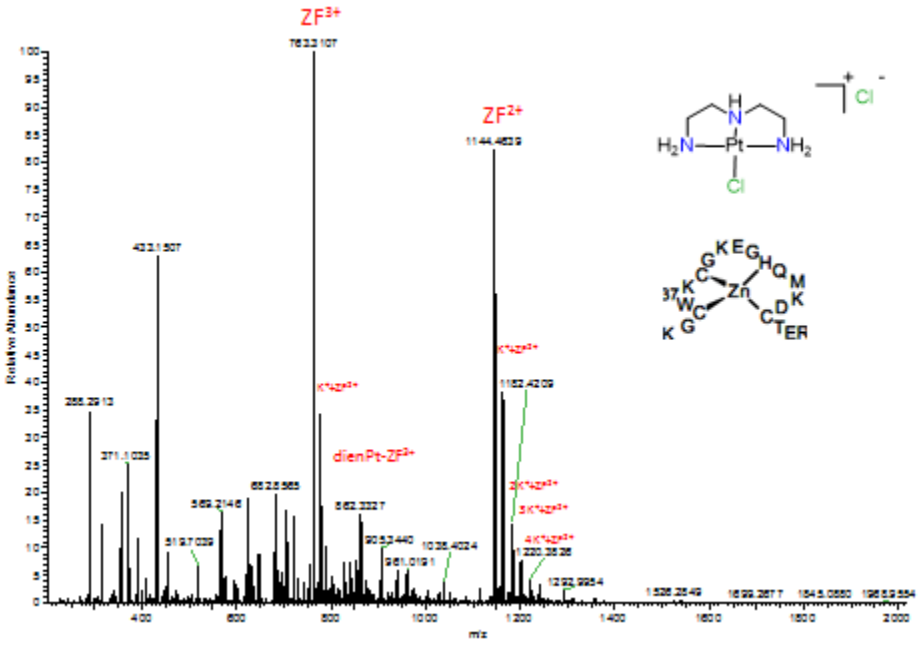

Figure 2.13. MS spectrum of the 1:1 mixture of [PtCl(dien)]Cl with ZF2 after 15h.

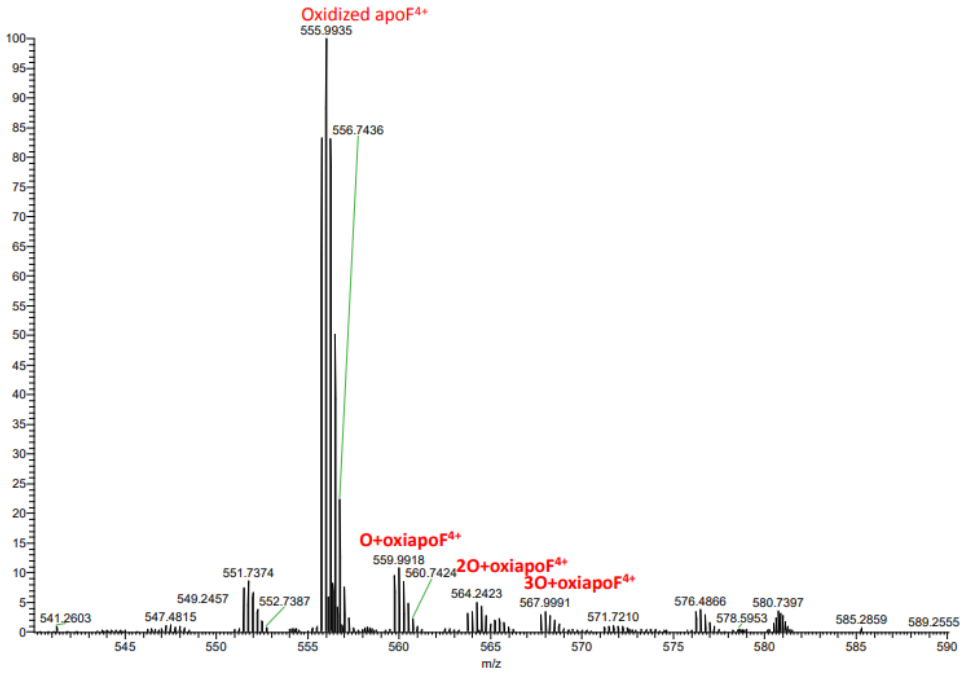

Figure 2.14. Expanded version of ESI-MS spectrum of the product of $[Au(Mebpma)Cl]^{2+}$ and C-terminal ZF2 showing the $apoF^{4+}$ ion and the presence of associated oxidized -SO, $-SO_2$ and $-SO_3$ adducts of the apopeptide.

Substitution-inert $[Pt(N_3)L]^{2+}$ Complexes.

For the incubation of the dmap-containing complex **PtL^{1}a** with ZF2, which contains a fourth nitrogen coordinated to the metallic ion, the mass spectrum (Figure 2.15) confirms the non-covalent interaction, as can be observed by the weak peaks assigned to the 1:1 adduct (**PtL^{1}a**:ZF) at m/z of 939.70 (**PtL^{1}a** -ZF^{3+}) (not shown), 1408.04 (**PtL^{1}a** -ZF^{2+}) and 1427.53 (K+ **PtL^{1}a**-ZF^{2+}). It is noteworthy that even for a weak non-covalent interaction these peaks can be observed in the ESI-MS spectrum under the appropriate conditions. No change is observed over time.

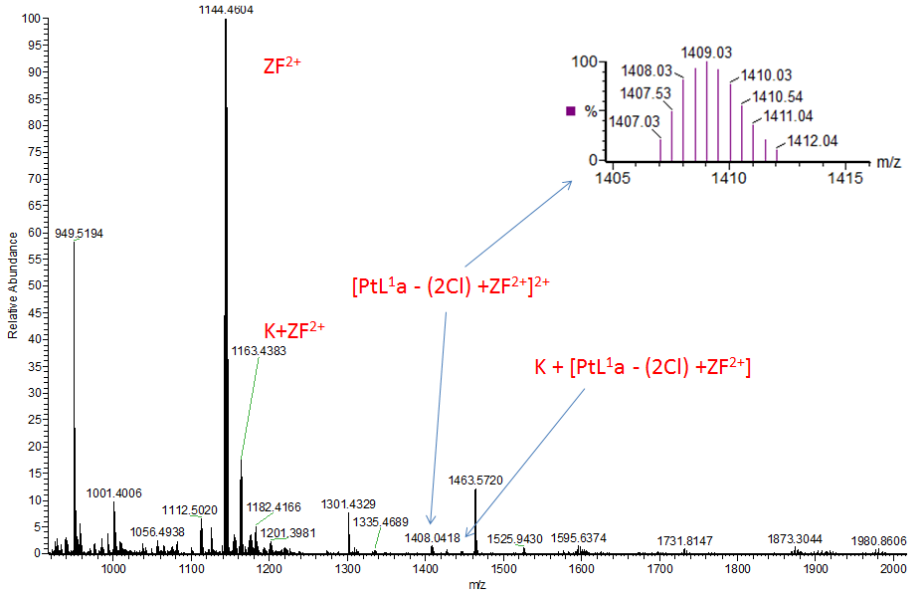

Figure 2.15. MS spectrum of the 1:1 mixture of [**PtL^{1}a]Cl$_2$** with the C-terminal zinc finger of HIV NCp7. The expansion of noncovalent adduct peak and the theoretical m/z are shown in the right.

2.4 Conclusions

The reactions of {MClN$_3$} species [PtCl(Mebpma)]Cl (**PtL^1**) and [AuCl(Mebpma)](PF$_6$)$_2$ (**AuL^1**) complexes and the analogous bpma complexes (**PtL^2** and **AuL^2**) with *N*-AcCys and NCp7 ZF2 have been investigated. Comparison of the ^{1}H NMR data suggest appreciable withdrawal of electron density from the N$_3$ ligand, which is more pronounced in the gold(III) complexes than in

the platinum(II) analogues, and explains the facile deprotonation of **AuL^2** and the relative instability of both gold(III) complexes, also associated with the ease of Au^{3+} reduction in both cases.[25] Indeed, only the platinum(II) *N*-heterocyclic compounds of the type $[Pt(N_3)L]Cl_2$ could be isolated in their pure form from the reactions of the precursors **PtL^1** and **PtL^2** with 4-dimethylaminopyridine (dmap), 9-ethylguanine (9-EtGua) and 4-methylpyridine (4-pic). Formation of the analogous $[Au(N_3)L]^{3+}$ complexes occurs in solution and can be monitored by ^{1}H NMR Spectroscopy but no stable solid products were isolated.

As shown by the reactivity assay, the $[Pt(N_3)L]^{2+}$ complexes are inert and react only very slowly with excess *N*-AcCys. In contrast, the $[PtCl(N_3)]^+$ complexes **PtL^1** and **PtL^2** react with *N*-AcCys almost immediately to yield substitution products $[Pt(N_3)Cys]^{2+}$, which seem to undergo decomposition with release of the chelate ligand after 24 h. The decomposition of the bpma containing species is faster than that for Mebpma. These results are consistent with the ESI-MS spectrometry results with the zinc finger which shows adducts M:F (apopeptide) adducts for **PtL^1** similar to that found for **AuL^1**. For both complexes the reactions with ZF2 occur with Zn^{2+} ejection, which is not seen for the $[PtCl(dien)]^+$ analogue. The reaction with **AuL^1** occurs quickly, as seen before for other gold(III) complexes, resulting in "gold fingers" and oxidized apoF peptide. These results suggest a greater deactivation/inhibition action of the NCp7 ZF2 by the Mebpma-containing complexes, especially for **AuL^1**.

Interaction of the inert $[Pt(N_3)L]^{2+}$ complexes with Trp was investigated and the results show that the presence of the dmap ligand results in complexes with considerable affinity for the amino acid. Furthermore, **PtL^{1}a** is one of the best Trp fluorescence quenchers among the complexes reported herein and previously studied platinum(II) and gold(III) analogues both for the free amino-acid and the NCp7 peptide sequence. The association constant determined with the full

NCp7 peptide is significantly higher than that found for $[Pt(dien)(9\text{-}EtGua)]^{2+}$ ($K_a = 20 \times 10^{-3}\ M^{-1}$) and comparable to values found for organic inhibitors of the HIVNCp7-RNA interaction.[44] The association constant with the C-terminal finger is sufficiently strong that formation of the non-covalent **PtL^{1}a**:ZF2 adduct may be confirmed by ESI-MS without Zn^{2+} ejection. In summary, it was possible to improve the non-covalent π-π stacking interaction of $[Pt(N_3)L]^{2+}$ complexes with Trp by tuning the ligands coordinated to the platinum(II) ion, with the potential for selective interaction with the HIV-NCp7 protein.

The results are overall consistent with a greater reactivity of bpma over dien chelate. The relative displacement of Cl^- from $[PtClN_3]^+$ (where N_3 = terpyridine, bpma and dien) by isosteric pyridine nucleophiles has been discussed in terms of the reactivity and discrimination ability of the $\{PtN_3\}$ reaction centre.[26] The reactivity is linearly related to the basicity of the isosteric entering nucleophiles and the ability of the substrates to discriminate among neutral nucleophiles of different basicity was considered a measure of their relative electrophilicity terpy > bpma > dien. Broadly, the results presented here and comparison with the previously studied $[PtCl(terpy)]^+$,[42] extrapolate these findings to biologically relevant thiols and thiol-containing peptides. Indeed, bpma represents an intermediate case between terpy and dien. In this respect is noteworthy that a peak at 311.0 m/z in the spectrum of **AuL^1** and the ZF2 may represent {Zn(Mebpma)Cl}(Figure 2.12) with chelate transfer as observed previously with the terpy analog.[43] Both the electronic structure and steric demands in going from sp^2 planar (terpy) to sp^2/sp^3 (bpma) to all sp^3 (dien) nitrogens may contribute to the kinetic differentiation as suggested.[25] Once again, these results indicate that it is possible to design new candidates to interact more selectively with biomolecules. The inertia of the $[Pt(N_3)L]^{2+}$ complexes could be useful in the search for more selective NCp7 inhibitors, once those complexes can react favorably

with strong nucleophilic amino acids residues as ZF Cys residues, avoiding "deactivation" reactions with other biomolecules (sulfur-containing Cys residues). The syntheses of novel complexes containing different *N*-donor ligands that are able to form relatively stable complexes with NCp7 or that lead to Zn^{2+} ejection are also under further investigation.

2.5 Experimental Section

Materials and methods.

[PtCl(dien)]Cl,[29] [AuCl(dien)]Cl_2,[30] [AuCl(bpma)]$(OTf)_2$,[25] and bis(2-pyridylmethyl)methylamine (Mebpma)[45] were synthesized according to the literature. All reagents used in this study were analytical grade and used without further purification. *N*-acetyltryptophan (*N*-AcTrp), *N*-acetylcysteine (*N*-AcCys), bis(2-pyridylmethyl)amine (bpma), 4-dimethylaminopyridine (dmap), 9-ethylguanine (9-EtGua) and 4-methylpyridine (4-pic), were purchased from Sigma Aldrich. Apo-peptides were purchased from GenScript Corporation and had the following sequences: NCp7 ZF2 (KGCWKCGKEGHQMKDCTER), and the full NCp7 (MQRGNFRNQRKNVKCFNCGKEGHTARNCRAPRKKGCWKCGKEGHQMKDCTERQAN). The zinc finger peptides were prepared according to our published procedures[14,43] and characterized by CD and mass spectrometry.

Synthesis.

[PtCl(Mebpma)]Cl (**PtL^1**)**.** cis-[$PtCl_2(DMSO)_2$] was stirred for 24 h in 20.0 mL of CH_2Cl_2 with 1.1 equiv. of Mebpma in the dark. The yellow solid was washed with CH_2Cl_2 and diethyl ether and dried in vacuo (60% yield). Anal. Calcd. (%) for $C_{13}H_{15}Cl_2N_3Pt(H_2O)_{1.5}$: C, 30.84; H, 3.58; N, 8.30. Found: C, 29.41; H, 3.13; N, 7.54. ^{1}H NMR (D_2O, 400 MHz): δ 3.05(s, 3H), 4.60 (d, *J* = 16.0 Hz, 2H), 5.17 (d, *J* = 12.0 Hz, 2H), 7,51 (t, *J* = 8.0 Hz, 2H), 7,65 (d, *J* = 8.0 Hz, 2H), 8.14 (t,

J = 8.0 and 4.0 Hz, 2H), 8.76 (d, *J* = 4.0 Hz, 2H). ^{195}Pt NMR (85.80 MHz, D_2O, δ/ppm): -2331.9. IR (KBr, selected peaks)/cm^{-1}: ν(PtCl) 377, ν(PtN) 441, 485.

[PtCl(bpma)]Cl (**PtL^2**). Synthesized as described for **PtL^1**, except for the use of 1.1 equiv. of bpma. The suspension was filtered and the light grey solid, washed with CH_2Cl_2 and diethyl ether and dried in vacuo (98% yield). Anal. Calcd. (%) for $C_{12}H_{13}Cl_2N_3Pt$: C, 30.98; H, 2.82; N, 9.03. Found: C, 30.77; H, 2.57; N, 8.79. ^{1}H NMR (D_2O, 400 MHz): δ 4.65 (d, *J* = 16.0 Hz, 2H), 4.96 (d, *J* = 16.0 Hz, 2H), 7.21 (t, *J* = 8.0 Hz, 2H), 7.52 (d, *J* = 8 Hz, 2H), 7.98 (td, *J* = 8.0 and 4.0 Hz, 2H), 8.53 (d, *J* = 4.0 Hz, 2H). ^{195}Pt NMR (85.80 MHz, D_2O, δ/ppm): -2301.8. IR (KBr, selected peaks)/cm^{-1}: ν(PtCl) 322, ν(PtN) 449, 491.

[Pt(Mebpma)(dmap)]Cl_2 (**PtL^{1}a**). **PtL^1** was stirred in the dark under reflux for 5 h in 15.0 mL of distilled water with 1 equiv. of dmap. The solution was stirred at room temperature for an additional 19 h. The solvent was evaporated to near dryness and 20.0 mL of acetone were added and the mixture, stirred for 30 min. The suspension was filtered and the brownish solid, washed with acetone and diethyl ether and dried in vacuo (47% yield). Anal. Calcd. (%) for $C_{20}H_{25}Cl_2N_5Pt(H_2O)_5$: C, 34.74; H, 5.10; N, 10.13. Found: 34.12; H, 4.84; N, 9.78. ^{1}H NMR (D_2O, 400 MHz): δ 3.06 (s, 3H), 3.15 (s, 6H), 4.66 (d, *J* = 16.0 Hz, 2H), 5.17 (d, *J* = 16.0 Hz, 2H), 6.84 (br s, 2H), 7.43 (t, *J* = 8.0 Hz, 2H), 7.73 (m, 4H), 8.18 (td, *J* = 8.0 and 4.0 Hz, 2H), 8.38 (br s, 2H). ^{195}Pt NMR (85.80 MHz, D_2O, δ/ppm): -2413.1. IR (KBr, selected peaks)/cm^{-1}: ν(PtN) 446, 489.

[Pt(bpma)(dmap)]Cl_2 (**PtL^{2}a**). Synthesized as described for **PtL^{1}a** starting with **PtL^2**, and obtained as a white solid (87% yield). Anal. Calcd. (%) for $C_{19}H_{23}Cl_2N_5Pt(H_2O)_5$: C, 33.68; H, 4.91; N, 10.34. Found: C, 32.82; H, 4.77; N, 9.88. ^{1}H NMR (D_2O, 400 MHz): δ 3.15 (s, 6H), overlapped (4H), 6.85 (br s, 2H), 7.37 (t, *J* = 8.0 Hz, 2H), 7.67 (m, 4H), 8.13 (td, *J* = 8.0 and 4.0

Hz, 2H), 8.46 (br s, 2H). ^{195}Pt NMR (85.80 MHz, D_2O, δ/ppm): -2401.5. IR (KBr, selected peaks)/cm–1: ν(PtN) 450, 496, 526.

[Pt(bpma)(4-pic)]Cl_2 (**PtL^{2}b**). Synthesized as described for **PtL^{2}a** except for the use of 1.15 equiv. of 4-pic, and obtained as a white solid (83% yield). Anal. Calcd. (%) for $C_{18}H_{20}Cl_2N_4Pt(H_2O)_{2.5}$: C, 35.83; H, 4.18; N, 9.29. Found: C, 34.38; H, 3.74; N, 8.88. ^{1}H NMR (D_2O, 400 MHz): δ 2.58 (s, 3H), overlapped (m, 4H), 7.35 (t, *J* = 8.0 Hz, 2H), 7.56 (d, *J* = 4.0 Hz, 2H), 7.67 (d, *J* = 8.0 Hz, 2H), 7.67 (br s, 2H), 8.15 (td, *J* = 8.0 and 4.0 Hz, 2H), 8.92 (br s, 2H). ^{195}Pt NMR (85.80 MHz, D_2O, δ/ppm): -2405.5. IR (KBr, selected peaks)/cm^{-1}: ν(PtN) 449, 494.

[Pt(bpma)(9-EtGua)]Cl_2 (**PtL^{2}c**). Synthesized as described for **PtL^{2}a** except for the use of 1.15 equiv. of 9-EtGua and obtained as a light yellow solid (93% yield). Anal. Calcd. (%) for $C_{19}H_{22}Cl_2N_8OPt(H_2O)_{3.5}$: C, 32.26; H, 4.13; N, 15.84. Found: C, 31.58; H, 4.10; N, 15.37. ^{1}H NMR (D_2O, 400 MHz): δ 1.48 (syn) and 1.58 (anti) (t, *J* = 8.0 Hz, 3H), 4.22 (syn) and 4.31 (anti) (q, *J* = 8.0 Hz, 2H), 4.95(m, 4H), 7.33 (q, *J* = 8.0 Hz, 2H), 7.57-7.66 (m, 4H), 8.12 (t, *J* = 8.0 Hz, 2H), 8.51 (syn) and 8.88 (anti) (s, 1H). ^{195}Pt NMR (85.80 MHz, D_2O, δ/ppm): -2362.7; -2379.0. IR (KBr, selected peaks)/cm^{-1}: ν(PtN) 447, 491.

[AuCl(Mebpma)]$(PF_6)_2$ (**AuL^1**) Synthesized analogously to [Au(bpma)Cl](PF_6). To a stirring solution of tetrachloroauric acid was added 1 equiv. of Mebpma in the presence of 2 equiv. of ammonium hexafluorophosphate. The tan precipitate isolated by filtration and washed with water (53.5% yield). Anal. Calcd (%) for $[(C_{13}H_{15}N_3)AuCl](PF_6)_2$: C, 21.23; H, 2.06; N, 5.71. Found: C, 21.29; H, 1.59; N, 5.93. ^{1}H NMR (DMF-d_7, 300 MHz): δ 3.94 (s, 3H), 5.47 (d, 2H), 6.35 (d, 2H), 8.13 (t, 2H), 8.31 (d, 2H), 8.72 (t, 2H), 9.13 (d, 2H).

[AuCl(bpma-H)](PF_6) (**Au(L^2-H)**) [Au(bpma-H)Cl](PF_6) was synthesized by addition of 1 equiv. of BPMA to a solution of tetrachloroauric acid in water in the presence of 1 equiv. of

ammonium hexafluorophosphate. The red precipitate was filtered and washed with water (70.7% yield). Anal. Calcd. (%) for $[Au(C_{12}H_{12}N_3)Cl](PF_6)$: C, 25.04; H, 2.10; N, 7.30. Found: C, 24.91; H, 1.87; N, 7.14. ^{1}H NMR (DMF-d_7, 300 MHz): δ 4.40 (s, 4H), 7.96 (m, 2H), 8.21 (d, 2H), 8.55 (m, 2H), 9.14 (d, 2H).

NMR experiments.

^{1}H and ^{195}Pt NMR spectra were recorded on a Bruker AVANCE III 400 MHz spectrometer. ^{1}H NMR are reported with reference to solvent resonances of D_2O at δ 4.79 – the dmf-d_7 spectral shifts were adjusted appropriately. The ^{195}Pt{^{1}H} NMR spectra including those of the *N*-AcCys assay were obtained in D_2O, at room temperature, with 40 mM solutions, at an operating frequency of 85.80 MHz, range of -1900 to -3500 ppm and 5000 scans. The spectra were referenced externally using standards of Na_2PtCl_6 in D_2O (δ = 0 ppm). The ^{1}H NMR spectra of the 4-pic and dmap platinum complexes were recorded on a Varian Mercury-300 MHz, at 293 and 333 K (60ºC). The samples were prepared in D_2O, at 20 mM approximate concentration and the spectra, obtained with an average number of 32 scans.

Fluorescence spectroscopy.

Fluorescence studies were recorded on a Varian Cary Eclipse fluorometer. Solutions of the $[Pt(N_3)L]Cl_2$ species were prepared in water to a final concentration of 1.5 mM. 1 mM stock solutions of *N*-AcTrp, ZF2 and NCp7 were prepared in 20 mM tris buffer with 50 mM NaCl at pH 7.4. In a fluorescence cuvette, 3 mL of a 5 μM solution of *N*-AcTrp, ZF2 and NCp7 was titrated with volumes of 10 μL of the stock solution of the platinum(II) compounds at molar ratios from 1 to 10, and the fluorescence emission was measured in a 300-450 nm range, with an excitation wavelength of 280 nm and a detector voltage of 700 V for *N*-AcTrp and 750 V for ZF2 and NCp7 at room temperature. The emission maximum (360 nm) was measured after each titration. The Ka

values were determined from Eadie-Hofstee plots and were determined from an average of 3 trials using the following equation: $\Delta F = (K_a)^{-1}\Delta F/[\text{quencher}] + \Delta F_c$.

Mass Spectrometry.

For the electrospray ionization mass spectrometry experiments, 1:1 mixtures of **PtL^{1}a**:ZF2 was prepared. The samples were sprayed immediately using a final concentration of ~100 μM. Experiments were carried out on an Orbitrap Velos from Thermo Electron Corporation operating in positive mode. Samples were diluted with methanol and directly infused at a flow rate of 0.7 μL/min using a source voltage of 2.30 kV. The source temperature was maintained at 230°C throughout. MCl(N_3) complexes were incubated with *N*-AcCys or NCp7 ZF2 at 1: 1 molar ratios, and the reaction mixtures at t = 0 and 24 hours were monitored by ESI-MS under the same conditions.

Far infrared-(FIR) Spectroscopy.

Far Infrared (FIR) Fourier Spectra were obtained in KBr pellets in a Nicolet – Nexus 670 FT-IR in the 600–200 cm^{-1} frequency range, with an average number of 32 scans.

Corresponding Author

*E-mail: npfarrell@vcu.edu. Fax: 1-804-828-8599. Phone: 1- 804-828-6320.

Acknowledgments.

This work was supported by NSF CHE-1413189 and Ciencia Sem Fronteiras CAPES PVES 154/2012. VHFB and MDV T would like to thank the Brazilian agencies National Council for Scientific and Technological Development (CNPq for a research fellowship to MDV), Brazilian Federal Agency for Support and Evaluation of Graduate Education (CAPES) and Rio de Janeiro Research Foundation (FAPERJ) for financial support. We thank Raphael E.F. da Paiva for stimulating discussions.

2.6 References

1. Mori, M.; Lesia Kovalenko; Lyonnais, S.; Antaki, D.; Torbett, B. E.; Botta, M.; Mirambeau, G.; Mély, Y. Nucleocapsid Protein: A Desirable Target for Future Therapies Against HIV-1. *Curr. Top. Microbiol. Immitramunol.*, **389,** 53–92, 2015.

2. de Rocquigny, H.; Shvadchak, V.; Avilov, S.; Dong, C. Z.; Dietrich, U.; Darlix, J.L.; Mély, Y. Targeting the Viral Nucleocapsid Protein in Anti-HIV-1 Therapy. *Mini Rev. Med. Chem.* **8,** 24–35, 2008.

3. Godet, J.; Kenfack, C.; Przybilla, F.; Richert, L.; Duportail, G.; Mélly, Y. Site-selective Probing of cTAR Destabilization Highlights the Necessary Plasticity of the HIV-1 Nucleocapsid Protein to Chaperone the First Strand Transfer. *Nucleic Acids Res.* ***41,*** 5036–5048, 2013.

4. Keane, S. C.; Heng, X.; Lu, K.; Kharytonchyk, S.; Ramakrishnan, V.; Carter, G.; Barton, S.; Hosic, A.; Florwick, A.; Santos, J.; Bolden, N. C.; McCowin, S.; Case, D. A.; Johnson, B.; Salemi, M.; Telesnitsky, A.; Summers, M. F. Structure of the HIV-1 RNA Packaging Signal. *Science*. ***384,*** 917–921, 2015.

5. Wu, H.; Mitra, M.; McCauley, M. J.; Thomas, J. A.; Rouzina, I.; Musier-Forsyth, K.; Williams, M. C.; Gorelick, R. J. Aromatic Residue Mutations Reveal Direct Correlation between HIV-1 Nucloecapsid Protein's Nucleic Acid Chaperone Activity and Retroviral Replication. *Virus Res.* **171,** 263–277, 2013.

6. Rice, W. G.; Supko, J. G.; Malspeis, L.; Jr, R. W. B.; Clanton, D.; Bu, M.; Graham, L.; Schaeffer, C. A.; Turpin, J. A.; Domagala, J.; Gogliotti, R.; Bader, J. P.; Halliday, S. M.; Coren,

L.; Sowder, R. C.; Arthur, L.; Henderson, L. E. Inhibitors of HIV Nucleocapsid Protein Zinc Fingers as Candidates for the Treatment of AIDS. *Science.* **270,** 1194–1197, 1995.

7. Musah, R. A. The HIV-1 Nucleocapsid Zinc Finger Protein as a Target of Antiretroviral Therapy. *Curr. Top. Med. Chem.* **4,** 1605–1622, 2004.

8. Ramboarina, S.; Morellet, N.; Fournié-Zaluski, M. C.; Roques, B. P.; Moreller, N. Structural Investigation on the Requirement of CCHH Zinc Finger Type in Nucleocapsid Protein of Human Immunodeficiency Virus 1. *Biochemistry* **38,** 9600–9607, 1999.

9. Bhattacharya, S.; Osman, H. Novel Targets for Anti-retroviral Therapy. *J. Infect.* **59,** 377–386, 2009.

10. Stephen, A. G.; Worthy, K. M.; Towler, E.; Mikovits, J. A.; Sei, S.; Roberts, P.; Yang, Q. en; Akee, R. K.; Klausmeyer, P.; McCloud, T. G.; Henderson, L.; Rein, A.; Covell, D. G.; Currens, M.; Shoemaker, R. H.; Fisher, R. J. Identification of HIV-1 Nucleocapsid Protein:Nucleic Acid Antagonists with anti-HIV Activity. *Biochem. Biophys. Res. Commun.* **296,** 1228–1237, 2002.

11. Morellet, N.; Demene, H.; Teilleux, V.; Huynh-Dinh, T.; De Rocquigny, H.; Fournie-Zaluski, M.-C.; Roques, B. P. Structure of the Complex between the HIV-1 Nucleocapsid Protein NCp7 and the Single-stranded Pentanucleotide d(ACGCC). *J. Mol. Biol*. **283,** 419−434, 1998.

12. Quintal, S. M.; DePaula, Q. A.; Farrell, N. P. Zinc Finger Proteins as Templates for Metal Ion Exchange and Ligand Reactivity. Chemical and Biological Consequences. *Metallomics* **3,** 121–139, 2011.

13. Anzellotti, A. I.; Ma, E. S.; Farrell, N. P. Platination of Nucleobases to Enhance Noncovalent Recognition in Protein-DNA/RNA Complexes. *Inorg. Chem.* **44,** 483–485, 2005.

14. Anzellotti, A. I.; Liu, Q.; Bloemink, M. J.; Scarsdale, J. N.; Farrell, N. P. Targeting Retroviral Zn Finger-DNA Interactions: A Small-Molecule Approach Using the Electrophilic Nature of *trans*-Platinum-Nucleobase Compounds. *Chem. Biol.* **13,** 539–548, 2006.

15. Abbehausen, C.; Peterson, E. J.; de Paiva, R. E. F.; Corbi, P. P.; Formiga, A. L. B.; Qu, Y.; Farrell, N. P. Gold(I)-Phosphine-N-Heterocycles: Biological Activity and Specific (Ligand) Interactions on the C-Terminal HIVNCp7 Zinc Finger. *Inorg. Chem.* **52,** 11280–11287, 2013.

16. Anzellotti, A. I.; Sabat, M.; Farrell, N. P. Covalent and Noncovalent Interactions for [Metal(dien)nucleobase]$^{2+}$ Complexes with L-Tryptophan Derivatives: Formation of Palladium-Tryptophan Species by Nucleobase Substitution under Biologically Relevant Conditions. *Inorg. Chem.* **45,** 1638–1645, 2006.

17. Anzellotti, A. I.; Bayse, C. A; Farrell, N. P. Effects of Nucleobase Metalation on Frontier Molecular Orbitals: Potential Implications for π-Stacking Interactions with Tryptophan. *Inorg. Chem.* **47,** 10425–10431, 2008.

18. Tsotsoros, S. D.; Bate, A. B.; Dows, M. G.; Spell, S. R.; Bayse, C. A.; Farrell, N. P. Modulation of the Stacking interaction of MN4 (M=Pt, Pd, Au) Complexes with Tryptophan through N-Heterocyclic Ligands. *J. Inorg. Biochem.* **132,** 2–5, 2014.

19. Spell, S. R.; Farrell, N. P. Synthesis and Properties of the First [Au(dien)(N-heterocycle)]$^{3+}$ Compounds. *Inorg Chem* **53,** 30–32, 2014.

20. de Paula, Q. A.; Tsotsoros, S. D.; Qu, Y.; Bayse, C. A.; Farrell, N. P. Platinum-nucleobase PtN_4 Complexes as Chemotypes for Selective Peptide Reactions with Biomolecules. *Inorg. Chim. Acta* **393,** 222–229, 2012.

21. Guney, E.; Yilmaz, V. T.; Ari, F.; Buyukgungor, O.; Ulukaya, E. Synthesis, Characterization, Structures and Cytotoxic Activity of Palladium(II) and Platinum(II) Complexes Containing bis(2-pyridylmethyl)amine and Saccharinate. *Polyhedron* **30,** 114–122, 2011.

22. Durović, M. D.; Bugarčić, Z. D.; Heinemann, F. W.; van Eldik, R. Substitution versus Redox Reactions of Gold(III) Complexes with L-cysteine, L-methionine and Glutathione. *Dalton Trans.* **43,** 3911–3921, 2014.

23. Pitteri, B.; Annibale, G.; Marangoni, G.; Bertolasi, V.; Ferretti, V. Base Hydrolysis Kinetics and Equilibria of [bis(2-pyridylmethyl)amine]chloroplatinum(II) and Crystal and Molecular Structures of [Pt(bpma)Cl]Cl·H_2O and [Pt(bpma)(OH_2)](ClO_4)·2H_2O. *Polyhedron* **21,** 2283–2291, 2002.

24. Cao, L.; Jennings, M. C.; Puddephatt, R. J. A Dipalladium Complex with a Single Hydroxo Bridge and its Methylpalladium Precursor. *Dalton Trans.* 5171–5176, 2009.

25. Cao, L.; Jennings, M. C.; Puddephatt, R. J. Amine-Amide Equilibrium in Gold(III) Complexes and a Gold(III)-Gold(I) Aurophilic Bond. *Inorg. Chem.* **46,** 1361–1368, 2007.

26. Pitteri, B.; Marangoni, G.; Cattalini, L.; Visentin, F.; Bertolasi, V.; Gilli, P. The Role of the Non-Participating Groups in Substitution Reactions at Cationic Pt(II) Complexes Containing Tridentate Chelating Nitrogen Donors. Crystal Structure of {Pt[bis(2-pyridylmethyl)amine](py)}(CF_3SO_3)$_2$. *Polyhedron* **20,** 869–880, 2001.

27. Andrepont, C.; Marzilli, P. A.; Marzilli, L. G. Guanine Nucleobase Adducts Formed by [Pt(di-(2-picolyl)amine)Cl: Evidence that a Tridentate Ligand with Only in-Plane Bulk Can Slow Guanine Base Rotation. *Inorg. Chem.* **51,** 11961–11970, 2012.

28. Topolski, A.; Bugarčić, Ž. Kinetics of Chloride Substitution in $[Pt(bpma)Cl]^+$ and [Pt(gly-met-*S*,*N*,*N*)Cl] Complexes by Thiourea, Nitrates, and Iodides. *Chem. Pap.* **68,** 130–135, 2014.

29. Annibale, G.; Brandolisio, M.; Pitteri, B. New Routes for the Synthesis of Chloro(diethylenetriamine) Platinum(II) Chloride and Chloro(2,2':6',2"-terpyridine) Platinum(II) Chloride Dihydrate. *Polyhedron* **14,** 451–453, 1995.

30. Nardin, G.; Randaccio, L.; Annibale, G.; Natile, G.; Pitteri, B. Comparison of Structure and Reactivity of bis(2-aminoethyl)amine- and bis(2-aminoethyl)amido-chlorogold(III) Complexes. *J. Chem. Soc., Dalton Trans.* 220–223, 1980.

31. Spell, S. R.; Farrell, N. P. $[Au(dien)(N\text{-heterocycle})]^{3+}$: Reactivity with Biomolecules and Zinc Finger Peptides. *Inorg. Chem.* **54,** 79–86, 2015.

32. Baddley, W. H.; Basolo, F.; Gray, H. B.; Nolting, C.; Poe, A. J. Acidodiethylenetriaminegold(III) Complexes: Preparation, Solution, Chemistry, and Electronic Structure. *Inorg. Chem.* **2,** 921-928, 1963.

33. Best, S. L.; Guo, Z.; Djuran, M. I.; Sadler, P. J. $[Au(dien)Cl]Cl_2$: Exchange Phenomena Observed by H1 and C13 NMR Spectroscopy. *Met. Based Drugs* **6,** 261–269, 1999.

34. Romeo, R.; Minniti, D.; Alibrandi, G.; De Cola, L.; Tobe, M. L. Acidic Properties of (dimethyl sulfoxide)(1,5-diamino-3-azapentane)platinum(II) Perchlorate and Kinetics of the Displacement of Dimethyl Sulfoxide from the Conjugate Base. *Inorg. Chem.* **25,** 1944–1947, 1986.

35. Still, B. M.; Kumar, P. G. A.; Aldrich-Wright, J. R.; Price, W. S. ^{195}Pt NMR - Theory and Application. *Chem. Soc. Rev.* **36,** 665–686, 2007.

36. Berners-Price, S. J.; Ronconi, L.; Sadler, P. J. Insights into the Mechanism of Actoin of Platinum Anticancer Drugs from Multinuclear NMR Spectroscopy. *Prog. Nucl. Magn. Reson. Spectrosc.* **49,** 65–98, 2006.

37. Andrepont, C.; Pakhomova, S.; Marzilli, P.A.; Marzilli, L.G. Unusual Example of Chelate Ring Opening upon Coordination of the 9-Ethylguanine Nucleobase to [Pt(di-(6-methyl-2-picolyl)amine)Cl]Cl. *Inorg. Chem*., **54,** 4895-4908, 2015.

38. Djuran, M. I.; Lempers, E. L. M.; Reedijk, Reactivity of Chloro- and Aqua(diethylenetriamine)platinum(II) Ions with Glutathione, S-methylglutathione, and Guanosine 5'-monophosphate in Relation to the Antitumor Activity and Toxicity of Platinum Complexes. *J. Inorg. Chem.* **30,** 2648–2652, 1991.

39. Bose, R. N.; Moghaddas, S.; Weaver, E. L.; Cox, E. H. Reactivity of Glutathione and Cysteine toward Platinum(II) in the Presence and Absence of Guanosine 5'-Monophosphate. *Inorg. Chem.* **34,** 5878–5883, 1995.

40. Wang, X.; Guo, Z. The Role of Sulfur in Platinum Anticancer Chemotherapy. *Anticancer Agents Med. Chem.* **7,** 19–34, 2007.

41. Glišić, B. Đ.; Rychlewska, U.; Djuran, M. I. Reactions and Structural Characterization of Gold(III) Complexes with Amino Acids, Peptides and Proteins. *Dalton Trans.* **41,** 6887-6901, 2012.

42. Djeković, A.; Petrović, B.; Bugarčić, Ź.D.; Puchta, R.; van Eldik, R. Kinetics and Mechanism of the Reactions of Au(III) Complexes with Some Biologically Relevant Molecules. *Dalton Trans*. **41,** 3633-3641, 2012.

43. de Paula, Q. A.; Mangrum, J. B.; Farrell, N. P. Zinc Finger Proteins as Templates for Metal Ion Exchange: Substitution Effects on the C-Finger of HIV Nucleocapsid NCp7 Using M(chelate) Species (M=Pt, Pd, Au). *J. Inorg. Biochem.* **103,** 1347–1354, 2009.

44. Tsotsoros, S.D.; Lutz, P.B..; Daniel, A.G.; Peterson, E.J.; da Paiva, R.E.F., Qu, Y.; Bayse, C.A.; Farrell, N.P. Enhancement of the Physiochemical Properties of [Pt(dien)(nucleobase)]$^{2+}$ for HIVNCp7 Targeting. *Chem. Sci.* **2,** 1269-1281, 2017.

45. Astner, J.; Weitzer, M.; Foxon, S. P.; Schindler, S.; Heinemann, F. W.; Mukherjee, J.; Gupta, R.; Mahadevan, V.; Mukherjee, R. Synthesis, Characterization, and Reactivity of Copper Complexes with Tridentate N-donor Ligands. *Inorg. Chim. Acta* **361,** 279–292, 2008.

2.7 Appendix

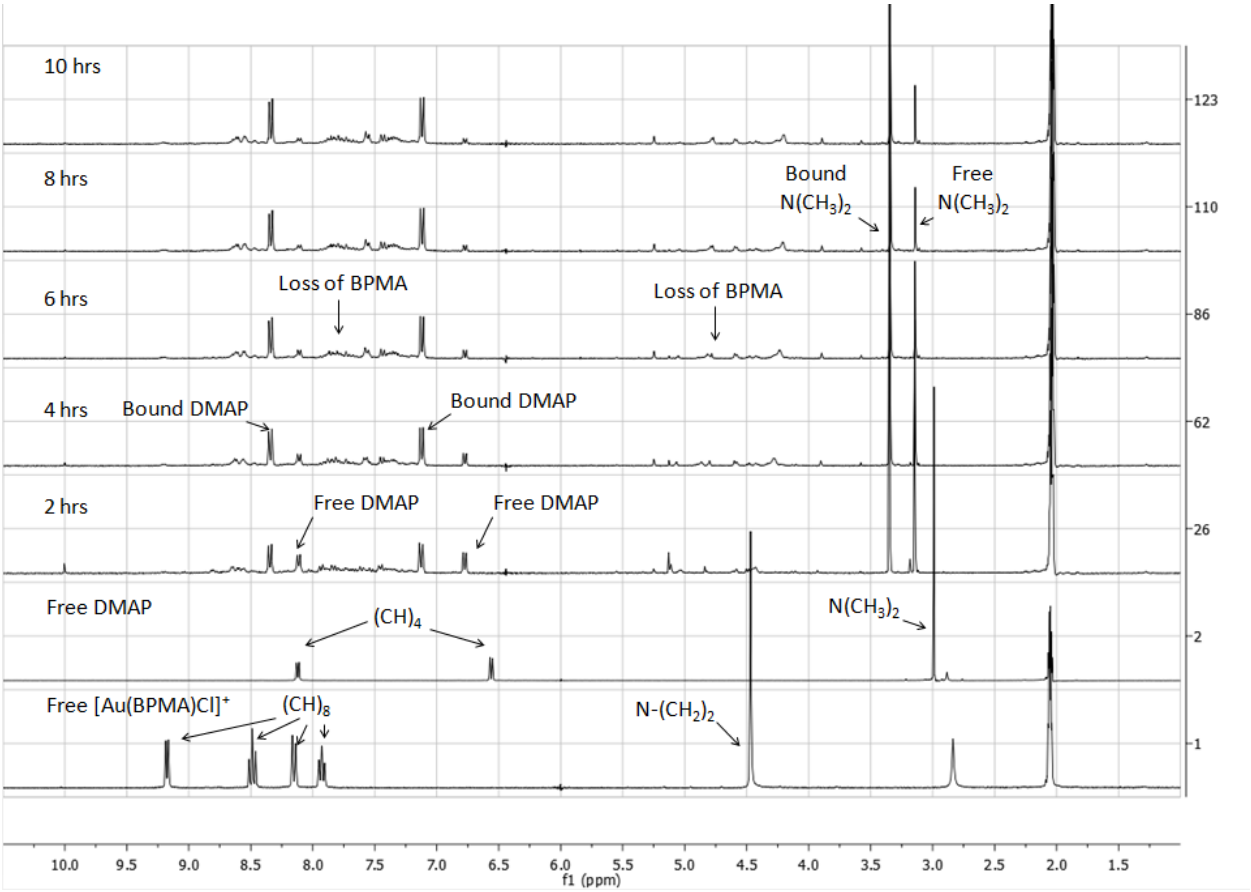

Figure 2.16. Interaction of $[Au(BPMA)Cl]^+$ with one equivalent of DMAP monitored by ^1H-NMR for 10 hours.

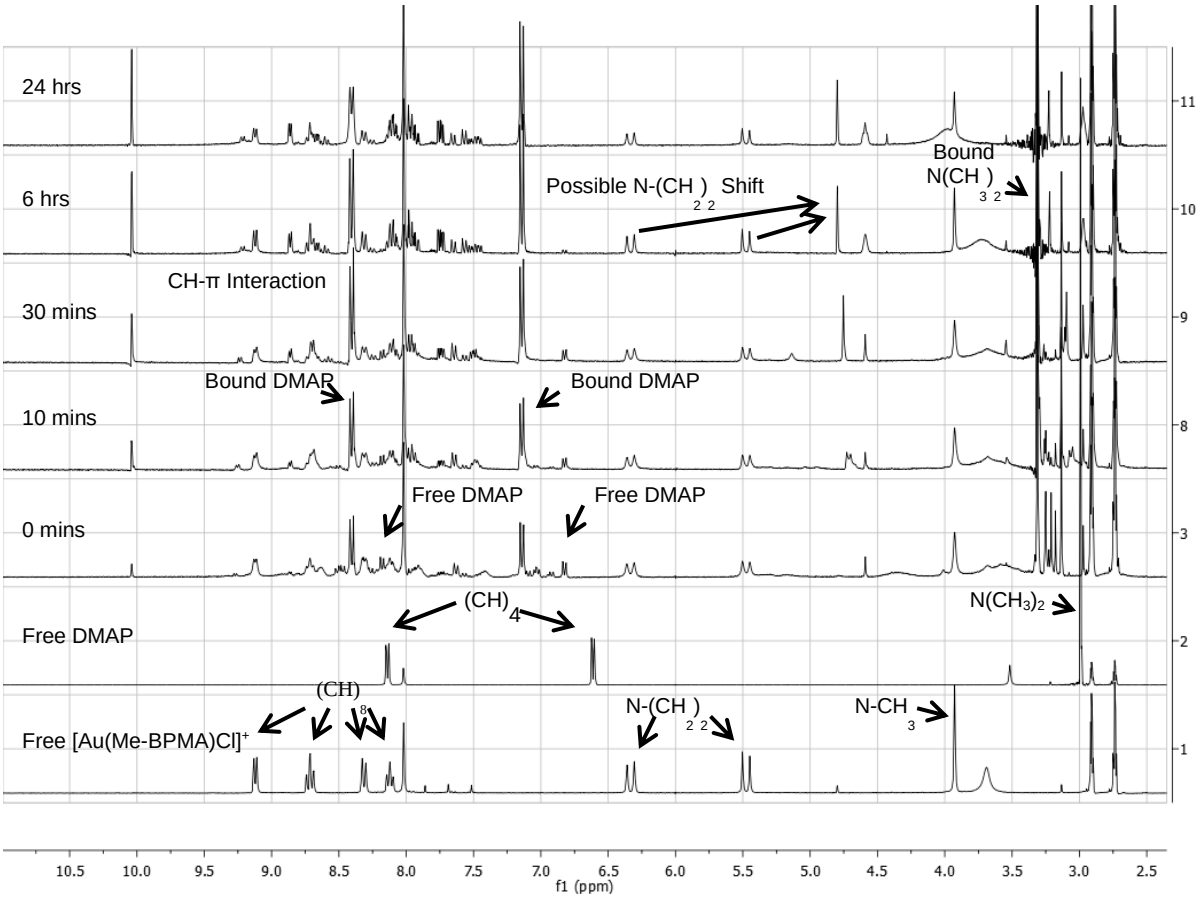

Figure 2.17. Interaction of $[Au(Me\text{-}BPMA)Cl]^{2+}$ with one equivalent of DMAP monitored by ^{1}H-NMR for 10 hours.

Chapter 3: Investigation of 1-Methylcytosine as a Ligand in Gold(III) Complexes: Synthesis and Protein Interactions

James Beaton [1] and Nicholas P. Farrell [1,*]

[1]Department of Chemistry, Virginia Commonwealth University, Richmond, Virginia 23284-2006, United States

3.1 Abstract

The HIV nucleocapsid protein NCp7 has been previously shown to play a number of roles in the viral life cycle, and has previously been identified as a potential target for small molecule intervention. In this work, the synthesis of the previously unreported complexes $[Au(dien)(1MeCyt)]^{3+}$, $[Au(N\text{-}Medien)(1MeCyt)]^{3+}$, and $[Au(dien)(Cyt)]^{3+}$ is detailed, and the interactions of these complexes with models for NCp7 are described. The affinity for these complexes with the target interaction site, the "essential" tryptophan of the C-terminal zinc finger motif of NCp7, was investigated through the use of a fluorescence quenching assay and by ^{1}H-NMR spectroscopy. The association of $[Au(dien)(1MeCyt)]^{3+}$ as determined through fluorescence quenching is intermediate between the previously reported DMAP and 9-EtGua analogs, while the associations of $[Au(N\text{-}Medien)(1MeCyt)]^{3+}$ and $[Au(dien)(Cyt)]^{3+}$ are lower than the previously reported complexes. Additionally, NMR investigation of this interaction shows that the association of complexes of this nature may be weaker than previously reported. The specifics of the interaction with the C-terminal zinc finger were investigated by circular dichroism spectroscopy

and electrospray-ionization mass spectrometry. The interaction is complete nearly immediately upon mixing, and the formation of Au_xF^{n+} (x = 1, 2, or 4; F = apopeptide) concomitant with the loss of all ligands was observed. Additionally, for the first time oxidized dimerized peptide was observed as a product, indicating reaction via a charge transfer mechanism.

3.2. Introduction

Gold compounds have a long history in medicinal chemistry. The thiophilic nature of gold suggests sulfur-rich proteins such as thioredoxin as reasonable cellular targets for gold action.[1] Au(III) is quite labile in its chemistry and susceptible to reduction to Au(I).[1] Apart from the inherent difficulty in understanding speciation of a Au(III) complex in a biological medium, non-selective interactions are also highly likely. This is especially true when highly nucleophilic sulfur sites in proteins are considered as viable targets. Formally substitution-inert coordination spheres such as MN_4 or MN_3L (where M = Pt, Au and N_4 may be an N_3 chelate such as diethylenetriamine (dien) and L a purine or pyrimidine ligand) have been explored by our group for greater specificity with biomolecules.[2] In principle, we have suggested that highly nucleophilic cysteines of biomolecules can be targeted using weak nucleophiles such as Platinum-Nucleobase PtN_4 Complexes for selective peptide reactions. While Au(III) is chemically more reactive than Pt(II) the same principle applies. A complementary approach to enhance selectivity in metal ion-biomolecule interactions is to use an inherent property of the protein along with appropriate design of the small molecule. A two-stage approach to selectivity can then be envisaged – molecular recognition followed by "fixation" where the inorganic moiety forms covalent linkages to the protein of interest. In this contribution we summarize how this approach might work using formally substitution-inert gold-metal nucleobase complexes and a tryptophan-containing zinc finger peptide from the HIV nucleocapsid protein HIVNCp7. Specifically, we describe the

synthesis and properties of Au(III)-1-MeCytosine complexes and their interactions with the C-terminal NCp7-F2 targeting the essential tryptophan of the protein.

Zinc binding proteins are one of the most common types of metalloprotein, and make up as much as 10% of proteins found in humans.[3] In these proteins, zinc can serve a catalytic role, a structural role, and even a recently discovered inhibitory role.[4,5] In zinc finger proteins, the zinc serves a structural role binding in a tetrahedral geometry to four surrounding amino acids.[6] These amino acids are generally a combination of cysteines and histidines, and take the forms Cys_2His_2, $Cys_2HisCys$ (Cys_3His), or Cys_4, and modification of the zinc-coordinating residues can have a dramatic effect on protein function.[7] The HIV nucleocapsid protein (NCp7), a 55 amino acid protein that contains two Cys_3His zinc fingers (Figure 3.1), has been identified as a potential target for chemical intervention through the modification of these structural elements, and it has been previously shown that alteration of the zinc coordination sphere significantly hinders viral replication.[4] NCp7 interacts with its polynucleotide substrate, viral RNA, through guanine stacking with both W37 on the second C-terminal zinc finger motif, as well as through the phenylalanine (F16) located on the first zinc finger.[4,8]

NCp7 recognition by small molecules can be optimized through a noncovalent π-π stacking interaction between the "essential" tryptophan residue and metallated nucleobases, analogous to the RNA(DNA) interaction. Previously reported gold (III) complexes based on $[Au(dien)L]^{3+}$ (dien = diethylenetriamine; L = N-heterocycle) have been investigated for their ability to stabilize the Au(III) oxidation state, as well as their ability to eject zinc from zinc finger proteins.[9-12] In the case of coordination complexes, this interaction brings the metal center in close contact with the highly nucleophilic zinc bound cysteine residues, allowing for secondary electrophilic attack by the metal center, resulting in zinc ejection.[2,9] Changing the N-heterocyclic ligand can be used to

fine-tune the electronic properties of the metal center to impart higher selectivity for the protein of interest. To this end, the $[Au(dien)L]^{3+}$ coordination sphere was studied with the previously uninvestigated ligand 1-methylcytosine (1-MeCyt). Compared to the N-heterocycles 4-Dimethylaminopyridine (DMAP) and 9-Etylguanine (9-EtGua), the free ligand 1-MeCyt has a higher association constant with tryptophan.[13] Additionally, 1-MeCyt has an intermediate basicity (pKa = 4.45) relative to DMAP (pKa = 9.1) and 9-EtGua ($pK_{a(N7)}$ = 2.7).[14] Previously, basicity of the heterocycle was thought to be proportional to association constant in the $[Au(dien)(N\text{-heterocycle})]^{3+}$ motif.[9] The $[Au(dien)(1\text{-MeCyt})]^{3+}$ is, to our knowledge, the first 1-MeCytosine compound of Au(III) to be synthesized and completes the series of Pt(II) and Pd(II) complexes $[M(dien)L]^{n+}$ (L = 9-EtGua, 1-MeCyt) studied for their isostructural and isoelectronic similarities.[13,15,16] We report the synthesis of the $[Au(dien)(1\text{-MeCyt})]^{3+}$ (**A**), $[Au(N\text{-Medien})(1\text{-MeCyt})]^{3+}$ (**B**), and $[Au(dien)(Cyt)]^{3+}$ (**C**) (Figure 3.1). The associative interaction with N-Acetyl-L-tryptophan (NAcTrp) as a model for the recognition site of NCp7 (W37) was probed through the use of a fluorescence quenching assay. Additionally, the interactions with the C-terminal zinc finger of NCp7 (Figure 3.1) were investigated by mass spectrometry and circular dichroism spectroscopy.

3.3. Results

Synthesis and Characterization

The previously unreported complexes **A**, **B**, and **C** (Figure 3.1) were successfully synthesized in accordance with the previously published methods.[9] The ^{1}H-NMR spectra of the complexes **A** and of **B** show multiple protonation states with varying pH* (Figure 3.2), analogous to the previously reported 9-EtGua analogs.[9] As 1-MeCyt does not have a labile proton, the changes in the shifts observed with changing pH may be due to the previously reported deprotonation of the

dien chelate, likely at the central nitrogen (pK_a = 3.3 for 9-EtGua analog).[9] By analogy with the Pd and Pt complexes (see reference 13), the N3 is assigned as the binding site to Au(III). Unique to the 1-MeCyt complexes, the signals for the aromatic H6 protons split. This splitting of the aromatic protons is not observed in the complex of C nor in the platinated analog, and highlights the increased electronegativity of Au(III) relative to Pt(II).[16,17]

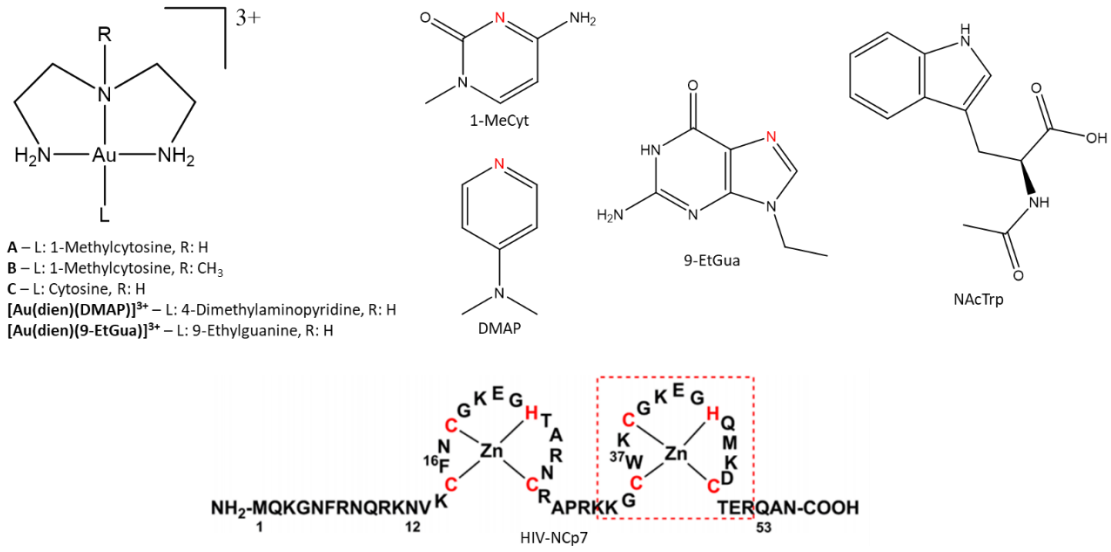

Figure 3.1. Structures of the complexes studied. Metal binding sites are highlighted in red.

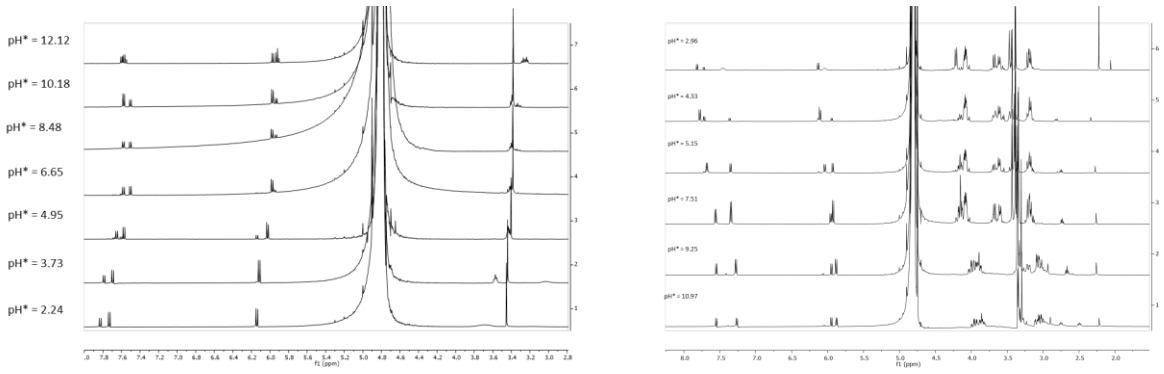

Figure 3.2. The ^{1}H-NMR spectra of **A** (left) and **B** (right) at varying pH* values, where pH* is the reading of the pH meter.

The mass spectra of **A** and **B** are typical of many coordination complexes, in that the parent ion peak is nearly indistinguishable from the background but the Au(III)-diethylenetriamine

backbone bound to fragments of 1-MeCyt is observed, indicating that the desired product had been obtained (Figure 3.3). Synthesis of the ribosylated analog of $[Au(Dien)(Cyd)]^{3+}$ (Cyd = cytidine) was attempted, but the recovered yellow product quickly turned purple, indicating the formation of colloidal gold (reduction of the metal center to Au(0)).

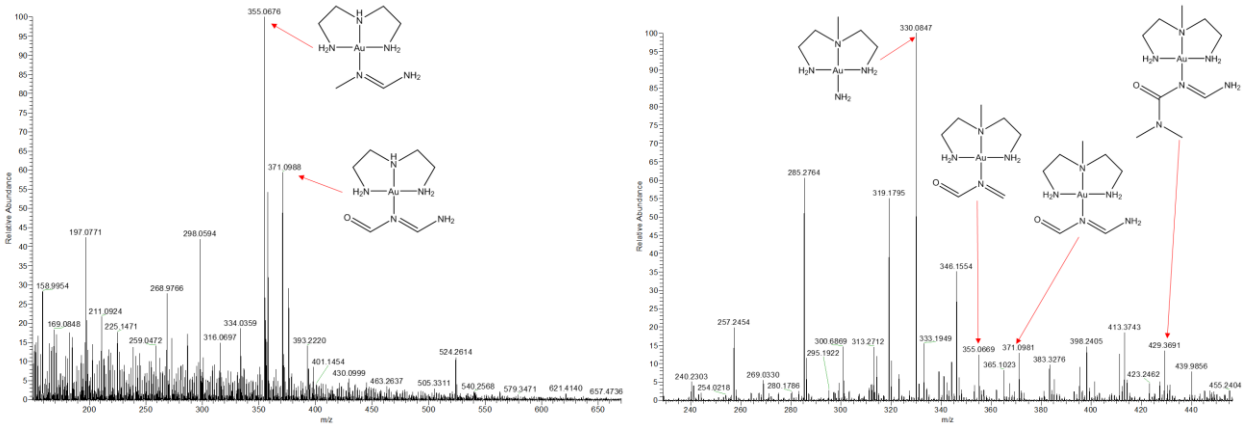

Figure 3.3. Mass spectra of **A** (left) and **B** (right).

Determination of Tryptophan Affinity by Fluorescence Quenching

Complexes **A**, **B**, and **C** were titrated into a solution of NAcTrp, and fluorescence quenching was used to determine the affinity (Figure 3.4). Complex **B** shows a lower affinity for NAcTrp (K_a = 13.0 × 10^3 M^{-1}) than the DMAP and 9-EtGua analogs. The association constant for **A** as determined by tryptophan quenching (24.2 × 10^3 M^{-1}) is intermediate between that of the DMAP and 9-EtGua analogs, while **C** has a lower association constant (9.31 × 10^3 M^{-1}). The synthesis and study completes the isoelectronic and isostructural series $[M(dien)L]^{n+}$ where M = Pd(II), Pt(II) and Au(III) and L = purine, 9-Ethylguanine, or pyrimidine, 1-meCytosine.[9,16] Figure 3.4 shows how, for this closely related series, the electronic factors from individual metal ions can be modulated to control to some extent the tryptophan affinity.[13]

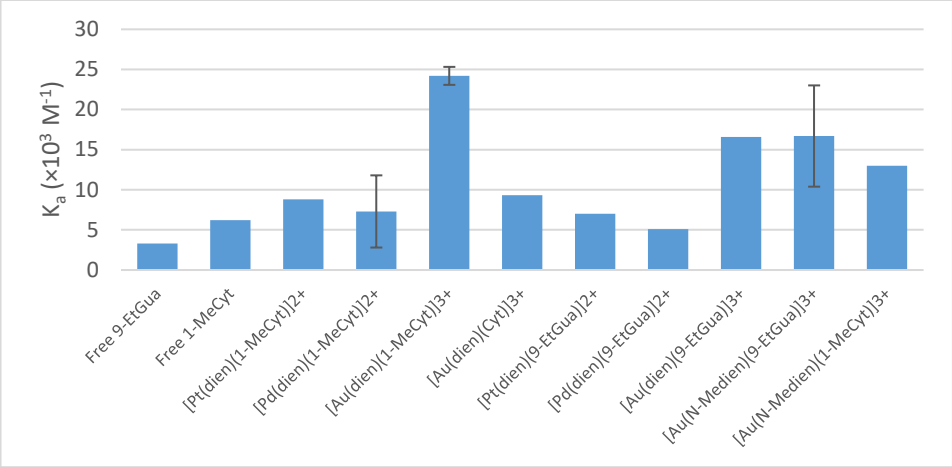

Figure 3.4. Association constants for $[M(dien)(nucleobase)]^{n+}$ determined by fluorescence quenching of NAcTrp.[9,15,16]

Interactions with Zinc Finger Proteins

Circular dichroism (CD) can be used to gain qualitative information about the structure of the zinc finger protein. As previously described, the zinc finger structural motif, as seen in the second finger of HIV-NCp7, has a characteristic positive band at 220 nm and a negative band at 195-200 nm.[18] The CD spectrum of the C-terminal zinc finger motif of NCp7 (NCp7-F2) was recorded before and after incubation with one equivalent of **A**, and the interaction was monitored for four hours (Figure 3.5).

Similarly to all previously studied gold(III)-dien complexes, the interaction with **A** results in rapid zinc ejection. The decrease seen in the positive band at 220 nm and the increase seen in the negative band at 200 nm upon interaction are indicative of random coil, and are similar to the previously reported CD spectrum of the apopeptide.[10] Thus, it is assumed that the zinc has been ejected very rapidly. Additionally, the spectrum does not change over the remainder of the next four hours, indicating that the reaction is complete after 15 minutes. After a 15 minute incubation with B, the result was also zinc ejection (data not shown).

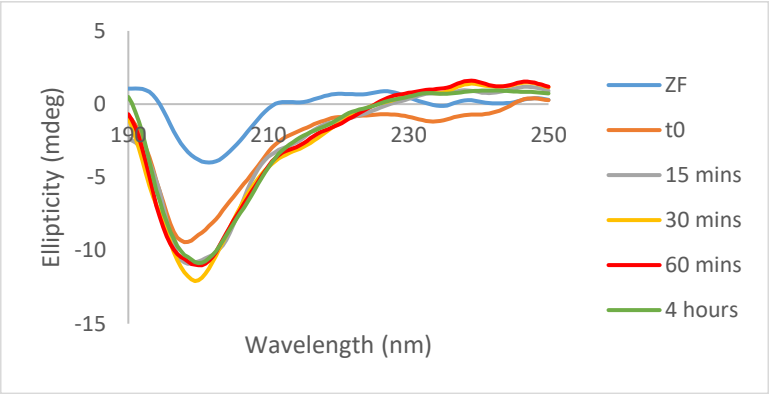

Figure 3.5. Circular dichroism spectrum of a 1:1 mixture of the C-terminal Zinc Finger of NCp7 and A, monitored over 4 hours.

Mass spectra of a 1:1 mixture of NCp7-F2 and **A** were recorded immediately after mixing, after 6 hours, and after 24 hours (Figure 3.6a, 3.7, and 3.8). The spectra did not change substantially from the initial timepoint to the final measurement, supporting the results obtained in the CD spectra and in the previous literature that the interaction between Au(III) complexes and zinc finger peptides occurs rapidly. At the time of the initial measurement, the zinc-coordinated peptide is not observed. Additionally, all Au-bound ligands are lost and only the well described "gold fingers" are observed.[10] Replacement of zinc by one, two, and four atoms of gold was observed: 605.4805 *m/z* (4+), 438.1595 *m/z* (6+), and 1003.2671 *m/z* (3+) respectively. This is the first instance that incorporation of four gold atoms has been observed upon interaction with a single zinc finger motif. Oxidized apopeptide (without zinc) is the most readily observable species; 741.3176 *m/z* (3+), 1111.4739 *m/z* (2+). An unusual feature, not seen previously in our studies, is the presence of oxidized dimerized apopeptide assigned to the mass observed at 889.5802 *m/z* for the n=5 charge state.

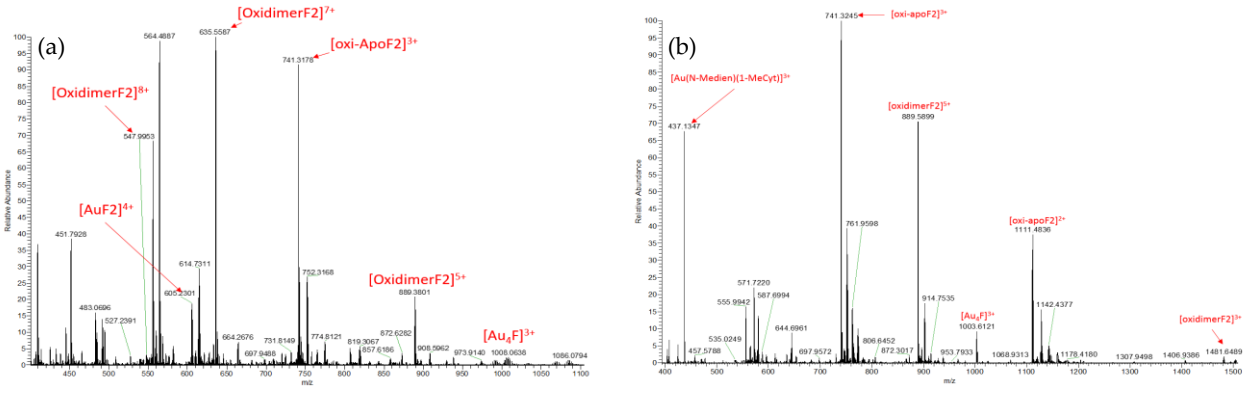

Figure 3.6. Mass spectra of a 1:1 mixture of **A** (a) and **B** (b) with the C-terminal zinc finger of NCp7.

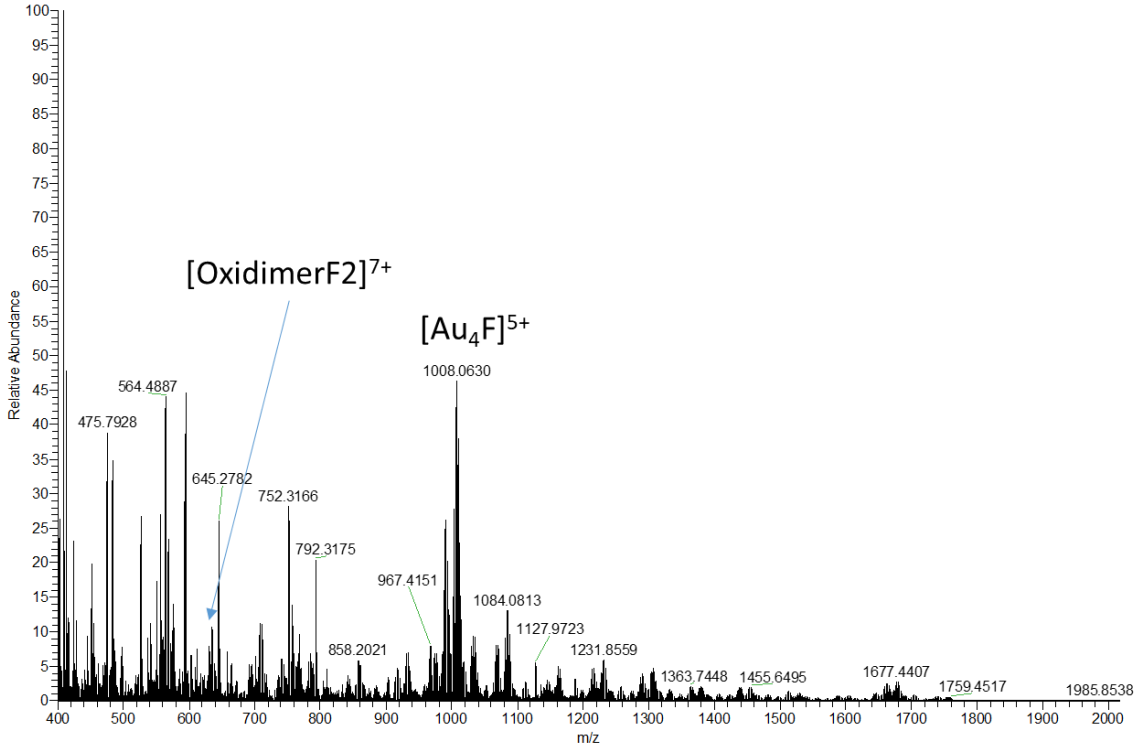

Figure 3.7. Mass spectrum of **A** with NCp7-F2 immediately after mixing.

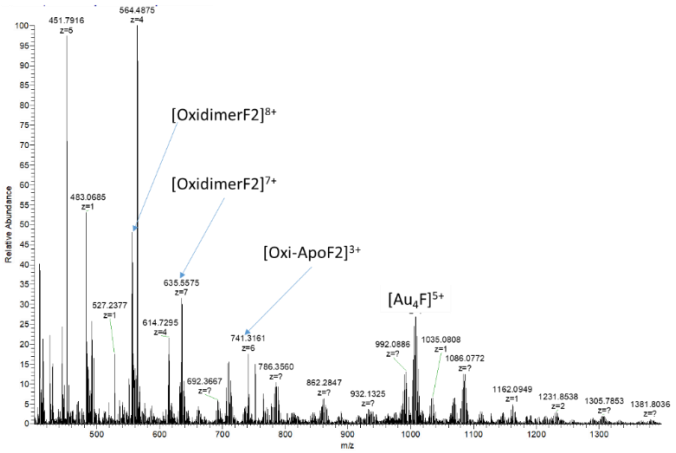

Figure 3.8. Mass spectrum of **A** with NCp7-F2 6 hours after mixing.

Mass spectra of a 1:1 mixture of NCp7-F2 and **B** taken immediately upon mixing and after one hour of incubation show essentially the same products as the spectra observed upon interaction with **A** (Figure 3.6b, Figure 3.9). Additionally, there is little difference in the initial spectrum and spectra obtained at later time points, again indicating that the reaction between NCp7-F2 and **B** is very rapid. Oxidized peptide and oxidized dimerized peptide were again seen, as well as incorporation of one, two, and four gold ions. Generally, because the ligands are not observed attached to gold after interaction with zinc finger proteins, the species observed in the mass spectra of the reaction with **A** and **B** are identical.

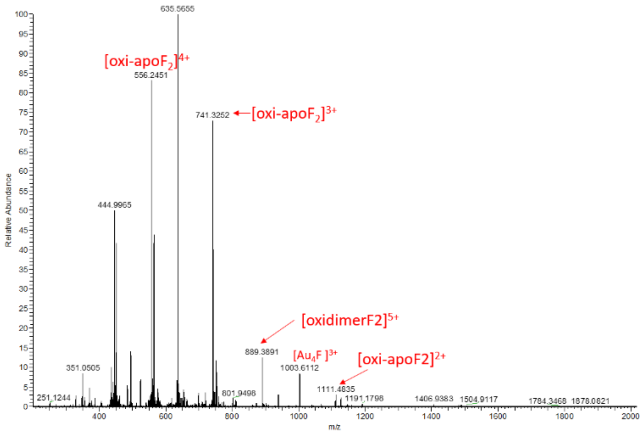

Figure 3.9. Mass spectrum of **B** with NCp7-F2 1 hour after mixing.

Cyclic Voltammetry

CV studies of complexes **A** and **B** showed that the new complexes follow the trend of resistance towards reduction seen in the previously studied DMAP and 9-EtGua analogs (Table 3.1).[9] The reduction potentials were determined relative to $[AuCl(dien)]^{2+}$. The reduction potential of **A** is intermediate between the previously studied DMAP and 9-EtGua analogs, and the Au(III) oxidation state is stabilized relative to the $AuClN_3$ coordination sphere. The reduction potential of **B** is slightly higher than the previously studied DMAP analog, but is still slightly lower than the chloride analog.

Complex	ΔE_p (V)	Ref.
$[Au(dien)(9\text{-EtGua})]^{3+}$	-0.069	9
$[Au(dien)(DMAP)]^{3+}$	-0.048	9
$[Au(dien)(1\text{-MeCyt})]^{3+}$ (**A**)	-0.052	
$[AuCl(N\text{-Medien})]^{2+}$	+0.048	9
$[Au(N\text{-Medien})(9\text{-EtGua})]^{3+}$	+0.017	9
$[Au(N\text{-Medien})(DMAP)]^{3+}$	+0.042	9
$[Au(N\text{-Medien})(1\text{-MeCyt})]^{3+}$ (**B**)	+0.045	

Table 3.1. Peak Potential Values (vs Ag/AgCl) for the reduction of selected Au(III) complexes at a Platinum disc electrode relative to $[AuCl(dien)]^{2+}$.

3.4 Discussion

The synthesis of complexes **A** and **B** serves to complete the series of complexes of the form $[M(dien)(1\text{-MeCyt})]^{n+}$, in which the Pt(II) and Pd(II) complexes, which are both isoelectronic and

isostructural to the Au(III) complexes investigated in this work, had been previously investigated, but the Au(III) analog had remained unreported up to this point.

Tryptophan is present on the C-terminal zinc finger of NCp7, and plays an essential role in protein-DNA/RNA recognition, which occurs through a π-π stacking interaction between the aromatic tryptophan (or in the case of the full peptide, phenylalanine) residues and the nucleobases in DNA/RNA.[13,19] Previously, it has been shown that association with free N-Acetyl-L-tryptophan (NAcTrp) is a good indicator of a compound's affinity for the full protein. The fluorescent emission of NAcTrp can be quenched by a complex that interacts with NAcTrp in a π-π stacking interaction, and the degree to which the fluorescent emission is quenched is directly related to the strength of the interaction.[9-11,13,15,17]

Compared to the Pt(II) and Pd(II) analogs, the Au(III) complexes show a higher affinity for NAcTrp, consistent with the previous literature.[4,20] The lower affinity of **B** for NAcTrp than the DMAP and 9-EtGua analogs is surprising given the intermediate basicity of 1-MeCyt. The result for **A** is as expected, as the basicity of free 1-MeCyt is intermediate between that of DMAP and 9-EtGua, but the results obtained for **B** and **C** show that there are factors other than the basicity that influence the associative interaction. Therefore, it is likely that the N-methyl group present on the chelating ligand in **B** causes a lower association constant for the π-π stacking interaction with NAcTrp than in **A**, shows that the modulation of the electronic environment of the metal center can influence the interactions between the complex and the protein recognition element. However, this reduction upon methylation of the chelating ligand is only observed to a lesser extent in the 9-EtGua analog.

Mass spectrometry studies with the previously reported Au(III) analogs showed that the formation of random coil observed by CD was accompanied by the formation of "gold fingers" in

which one or more atoms of gold replaced the zinc in the zinc finger structure upon zinc ejection.[9] The observation of oxidized apopeptide is indicative of disulfide bond formation between cysteine molecules of the same peptide, while the observation of oxidized dimerized apopeptide is indicative of disulfide bond formation between cysteine residues of different protein molecules. These interactions would likely be facilitated by the reduction of the metal center from Au(III) to Au(I)/Au(0). This interaction is in contrast to the interactions observed in the Pt(II) analogs, in which reduction and incorporation of the Pt(II) metal center is not seen, and instead the metal center is observed with the ligands intact and with the zinc still incorporated.[4,17,20] As with the previously reported aurated DMAP and 9-EtGua analogs, but unlike the platinated analogs, peaks representing the unreacted zinc finger protein are not seen at the initial time point, highlighting the increased reactivity of the Au(III) metal center. The incorporation of four equivalents of gold was thought to be due to a difference in the redox properties of **A** and **B** when compared to the previously studied Au(III) analogs. Therefore, cyclic voltammetry studies were carried out in order to assess these differences.

Cyclic voltammetry showed that it is significantly easier to reduce cytosine and thymine than it is to reduce adenine and guanine.[21] In the context of interaction with zinc finger peptides, this reduction would be accompanied by disulfide bond formation. In this case, the greater ease of reduction may cause the occurrence of a charge transfer mechanism, in which the disulfide bond formation occurs across two equivalents of the peptide forming the oxidized dimerized peptide uniquely observed in the case of **A** and **B**, in contrast to the simple oxidation of one equivalent of zinc finger. Whereas this latter oxidation is easily understood with reduction of Au(III) to Au(I) and concomitant oxidation of two Zn-bound cysteines, the first step in peptide dimerization may be an electron transfer between the 1-MeCyt ligand to the tryptophan ligand. This suggestion

would explain why similar products would not be seen in the isostructural Pt(II) complexes, as the platinum center is not reduced upon interaction with zinc finger peptides, while a charge transfer mechanism must occur with concomitant reduction of the metal center.[22] No evidence for self-association was observed by NMR studies for **A** or for free ligands (Figure 3.10). Previously published work has discussed the reduction potential and accessibility of the cysteine residues of the C-terminal zinc finger, and this data suggests that disulfide bond formation would likely occur between C39 residues (Figure 3.11), as C39 has a reduction potential nearly as low as that of C49 (-33.35 vs. -35.91 mV), but has a much greater accessibility (52.88 vs. 15.17).[22] It is also possible that reduction of multiple molecules of **A** or **B** could also result in the formation of multiple disulfide bonds, in which case both C49 and C39 could form disulfide bonds to form the dimer.

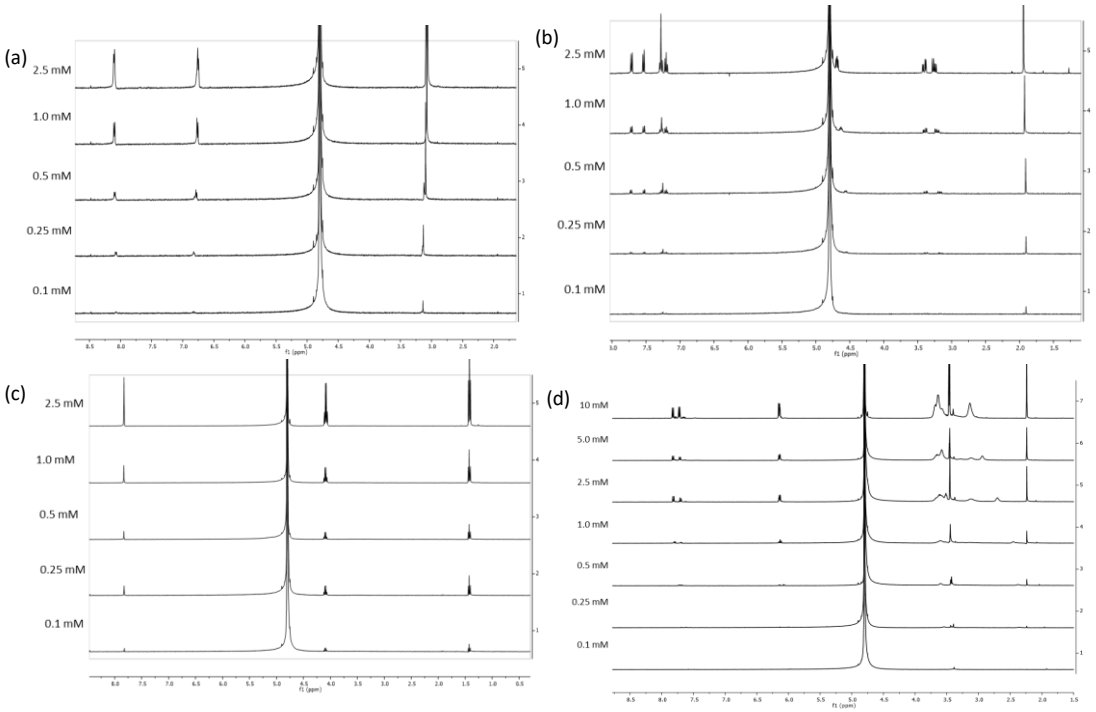

Figure 3.10. Self-association determination of (a) DMAP, (b) NAcTrp, (c) 9-EtGua, and (d) **A**. In each case, self-association was negligible on the scale of association between the complexes and NAcTrp.

Figure 3.11. Illustration of disulfide bond formation. Zinc coordinating residues are highlighted in red.

3.5. Materials and Methods

[AuCl(dien)]Cl_2 and [AuCl(N-Medien)]Cl_2 were synthesized according to previously published procedures.[23] 1-Methylcytosine was synthesized and purified according to previously published procedures.[24,25] Addition of the N-heterocycles were carried out analogously to previously published procedures.[9] All NMR studies were carried out in deuterium oxide on a Bruker AVANCE III (400 MHz). CD studies were carried out at 50 µM concentrations in water on a Jasco J-1500 spectrometer. Mass spectrometry studies were carried out on a Thermo Electron Corporation Orbitrap Velos mass spectrometer. Mass spectrometry samples were prepared at 10 µM concentrations in 10% methanol, and were sprayed at 2.30 kV and 0.9 µL/minute at 230 °C.

Synthesis of [Au(dien)(1-Mecyt)]$(NO_3)_3$ (**A**): [AuCl(dien)]Cl_2 (101.2 mg, 0.249 mmol) was dissolved in dH_2O (10 mL). 1-Methylcytosine (30.2 mg, 0.242 mmol) and Silver nitrate (125.4 mg, 0.738 mmol) were added, and the reaction mixture was stirred under light protection for 72 hours. The precipitated silver chloride was removed by filtration through celite, and the filtrate was evaporated to dryness under reduced pressure. The orange/yellow residue was dissolved in a small amount of dH_2O, and acetone was added to the cloud point. The orange/yellow solid product was collected by vacuum filtration, and characterized by ^{1}H-NMR, Infrared spectroscopy, and elemental analysis (experimental(theoretical)): C: 14.46% (14.62%) H: 2.81% (2.86%) N: 17.70% (17.17%). ^{1}H NMR (D_2O, 400 MHz): 7.83 (d, 0.35H), 7.73 (d, 0.65H), 6.14 (d, 1H), 3.69 (broad,

5.9), 3.45 (s, 3H), 3.18 (broad, 2.1H). UV-Vis (1 mM, H_2O): 237 nm (Abs = 3.98), 357 nm (Abs = 0.408).

Synthesis of [Au(N-Medien)(1-MeCyt)]$(NO_3)_3$ (**B**): [AuCl(N-MeDien)]Cl_2 (100.12 mg, 0.238 mmol) was dissolved in dH_2O (10 mL). Silver nitrate (121.4 mg, 0.715 mmol) and 1-methylcytosine (29.8 mg, 0.238 mmol) were added and the reaction mixture was stirred under light protection for 4 days. The reaction mixture was filtered through celite and the solvent was evaporated under reduced pressure. The resulting crude product was dissolved in a small amount of water and excess acetone was added to precipitate the yellow product, characterized by ^{1}H-NMR, Far-IR, and elemental analysis (experimental(theoretical)): C: 16.77%(17.20%) H: 3.33%(3.46%) N: 17.69%(18.05%). ^{1}H NMR (D_2O, 400 MHz): 7.82 (d,0.66H), 7.72 (d, 0.38H), 6.13(d, 1H), 4.21 (d, 1.6H), 4.09 (m, 2.6H), 3.65 (m, 2.6H), 3.46 (d, 1.8H), 3.38 (s, 3H), 3.19 (m, 2.4H). UV-VIS (1 mM, H_2O): 237 nm (Abs = 3.94), 352 nm (Abs = 0.921).

Synthesis of [Au(dien)(Cyt)]$(NO_3)_3$ (**C**): [AuCl(dien)]Cl_2 (100.44 mg, 0.168 mmol) was dissolved in dH_2O (10 mL). Cytosine (28.2 mg, 0.164 mmol) and Silver nitrate (85.61 mg, 0.506 mmol) were added, and the reaction mixture was stirred under light protection overnight. The precipitated silver chloride was removed by filtration through celite, and the filtrate was evaporated to dryness under reduced pressure. The orange residue was dissolved in a small amount of dH_2O, and acetone was added to the cloud point. The orange solid product was collected by vacuum filtration. ^{1}H NMR (D_2O, 400 MHz): 7.64 (d, 1H), 6.06 (d, 1H), 3.52 (t, 4H), 2.99 (broad, 4H).

Fluorescence Quenching of Tryptophan

Tryptophan quenching methods were adapted from those previously published.[9] A solution of N-acetyl-L-tryptophan (5 μM) was titrated with the Au(III) complexes (7.5 mM) in amounts ranging from 1-10 equivalents of quencher.

Determination of Self-Association by NMR Spectroscopy

Varying concentrations (0.1-2.5 mM) of N-heterocycle and gold(III) complex were analyzed by ^{1}H-NMR. The degree of self-association was determined by previously published methods.[26] Microsoft Excel Solver was used to solve the three variable equation.

Determination of Tryptophan Association by NMR Spectroscopy

The association between NAcTrp and π-π stacking compounds was determined through the use of a Benesi-Hildebrand plot, adapted from the previously published method.[19]

Cyclic Voltammetry

Cyclic voltammetry studies were carried out following the previously published procedures.[9] A three-electrode cell was employed, containing a platinum disk working electrode, a platinum mesh counter electrode, and a silver/silver chloride reference electrode (0.1 M KCl). Solutions were degassed with nitrogen for 15 minutes before analysis. Measurements were obtained in 50 mM phosphate buffer (4 mM NaCl, pH = 7.4).

3.6 Conclusions

In conclusion, the previously unreported 1-methylcytosine complexes based on the [Au(dien)(N-heterocycle)]$^{3+}$ motif, **A** and **B**, have been synthesized and investigated for their ability to interact with the C-terminal finger of the HIV nucleocapsid protein NCp7 as a model for a protein with highly nucleophilic cysteines. Gold compounds are considered to primarily interfere

with protein, rather than DNA, function. In considering the series $[M(dien)L]^{n+}$ the electronic properties can be modulated systematically for optimal protein interaction. A key feature leading to the rational design of complexes of the form $[Au(dien)L]^{3+}$ is the enhancement of the redox stability of the complexes relative to the precursor $[AuCl(dien)]^{2+}$ due to the incorporation of a more substitution inert nitrogen donor in the form of an N-heterocycle.[9] In the case of the more sterically hindered complex **B**, the reduction potential is greater than the chloride analog [AuCl(N-Medien)]$^{2+}$, and is in line with the reduction in stabilization of the gold(III) oxidation state seen in the complex $[Au(N\text{-}Medien)(DMAP)]^{3+}$. Secondly, the aurated nucleobase may interact preferentially with an RNA(DNA) recognition motif such as tryptophan. Formation of oxidized dimerized peptide was observed in the mass spectrometry studies conducted with NCp7-F2 and indicated a difference in the reactivity profile of **A** and **B** compared to the previously studied DMAP and 9-EtGua analogs. These results further confirm that by tuning the electronic and steric properties of the ligands on the Au(III) coordination sphere, the strength of interaction between complexes of the $[Au(dien)(N\text{-heterocycle})]^{3+}$ motif and a zinc finger can be modulated in a systematic manner.

Funding: This research was funded by National Science Foundation.

Acknowledgments: We gratefully acknowledge Dr. Christopher J. Freeman and Dr. Maryanne M. Collinson for assistance in carrying out the CV experiments.

3.7 References

1. Berners-Price, S. J. and Filipovska, A. Gold Compounds as Therapeutic Agents for Human Diseases. *Metallomics*, **3,** 863-873, 2011.

2. De Paula, Q. A.; Tsotsoros, S. D.; Qu, Y.; Bayse, C. A.; and Farrell, N.P. Platinum-nucleobase PtN4 Complexes as Chemotypes for Selective Peptide Reactions with Biomolecules. *Inorganica Chimica Acta*. **393,** 222-229, 2012.
3. Andreini, C.; Banci, L.; Bertini, I.; and Rosato, A. Counting the Zinc-Proteins Encoded in the Human Genome. *Journal of Proteome Research*. ***5,*** 196-201, 2006.
4. Morellet, N.; Jullian, N.; De Rocquigny, H.; Maigret, B.; Darlix, J.; and Roques, B. P. Determination of the Structure of the Nucleocapsid Protein NCp7 from the Human Immunodeficiency Virus Type 1 by 1H NMR. *The EMBO Journal*. **11(8),** 3059-3065, 1992.
5. Daniel, A. G.; Peterson, E. J.; and Farrell, N. P. The Bioinorganic Chemistry of Apoptosis: Potential Inhibitory Zinc Binding Sites in Caspase-3. *Agew. Chem.* **126,** 4182-4185, 2014.
6. Klug, A. and Rhodes, D. Zinc Fingers: A Novel Protein Fold for Nucleic Acid Recognition. *Cold Spring Harbor Symposia on Quantitative Biology*. **52,** 473-482, 1987.
7. Krishna, S. S.; Majumdar, I.; and Grishin, N. V. Structural Classification of Zinc Fingers. *Nucleic Acids Research.* **31(2),** 532-550, 2003.
8. South, T. L.; Blake, P. R.; Sowder III, R. C.; Arthur, L. O.; Henderson, L. E.; and Summers, M. F. The Nucleocapsid Protein Isolated from HIV-1 Particles Binds Zinc and Forms Retroviral-Type Zinc Fingers. *Biochemistry*, **29,** 7786-7789, 1990.
9. Spell, S. R. and Farrell, N. P. Synthesis and Properties of the First [Au(dien)(N-heterocycle)]$^{3+}$ Compounds. *Inorg. Chem.* **53(1),** 30-32, 2014.
10. Spell, S. R. and Farrell, N. P. [Au(dien)(N-heterocycle)]3+: Reactivity with Biomolecules and Zinc Finger Peptides. *Inorg. Chem.* **54,** 79-86, 2015.

11. Spell, S. R.; Mangrum, J. B.; Peterson, E. J.; Fabris, D.; Ptak, R.; and Farrell, N. P. Au(III) Compounds as HIV Nucleocapsid Protein (NCp7)-Nucleic Acid Antagonists. *Chem. Commun.* **53,** 91-94, 2017.

12. Anzellotti, A. I. and Farrell, N. P. Zinc Metalloproteins as Medicinal Targets. *Chem. Soc. Rev*. **37,** 1629-1651, 2008.

13. Anzellotti, A. I.; Bayse, C. A.; and Farrell, N. P. Effects of Nucleobase Metalation on Frontier Molecular Orbitals: Potential Implications for π-Stacking Interactions with Tryptophan. *Inorg. Chem.* **47,** 10425-10431, 2008.

14. Verdolino, V.; Cammi, R.; Munk, B. H.; and Schlegel, H. B. Calculation of pK_a Values of Nucleobases and Guanine Oxidation Products Guanidinohydantoin and Spiroiminodihydantoin using Density Functional Theory and a Polarizable Continuum Model. *J. Phys. Chem. B.* **112,** 16860-16873, 2008.

15. Anzellotti, A. I.; Ma, E. S.; and Farrell, N. Platination of Nucleobases to Enhance Noncovalent Recognition in Protein-DNA/RNA Complexes. *Inorg. Chem.* **44,** 483-485, 2005.

16. Anzellotti, A. I.; Sabat, M.; and Farrell, N. Covalent and Noncovalent Interactions for [Metal(dien)nucleobase]2+ Complexes with L-Tryptophan Derivatives: Formation of Palladium-Tryptophan Species by Nucleobase Substitution under Biologically Relevant Conditions. *Inorg. Chem.* **45,** 1638-1645, 2006.

17. Bernardes, V. H. F.; Qu, Y.; Du, Z.; Beaton, J.; Vargas, M. D.; and Farrell, N. P. Interaction of the HIV NCp7 Protein with Platinum(II) and Gold(III) Complexes Containing Tridentate Ligands. *Inorg. Chem.* **55(21),** 11396-11407, 2016.

18. dePaula, Q. A.; Mangrum, J. B.; Farrell, N. P. Zinc Finger Proteins as Templates for Metal Ion Exchange: Substitution Effects on the C-Finger of HIV Nucleocapsid NCp7 Using M(chelate) Species (M=Pt, Pd, Au). *J. Inorg. Biochem*. **103,** 1347−1354, 2009.

19. Ma, E. S. F.; Daniel, A. G.; and Farrell, N. P. Dinuclear Platinum Complexes Containing Planar Aromatic Ligands to Enhance Stacking Interactions with Proteins. *ChemMedChem*, **9(6),** 1155-1160, 2014.

20. Tsotsoros, S. D.; Lutz, P. B.; Daniel, A. G.; Peterson, E. J.; de Paiva, R. E. F.; Rivera, E.; Qu, Y.; Bayse, C. A.; and Farrell, N. P. Enhancement of the Physiochemical Properties of $[Pt(dien)(nucleobase)]^{2+}$ for HIVNCp7 Targeting. *Chem. Sci.*, **8,** 1269-1281, 2017.

21. P. Manoj, H. Mohan, J.P. Mittal, V.M. Manoj, and C.T. Aravindakumar. Charge Transfer from 2-Aminopurine Radical Cation and Radical Anion to Nucleobases: A Pulse Radiolysis Study. *Chemical Physics*, **331,** 351-358, 2007.

22. Abbehausen C., de Paive, R.E.F., Bjornsson R., Gomes S.Q., Du Z., Corbi P.P., Lima F.A., and Farrell N. X-ray Absorption Spectroscopy Combined with Time-Dependent Density Functional Theory Elucidates Differential Substitution Pathways of Au(I) and Au(III) with Zinc Fingers. *Inorg. Chem.*, **57,** 218-230, 2018.

23. Nardin, G.; Randaccio, L; Annibale, G.; Natile, G.; Pitteri, B. Comparison of Structure and Reactivity of bis(2-aminoethyl)amine- and bis(2-aminoethyl)amido-chlorogold(III) Complexes. *J. Chem. Soc. Dalton Trans.*, **2,** 220-223, 1980.

24. Greco, E.; Aliev, A. E.; Lafitte, V. G. H.; Bala, K.; Duncan, D.; Pilon, L.; Golding, P.; and Hailes, H. C. Cytosine Modules in Quadruple Hydrogen Bonded Arrays. *New J. Chem.*, **34,** 2634-2642, 2010.

25. Helfer II, D. L.; Hosmane, R. S.; and Leonard, N. L. Selective Alkylation and Aralkylation of Cytosine at the 1-Position. *J. Org. Chem.*, **46,** 4803-4804, 1981.
26. Waterhous, D. V. and Muccio, D. D. ^{1}H and ^{13}C Studies on the Self-Association of Retinoic Acid. *Magnetic Resonance in Chemistry*, **28,** 223-226, 1990.
27. Fielding, L. Determination of Association Constants (K_a) from Solution NMR Data. *Tetrahedron*, **56,** 6151-6170, 2000.

3.8 Appendix

NMR Association Studies

The inner filter effect is a concern in studies of the association of complexes of the [Au(dien)(N-heterocycle)]$^{3+}$ structure, as there is some overlap in the absorbance spectrum of the gold(III) complexes with the fluorescent absorption/emission spectra of N-acetyltryptophan. This overlap would artificially inflate the association value determined for a complex with N-acetyltryptophan, as the incident photons or emitted photons may be absorbed by the free gold(III) complex in solution. In order to address this issue, NMR experiments were carried out in order to investigate the potential of NMR as a method of determining the association between the gold(III) complexes and N-acetyltryptophan. In order to prove this concept, the free N-heterocycle DMAP was first investigated, as it is easily purchased at a low cost. However, DMAP has a fluorescence emission of its own, meaning the data previously obtained for association of DMAP with N-acetyltryptophan by fluorescence quenching may also be artificially higher than expected. In order to confirm that the data obtained from the NMR determination of association constant was valid, the free N-heterocycle 9-Ethylguanine was also investigated, as the free 9-ethylguanine does not have any spectral overlap with the N-acetyltryptophan. Finally, **A** was investigated in order to determine the difference in show that this method can be applied to a gold(III) complex. In order

to confirm that the system was a simple equilibrium system, and not a system in which a pre-association was present, the ability of the complexes to self-associate was also investigated by ^{1}H-NMR. The self-association of the complexes was determined using the equation $\delta_{obs} = \{[-K_d + (K_d^2 + 8CK_d)^{1/2}]/4C\}(\delta_M - \delta_D) + \delta_D$, where δ_{obs} is the observed, or average, chemical shift, δ_M is the chemical shift of the monomer, δ_D is the chemical shift of the dimer, and C is the total concentration of the molecule. On the scale of the associations with N-acetyltryptophan, any pre-association was determined to be negligible.

In addition, the binding stoichiometry of free DMAP and [Au(dien)(DMAP)]$^{3+}$ with NAcTrp were investigated by Job's method as previously described.[27] The final total concentration was 2.5 mM.

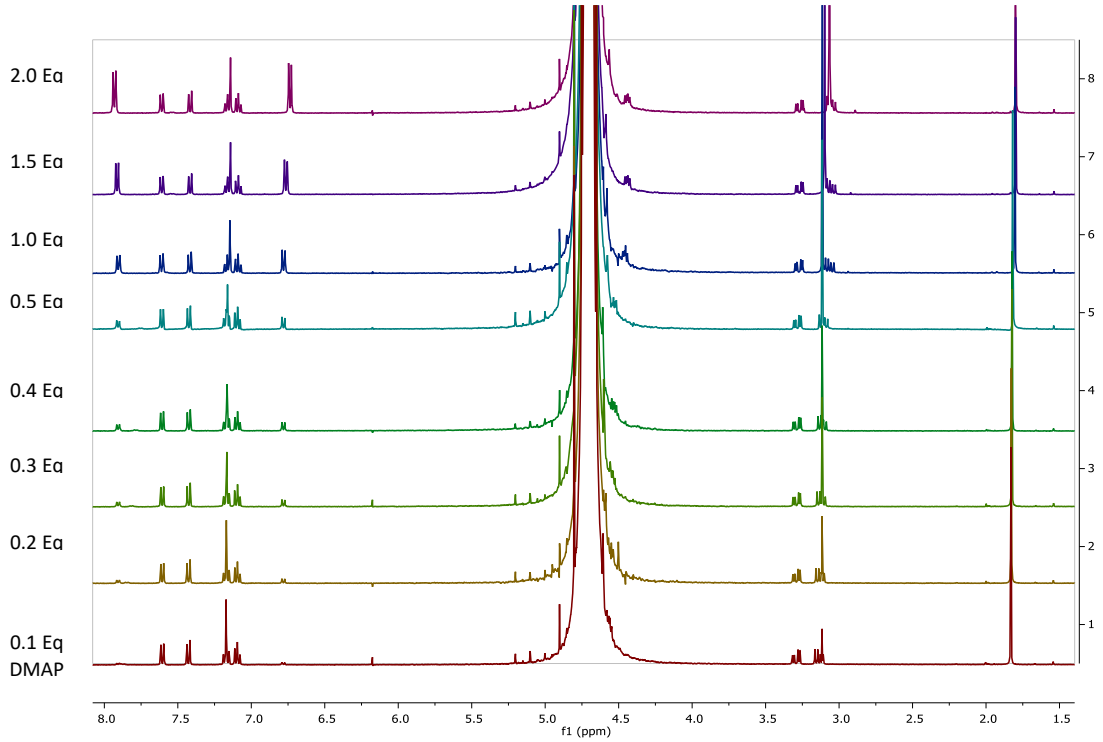

Figure 3.12. ^{1}H-NMR determination of the association between DMAP and N-acetyltryptophan.

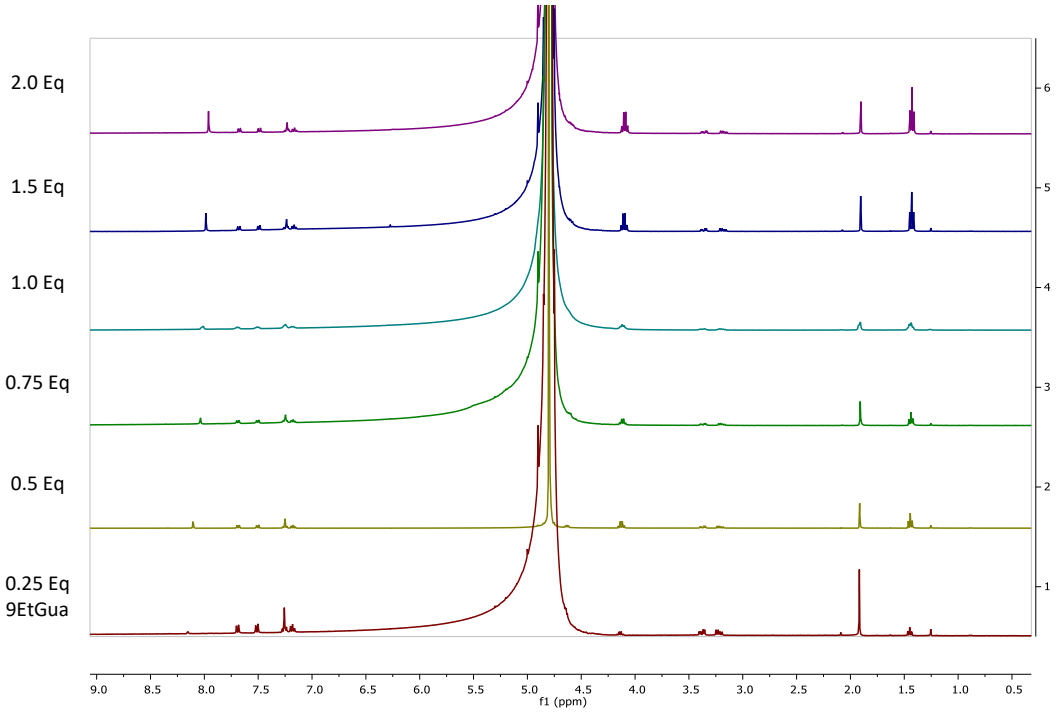

Figure 3.13. ^{1}H-NMR determination of the association between 9-EtGua and N-acetyltryptophan.

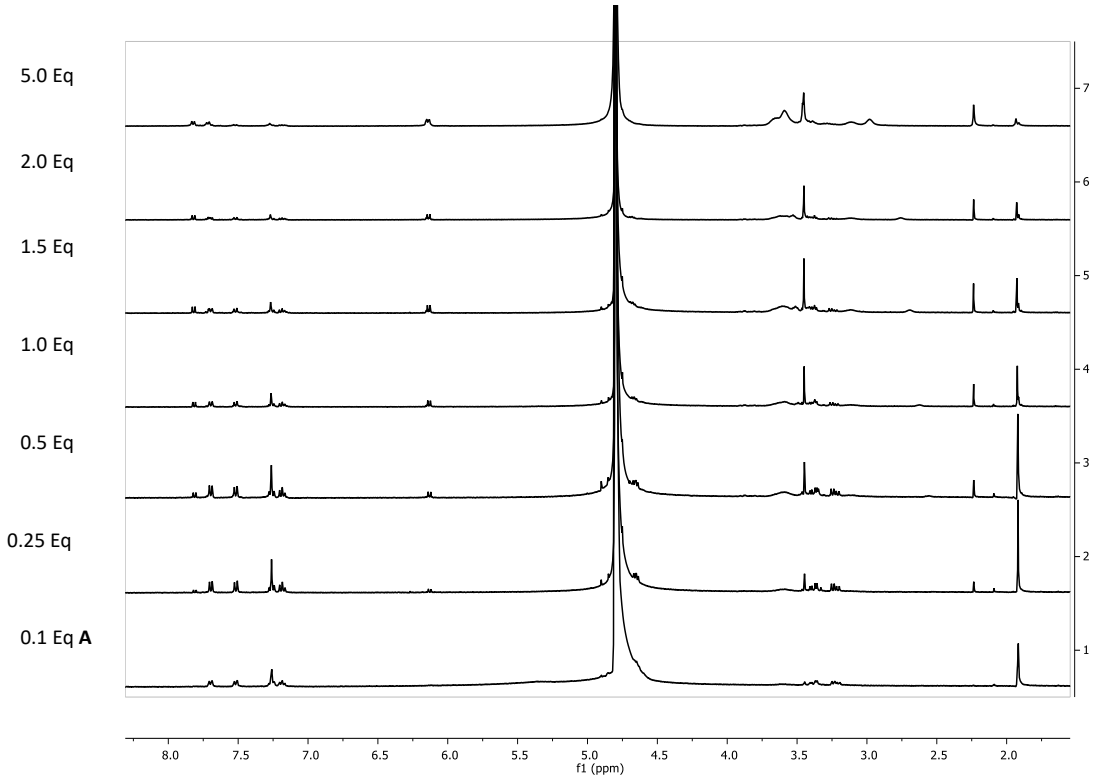

Figure 3.14. ^{1}H-NMR determination of the association between **A** and N-acetyltryptophan.

Complex	Ka ($\times 10^3$ M^{-1})
DMAP	0.236
9-EtGua	1.54
$[Au(dien)(1\text{-}MeCyt)]^{3+}$ (**A**)	2.68

Table 3.2. Association constants with N-acetyltryptophan as determined by Benesi-Hildebrand treatment of ^{1}H NMR data.

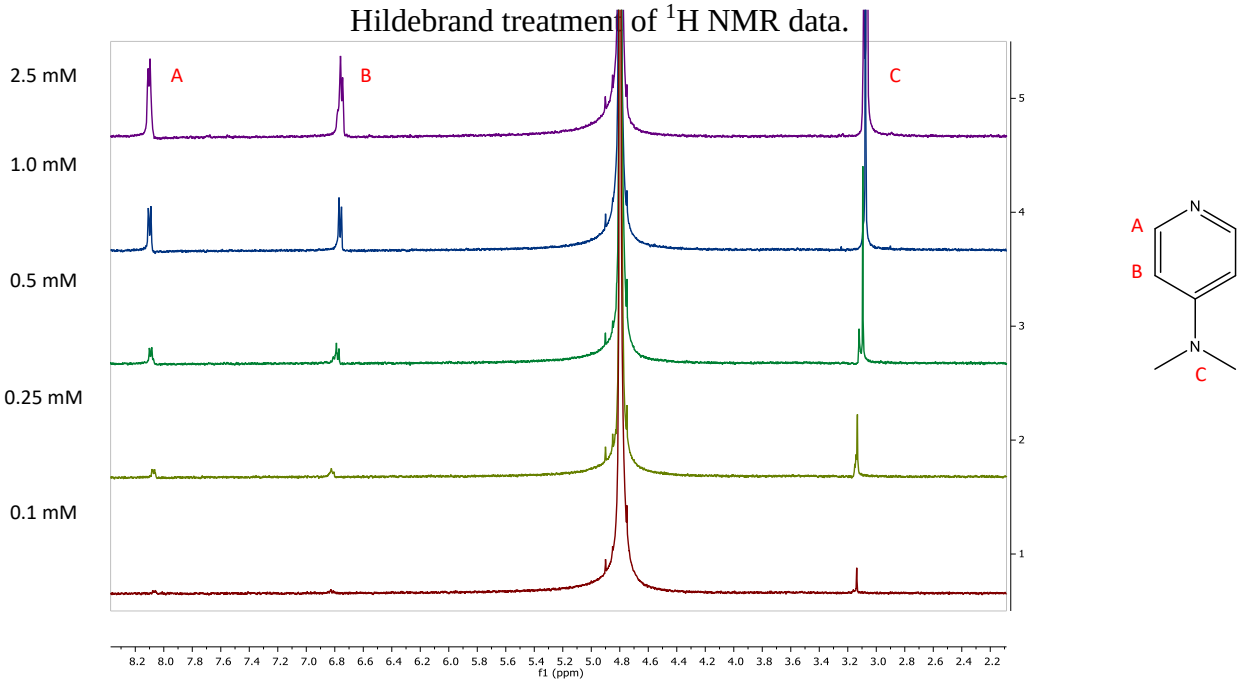

Figure 3.15. ^{1}H-NMR determination of the self-association of DMAP.

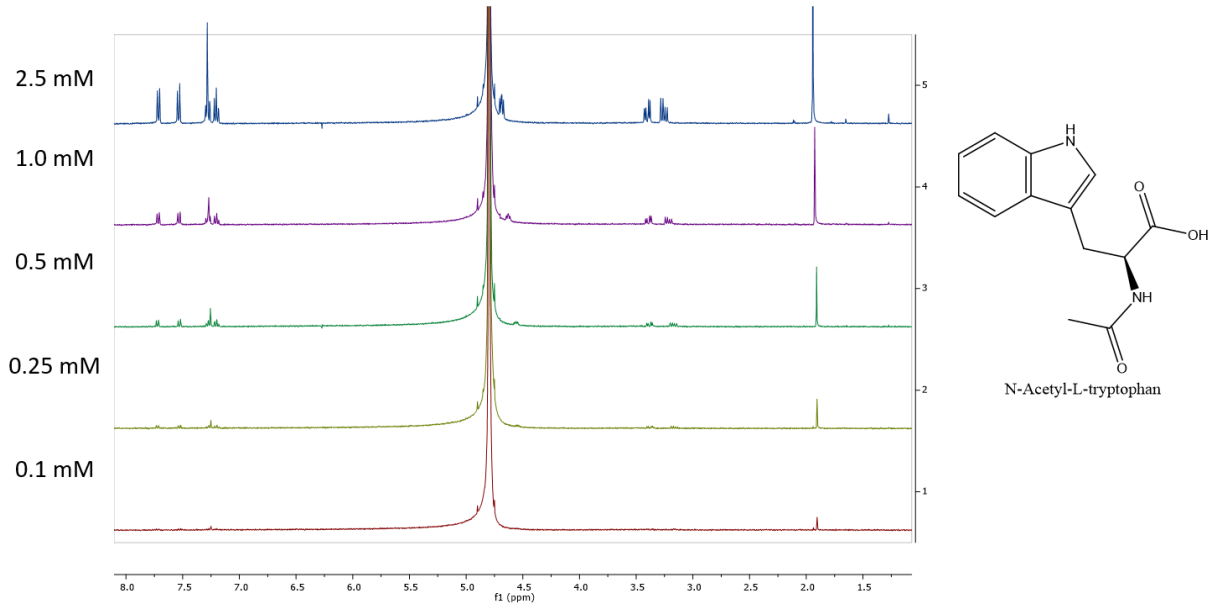

Figure 3.16. ^{1}H-NMR determination of the self-association of N-acetyltryptophan.

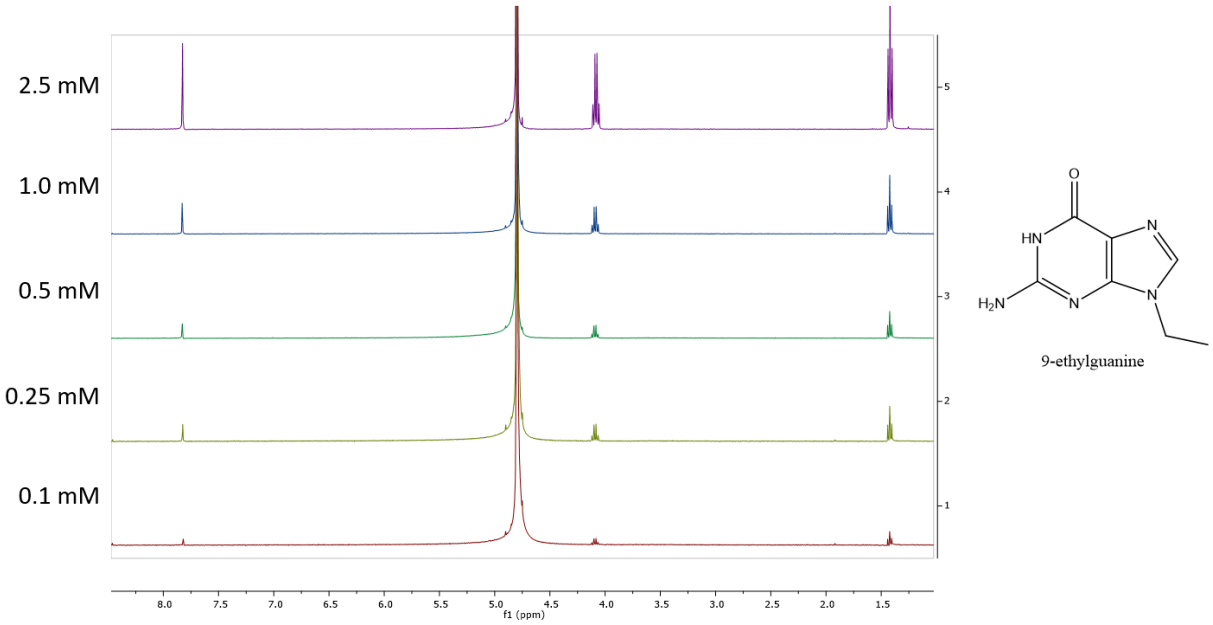

Figure 3.17. ^{1}H-NMR determination of the self-association of 9-ethylguanine.

B	C	D	E	F	G	H	I	J	K	L	M	N			
dObs	C	Kd	Kd*-1	Kd^2	8CKd	F+G	(F+G)^.5	E+I/4c	dm	dD	dm-dD	J*M	(N+L-B)=0		
6.821075	0.1	0.991789	-0.99179	0.983645	0.793431	1.777075	1.33307	0.853203	5.628532	8.830604	-3.20207	-2.73202	-0.72249	0.72249	Ka(avg) 0.998283
6.81615	0.25	0.9948	-0.9948	0.989627	1.9896	2.979228	1.726044	0.731244	5.696185	8.682557	-2.98637	-2.18377	-0.31736		
6.78025	0.5	1.000819	-1.00082	1.001638	4.003275	5.004913	2.237166	0.618174	5.75785	8.547614	-2.78976	-1.72456	0.042805		
6.76165	1	1.007608	-1.00761	1.015274	8.060865	9.076139	3.012663	0.501264	5.82077	8.409927	-2.58916	-1.29785	0.350426		
6.75235	2.5	1.013586	-1.01359	1.027357	20.27172	21.29908	4.615092	0.360151	5.89622	8.244816	-2.3486	-0.84585	0.646618		
	Average	1.00172											4.5E-10		
	Stdev	0.008983													

Table 3.3. Determination of the self-association of DMAP.

B	C	D	E	F	G	H	I	J	K	L	M	N			
dObs	C	Kd	Kd*-1	Kd^2	8CKd	F+G	(F+G)^.5	E+I/4c	dm	dD	dm-dD	J*M	(N+L-B)=0		
7.2507	0.1	0.985318	-0.98532	0.970851	0.788254	1.759105	1.326313	0.852487	6.134568	9.210439	-3.07587	-2.62214	-0.6624	Ka(avg)	1.013936
7.2513	0.25	0.982208	-0.98221	0.964733	1.964417	2.92915	1.711476	0.729268	6.179607	9.096052	-2.91645	-2.12687	-0.28212		
7.2554	0.5	0.983541	-0.98354	0.967353	3.934163	4.901516	2.213937	0.615198	6.22124	8.991453	-2.77021	-1.70423	0.031823		
7.27	1	0.987283	-0.98728	0.974728	7.898265	8.872993	2.978757	0.497868	6.263999	8.885084	-2.62108	-1.30496	0.310129		
7.2833	2.5	0.992927	-0.99293	0.985904	19.85854	20.84444	4.565571	0.357264	6.315184	8.758931	-2.44375	-0.87306	0.602567		
	Average	0.986255											1.08E-09		
	Stdev	0.004189													

Table 3.4. Determination of the self-association of N-acetyltryptophan.

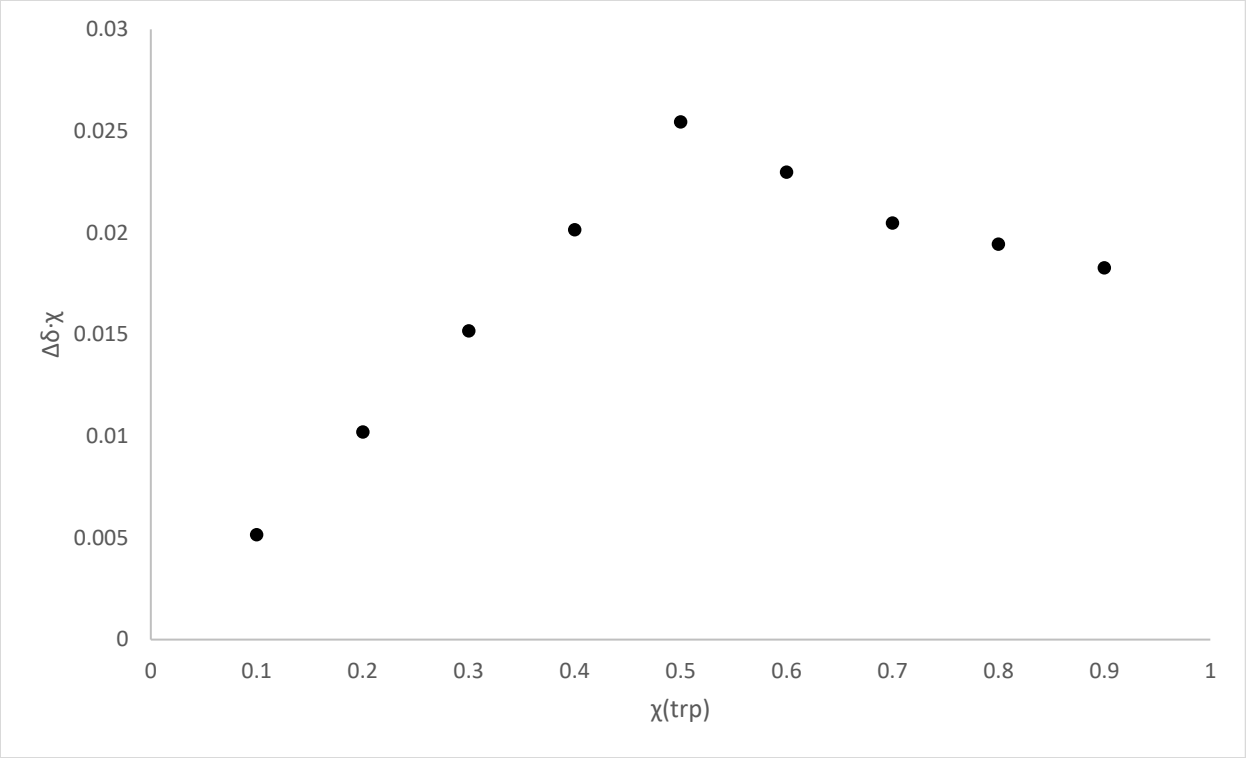

Figure 3.18. ^{1}H-NMR Job's Plot of the interaction between free DMAP and NAcTrp.

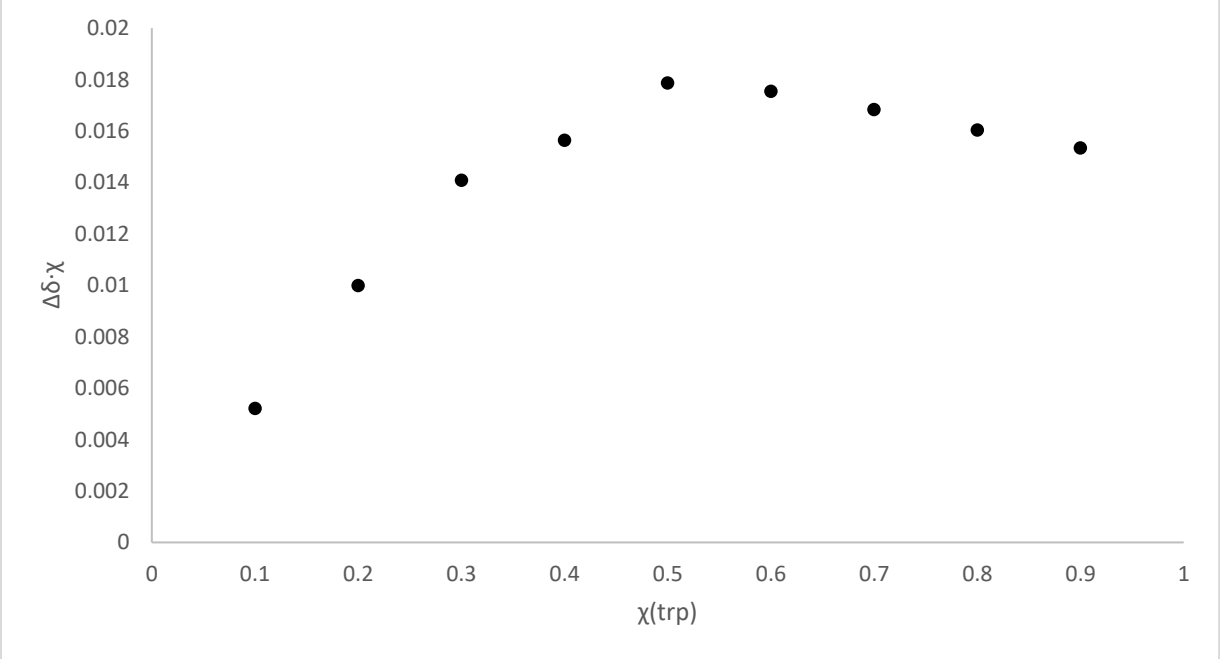

Figure 3.19. ^{1}H-NMR Job's Plot of the interaction between $[Au(dien)(DMAP)]^{3+}$ and NAcTrp.

Chapter 4: Synthesis, Crystal Structure, and Protein Interactions of a Triphenylphosphine Au(C^N) Complex – Carbon-Sulfur Transfer Mechanisms on HIV NCp7

James F. Beaton, Douglas H. Nakahata, Faik Musayev, Martin K. Safo, and Nicholas P. Farrell

4.1 Abstract

The synthesis, characterization, and crystal structure of the previously unreported complex $[AuCl(dampa)(PPh_3)]^{1+}$ are detailed. The interactions of this complex, and of the previously reported $AuCl_2(dampa)$, with NCp7 and smaller models show the possibility for gold-mediated transfer of the dampa and triphenylphosphine ligands to the sulfur of the protein and models. These interactions provide a novel method of targeting zinc finger proteins.

4.2 Introduction

The HIV Nucleocapsid Protein (NCp7) is involved in many critical processes in the viral life cycle, and is an example of a zinc finger protein.[1,2] NCp7 has two tetrahedrally coordinated zinc atoms, also known as zinc fingers, and modification or deletion of the zinc coordinating residues causes loss of protein function.[3,4] This loss of function has a strong negative impact on the efficacy of the virus.[4] Selective targeting of zinc finger proteins is a problem that has been widely discussed across the literature, but in many cases there are still significant challenges that must be addressed. The use of coordination complexes has been employed to obtain reactivity profiles that are unavailable through the use of organic molecules, including the leveraging of molecular

geometries and unique electronic properties to gain access to mechanisms of interaction beyond the use of an oxidation/reduction mechanism directly attacking the zinc coordinating residues. For example, the use of an N-heterocyclic ligand bound to a metal center such as Pt(II), Pd(II), or Au(III) allows for a π-π stacking with the tryptophan and phenylalanine residues.[5–14] This stacking interaction allows for a much weaker electrophile to attack the neighboring cysteine residues due to the proximity between the electrophile and the zinc coordinating residues. In the case of these complexes, it was shown that the use of a metal center enhanced the π-π stacking ability of the N-heterocyclic ligands to a greater extent than organic modification, highlighting the advantages of the use of coordination complexes in addressing complex challenges such as the selective targeting of zinc finger proteins.

Reaction mechanisms other than π-π stacking followed by electrophilic attack can also be achieved through the use of coordination complexes. Additionally, the "soft" nature of gold also suggests that it should interact readily with sulfur containing biomolecules, and indeed this phenomenon is borne out in the literature.[15,16] Most of the previous studies carried out between zinc finger proteins and gold-containing coordination complexes show that the major product is the replacement of the zinc ion with one or more gold atoms, referred to as the formation of "gold fingers".[10] Recently, however, Au(III) complexes containing a gold-carbon bond have been shown to have the ability to covalently modify polypeptides by transferring the C-donating ligand to a sulfur containing residue such as cysteine.[17,18] This work was expanded to zinc finger proteins in the case of the complex $Au(bnpy)Cl_2$ (bnpy = benzylpyridine), and it was shown that this covalent modification of the protein was possible by transfer of the benzylpyridine ligand to cysteine. This transfer is thought to occur by a ligand replacement, in which the cysteine replaces a gold bound chloride, followed by reductive elimination at the metal center, resulting in the covalent

modification of the zinc-coordinating residue.[19] By leveraging the unique ability of Au(III) to undergo this reaction, and by making use of the observation that altering the Au(III) coordination sphere gives the ability to tune the reactivity of the complex, may lead to the development of a Au(III) complex with a favorable reactivity profile that is selective for NCp7.

4.3 Results and Discussion

The structures of the complexes studied are shown in figure 4.1. The crystal structure of **A** has been previously reported.[20] Compound **B** crystallized in a monoclinic crystal system, *Cc* space group. The crystal structure is shown in figure 4.2. The asymetric unit confirms the formation of the Au-C^N chelate and the coordination of triphenylphosphine *trans* to the Au-N bond. The charge balance is achieved by the presence of hexafluorophosphate as a counterion, and chloroform molecule of crystallization was present. This configuration is contradictory to the expected geometry were the complex to follow the traditional *trans*-effect order of ligands. However, it is not the first time that a complex has defied the *trans*-effect when forming, and the phenomenon has previously referred to as "transphobia", in which a destabilizing effect is observed when two soft ligands are *trans* to one another. Other complexes with the dampa ligand also exemplify this effect, so that substituents containing donor atoms of high *trans* influence, such as S and C, are always located *trans* to the N rather than the C.[21–25] The gold atom deviates from planarity (as determined based on the four coordinating atoms) by 0.079 Å (r.m.s.), with a τ_4 parameter of 0.13.[26] The $-CH_2-$ group of the dampa ligand is located 0.466 Å away from the plane defined by N1–Au1–C1–C6, which may explain the observed splitting of the protons in the NMR spectrum.

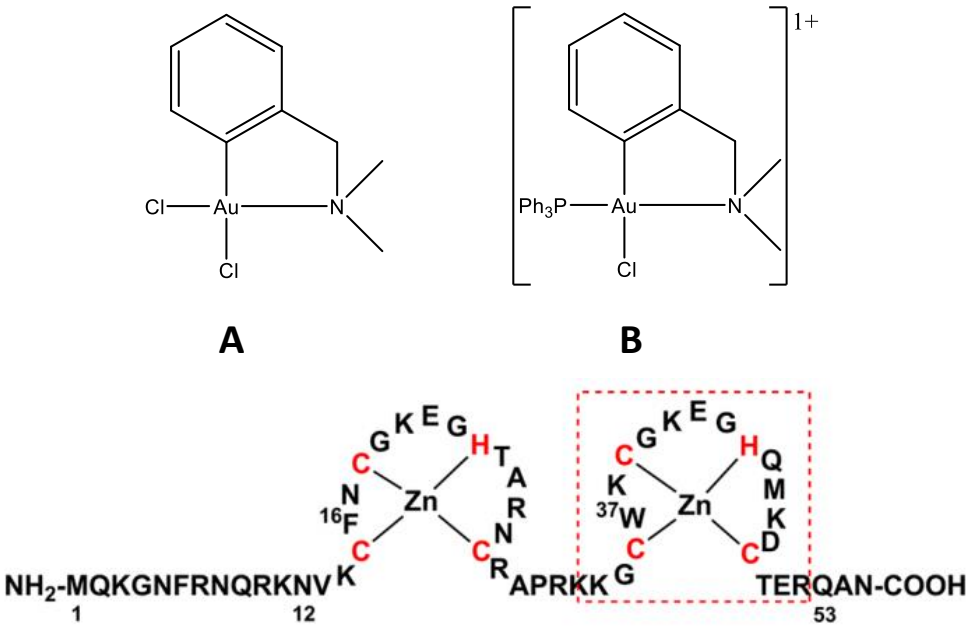

Figure 4.1. The structure of complex **A** (top left), **B** (top right), and NCp7 (bottom).

The main bond lengths and angles for **B** are listed in Table 4.1. The Au-N bond length was 2.141 Å, which consistent with the average for previously reported complexes of with similar C^N chelating systems of 2.12(7) Å. The Au-C bond length of 2.049 Å is shorter than the Au-N distance, and is also consistent with the average for previously reported complexes of 2.03(4) Å. This is consistent with the strong σ-donor character of the deprotonated phenyl ring. The Au-P bond length is the longest of the gold-coordinated ligands at 2.300 Å, but this is also consistent with the average Au-P bond length for reported Au(III) complexes of 2.30(2) Å. The crystal packing is stabilized by non-classical hydrogen bonding between the dampa CH_2 and the fluorine of hexafluorophosphate. This interaction is also present between the benzene hydrogen atoms and both the fluorine of hexafluorophosphate and chlorine of chloroform. The supramolecular structure of **B** is mainly formed by non-classical hydrogen bonding between the gold complex, hexafluorophosphate, and chloroform (see Appendix).

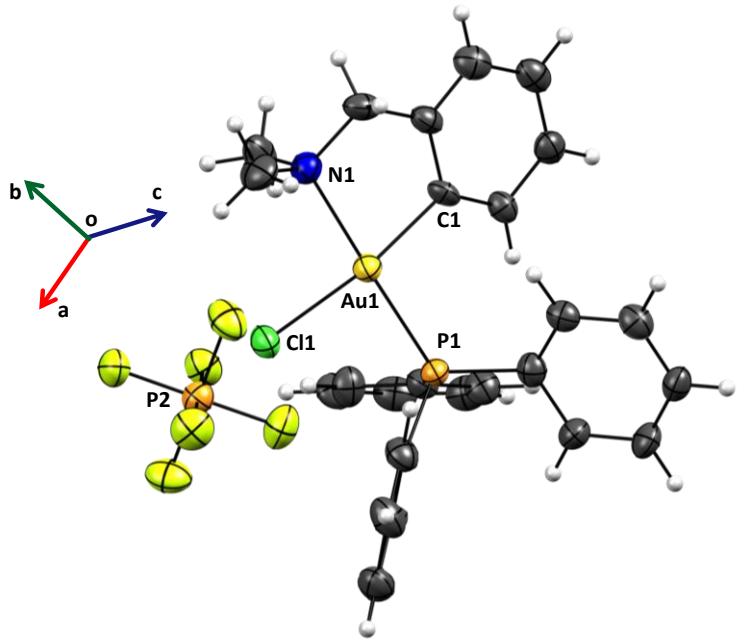

Figure 4.2. Molecular view of compound **B**. Displacement ellipsoids are drawn at the 50% probability level. The chloroform molecule was omitted for clarity.

Au1–C1	2.049 (13)	C1–Au1–N1	82.1 (5)
Au1–N1	2.141 (10)	P1–Au1–Cl1	91.15 (11)
Au1–P1	2.300 (3)	N1–Au1–Cl1	91.1 (3)
Au1–Cl1	2.360 (4)	C1–Au1–P1	95.5 (4)

Table 4.1. Selected bond lengths (Å) and bond angles (°) of the crystal structure of **B**.

In order to investigate the potential for **A** and **B** to target cysteine, the reaction between N-Acetyl-L-Cysteine (NAcCys) was studied by NMR spectroscopy (Figure 4.3) and mass spectrometry (Figure 4.6). Immediately upon mixing a 1:1 solution of **A** or **B** with NAcCys, the ^{1}H-NMR signals for the chelate aromatic protons and the NAcCys protons show that a reaction is underway. After 12 hours of time has elapsed, the signals have resolved, indicating that the reaction is complete and that a new product had formed. Additionally, in the NMR spectra of **A** and **B** the chelate –CH_2- peak is resolved into a singlet. This is in contrast to the analogous $AuCl_2$(bnpy), in which the rigid steric constraints imposed by the pyridine moiety cause splitting of the –CH_2-

protons.[19] This phenomenon was also previously observed in the complex $[Au(BPMA)Cl]^{2+}$ (BPMA = di-2-(picolyl)amine), and shows that there is the potential for modulation of the steric properties of the chelate, which could be leveraged to investigate new structure-activity relationships in order to effectively target NCp7.[27] However, this makes the NMR spectrum of the reaction product somewhat more difficult to interpret, as the resolution of the split peaks into a singlet was used to confirm C-S transfer in the case of $Au(bnpy)Cl_2$.[19]

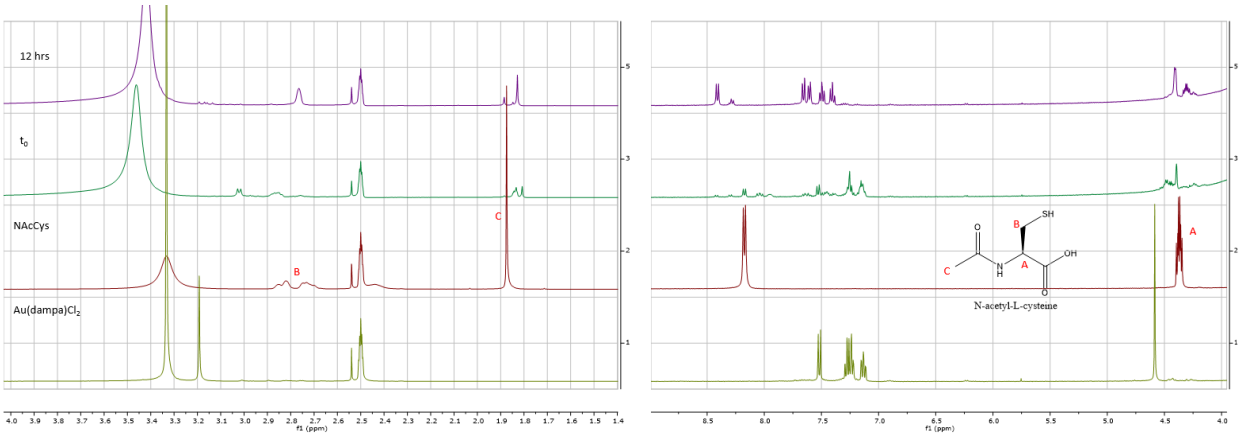

Figure 4.3. Interaction of **A** with NAcCys at time of mixing and 12 hours.

In order to determine the identity of the product that formed, a 1:1 mixture of **A** and NAcCys was examined by mass spectrometry. After 24 hours, signals representative of [dampa-Au-NAcCys] (*m/z* = 493.0801, 1+) and the carbon-sulfur transfer product [dampa-NAcCys] (*m/z* = 297.1237, 1+) are observed, confirming that the product observed by NMR is the result of a C-S transfer process. A 1:1 mixture of **B** and NAcCys showed presence of similar products, however in some cases two equivalents of dampa were observed bound to cysteine (*m/z* = 423.2828, 1+).

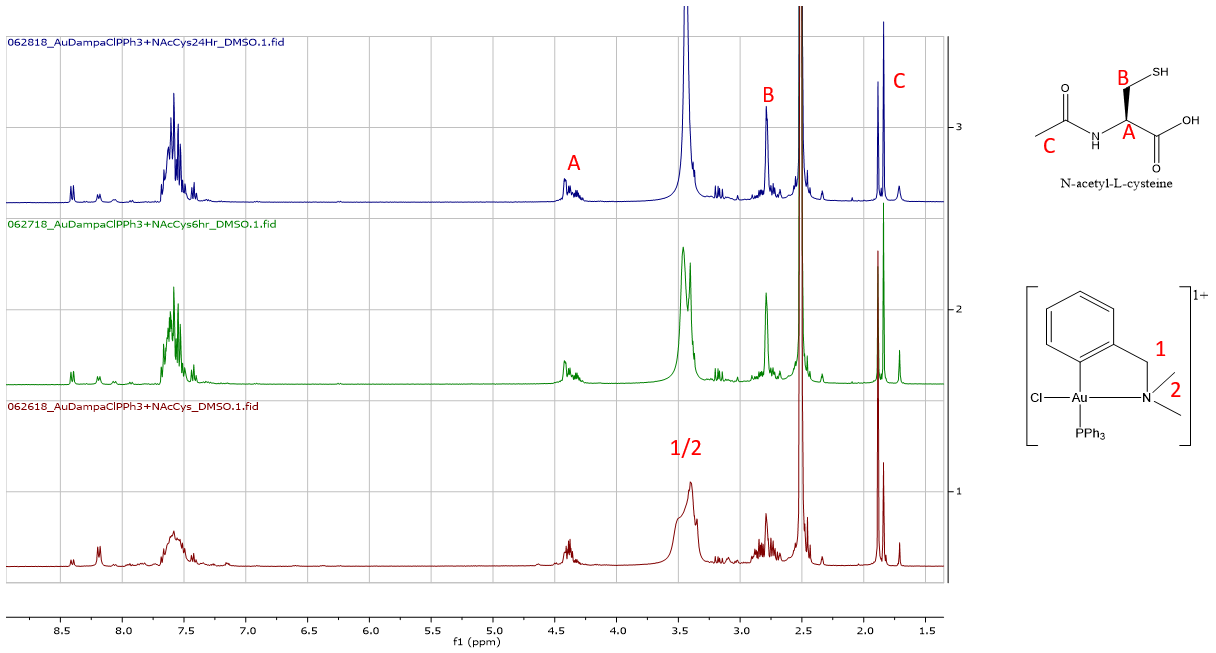

Figure 4.4. Interaction of **B** with NAcCys at time of mixing (bottom), 6 hours (middle), and 24 hours (top).

Similar studies were carried out using glutathione (GSH) to investigate the ability of **A** and **B** to interact with a larger sulfur containing biomolecule. As in the case of NAcCys, NMR spectroscopy shows that a distinct product has formed after 12 hours of reaction time (Figure 4.4). Similarly to the reaction with NAcCys, the mass spectrum of a 1:1 mixture of **A** and GSH showed formation of both the gold-bridged intermediate dampa-Au-GSH (*m/z* = 637.1356, 1+) and the C-S transfer product dampa-GSH (*m/z* = 441.1782, 1+) (Figure 3). Additionally, a signal representing $[Au(dampa)]_2$-GSH was observed (*m/z* = 966.1831, 1+). After 24 hours, the signals for all three products were still present, indicating that the reaction was incomplete or that it is possible for the final product to contain a bridging gold atom. Unlike the previously investigated $Au(bnpy)Cl_2$, the C-S transfer product was observed and the signal for oxidized glutathione ($GSSG^+$, *m/z* = 613.15) was not observed, indicating that reduction of the metal center is coupled to the C-S transfer

process in the case of **A**.[19] Mass spectrometric analysis of a reaction of **B** and GSH showed that identical products formed despite the presence of the triphenylphosphine ligand (Figure 4.7).

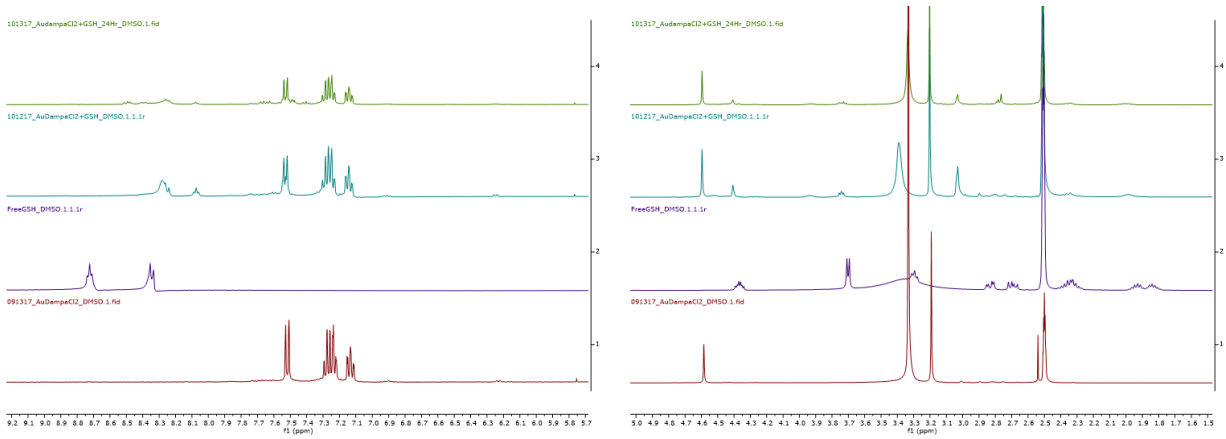

Figure 4.5. Interaction of **B** with NAcCys at time of mixing and 24 hours.

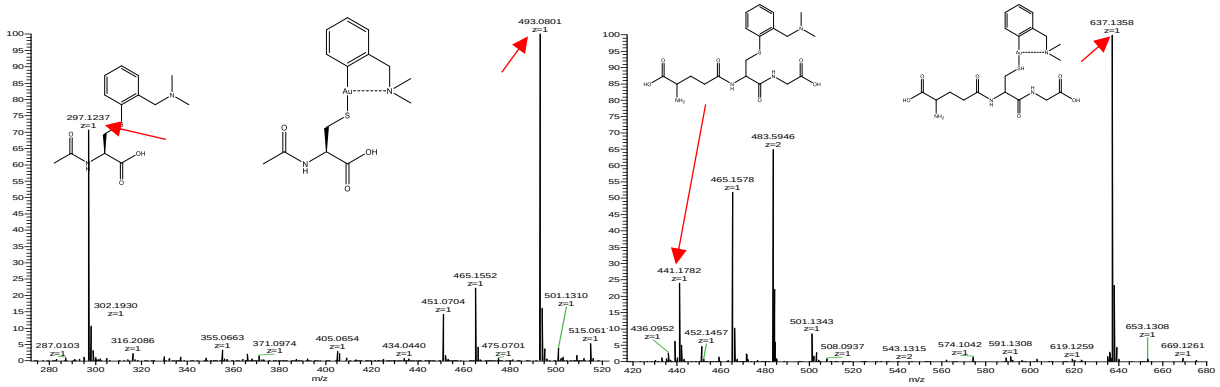

Figure 4.6. Interactions of **A** with NAcCys (left) and GSH (right).

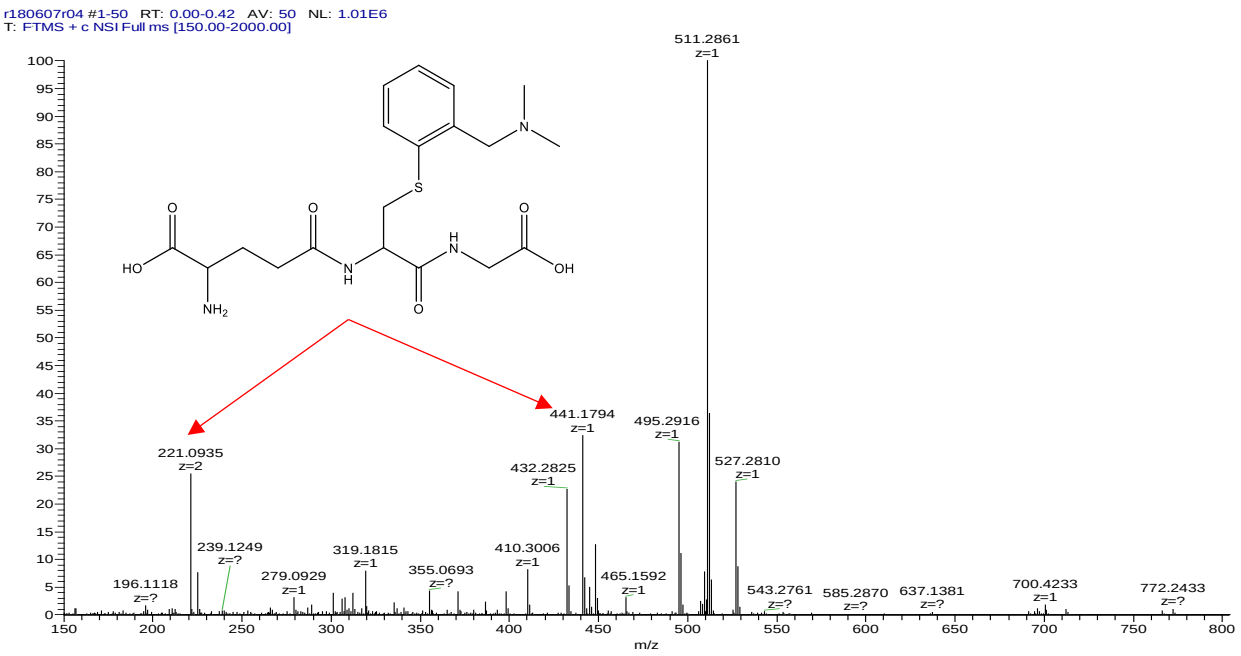

Figure 4.7. Mass spectrum of the product of the interaction of **B** with GSH after 24 hours.

The triphenylphosphine ligand on **B** also allows for the use of ^{31}P-NMR as a tool for elucidating the nature of the product formed. The chemical shift of the triphenylphosphine ligand on **B** appears at 36.94 ppm (relative to trimethylphosphate). This is a significant downfield shift with respect to previously reported Au(I) complexes, which appear at roughly 30 ppm.[28] The interactions of **B** with NAcCys and GSH are shown in figures 4.8 and 4.9 respectively. The ^{31}P-NMR studies conducted confirm that a reaction occurs between **B** and the sulfur containing molecules. After 24 hours of incubation time with NAcCys, an upfield shift is observed. The final product has a chemical shift of 32.13 ppm. The upfield shift observed in this case is in contrast to the product observed when Au(I) complexes are incubated with NAcCys, which produces a downfield shift and a final chemical shift of roughly 39 ppm. Instead, the final product has a chemical shift closer to the chemical shift of the previously studied Au(I) complexes, supporting the proposed reductive

elimination mechanism of C-S transfer, which would produce a triphenylphosphine containing Au(I) complex as a product.[28]

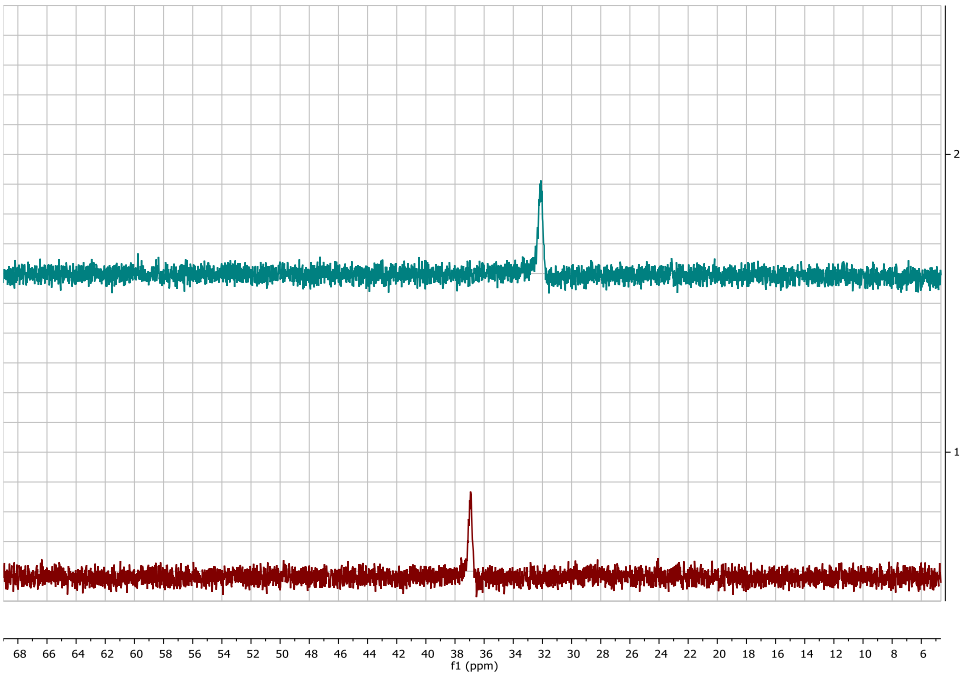

Figure 4.8. Interaction of **B** (bottom) with NAcCys after 24 hours (top) monitored by ^{31}P-NMR.

After 24 hours of incubation with GSH, two product peaks are observed, both of which are shifted upfield from **B**. The larger of the two has a chemical shift of 31.27 ppm and is likely the Au(I) reductive elimination product as seen in the reaction with NAcCys. The second smaller peak has a chemical shift of 23.17 ppm and may be representative of the intermediate in which the C-S transfer is not complete, indicating that the reaction is slower in the case of the more sterically hindered GSH. However, it is also possible that this peak is the result of the previously reported "ligand scrambling" effect observed in the case of phosphine-containing Au(I) complexes, but this is unlikely, as ligand scrambling has been reported to cause a downfield shift rather than an upfield shift.[28]

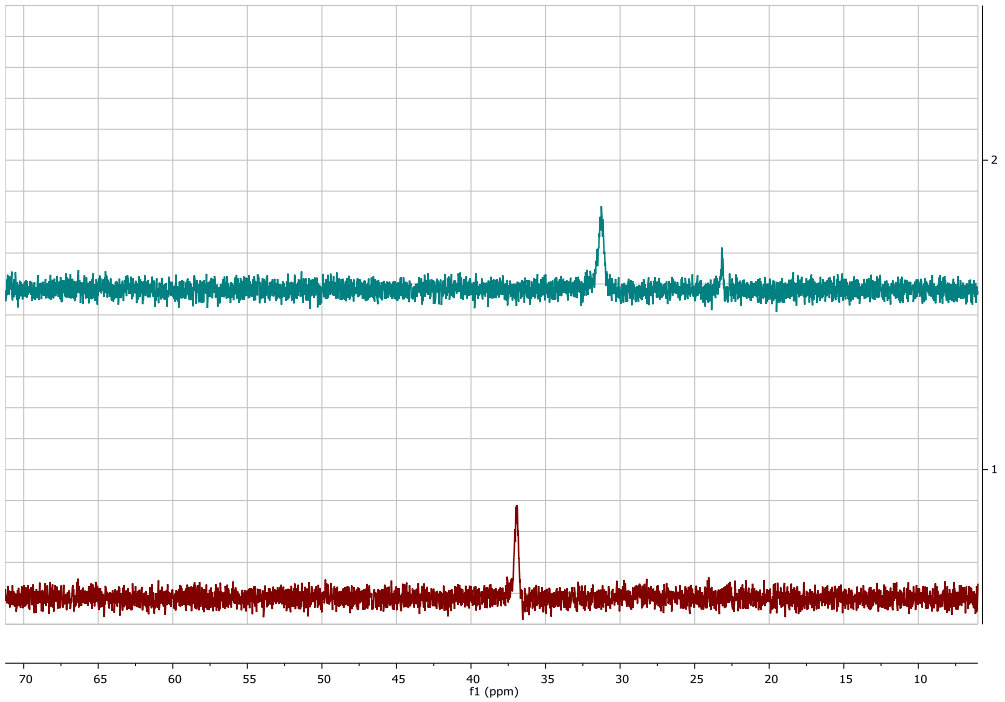

Figure 4.9. Interaction of **B** (bottom) with GSH after 24 hours (top) monitored by ^{31}P-NMR.

Upon interaction with the full NCp7 protein, a variety of products were identified by mass spectrometry (Figure 4.10). Immediately after mixing a solution of NCp7 with one equivalent of **A** per zinc finger, the presence of signals corresponding to both the gold bridged product, Peptide-$(Au(dampa))_2$ (*m/z* = 850.9478 (7+), 744.8303 (8+), 662.0722 (9+)), and the C-S transfer product, Peptide-$(dampa)_2$ (*m/z* = 617.2978 (9+), 556.5256 (10+)), were observed (where peptide is NCp7 in which the two coordinated zincs have been lost). The C-S transfer signals were present at a significantly lower abundance at this timepoint. Other signals that were identified include the formation of gold fingers with 2 (*m/z* = 677.1949 (8+), 609.6763 (9+)) and 5 (*m/z* = 909.3537 (8+), 808.5375 (9+)) equivalents of gold per finger were observed. Signals corresponding to [Peptide-Au_7-$dampa_2$] (*m/z* = 992.1113 (7+), 868.2231 (8+), 771.8650 (9+), 694.8798 (10+)) may be representative of an intermediate in which a gold finger containing 5 gold atoms is formed in place of one zinc finger, and gold bridged cysteines are present on the other finger. Signals

corresponding to [Peptide+Au+dampa] (*m/z* = 937.9295 (6+), 804.0841 (7+), 703.6997 (8+), 625.6223 (9+), 563.1609 (10+)) were also present in high abundance at the initial timepoint, which likely represent a peptide sequence in which one of the fingers has become a gold finger, and the other has complexed dampa through a C-S transfer reaction. This binding motif is more probable than a gold-bridged motif in this case, as both zinc atoms are lost. Interestingly, at the initial timepoint, signals representing [Peptide-(Au(dampa)Cl)$_2$] were observed (669.1698 (9+), 1002.5328 (6+)). This further shows that incorporation of the Au-C bond significantly slows the reaction between the gold complex and the protein, as in most previous examples chloride is not observed bound to gold at even the earliest timepoints.

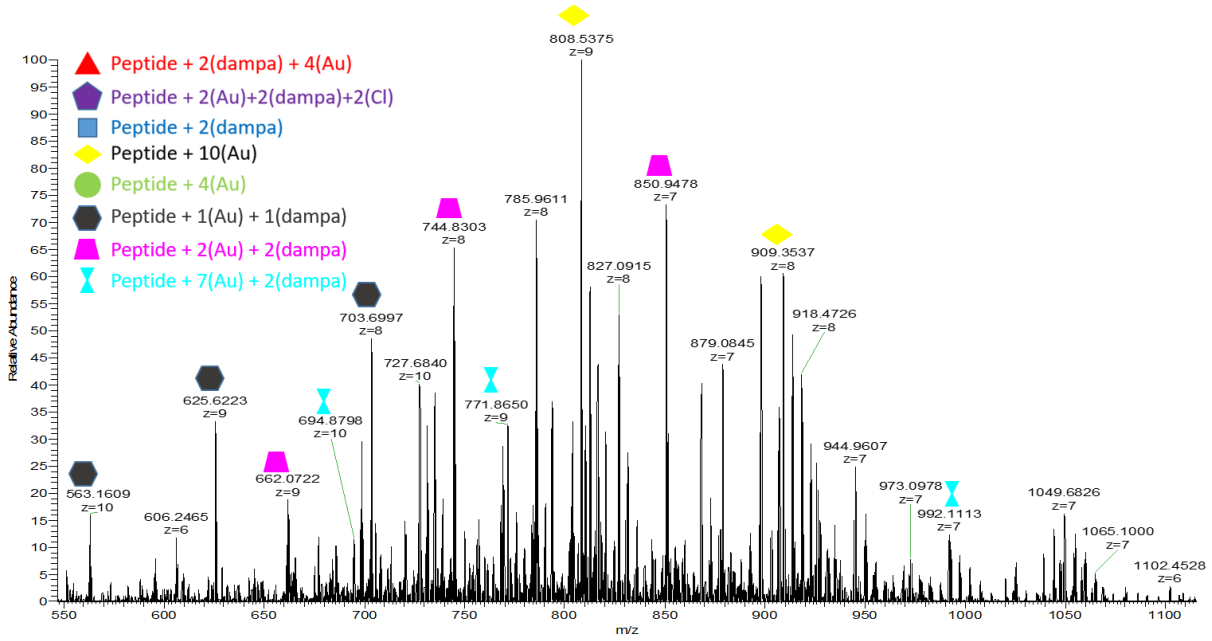

Figure 4.10. Interaction of **A** with NCp7 immediately after mixing.

Product Identity	Theoretical *m/z*	Observed *m/z*
Peptide + Au + dampa	703.71^{8+}	703.70^{8+}
	625.63^{9+}	625.62^{9+}
	563.17^{10+}	563.16^{10+}
Peptide + 2(Au) + 2(dampa)	850.95^{7+}	850.95^{7+}
	744.71^{8+}	744.83^{8+}
	662.08^{9+}	662.07^{9+}
Peptide + 7(Au) + 2(dampa)	992.08^{7+}	992.11^{7+}
	771.84^{9+}	771.87^{9+}
	694.76^{10+}	694.88^{10+}
Peptide + 10(Au)	909.42^{8+}	909.35^{8+}
	808.49^{9+}	808.54^{9+}

Table 4.2. Products of the reaction between **A** and NCp7 identified by mass spectrometry immediately after mixing.

After 24 hours of incubation with **A** (Figure 4.11), the most readily observable signals were those of [peptide-Au_4-$(dampa)_2$] (*m/*z = 1057.9220 (6+), 907.0779 (7+), 793.8193 (8+), 705.7289 (9+)). In this case, it is possible that the two equivalents of dampa are bridged by gold in the form [peptide-$\{Au(dampa)\}_2$-Au_2] in which dampa is still gold bridged, but it is also possible that all of the gold atoms and dampa ligands are bound to the peptide separately. The second most prominent set of signals present after 24 hours is that of the form [Peptide-Au_2-$(dampa)_2$-Cl_2] (*m/*z = 1002.0646 (6+), 858.9129 (7+), 751.9252 (8+), 669.1960 (9+), 602.3768 (10+)). The presence of these signals after 24 hours indicates that the gold bound to chloride state is significantly longer lived than in the previously studied AuN_4 complexes, in which gold bound to chloride was not observed after any significant length of time. In fact, even in the analogous complex Au(bnpy)Cl_2 (another complex with an Au-C bond), gold bound chloride was not observed[19]. Other signals observed after 24 hours of incubation include [Peptide-$(dampa)_2$] (*m/*z = 617.5116 (9+), 555.9616 (10+)), which is also observed at the initial timepoint, and signals representing the peptide with two gold fingers with two gold atoms each, [Peptide-Au_4] (*m/z* = 760.5781 (8+), 676.1805 (9+), 608.6635 (10+)), and peptide with two gold fingers with five gold atoms each, [Peptide-Au_{10}] (*m/z*

= 1039.1155 (7+), 909.4774 (8+), 808.5365 (9+)). The formation of gold fingers is analogous to the reactivity profile seen in the previously investigated gold(III) complexes possessing an AuN_4 coordination sphere, and shows that although a different product, in the form of the C-S transfer product, is obtainable through the use of the Au-C containing complex, mechanisms similar to the previously observed are still possible[10]. In the case of **A**, it is likely that the two labile Au-Cl bonds are responsible for the formation of gold finger products, as even at the initial timepoint the formation of the gold finger motifs were observed (ex. [Peptide-Au_7-$(dampa)_2$]).

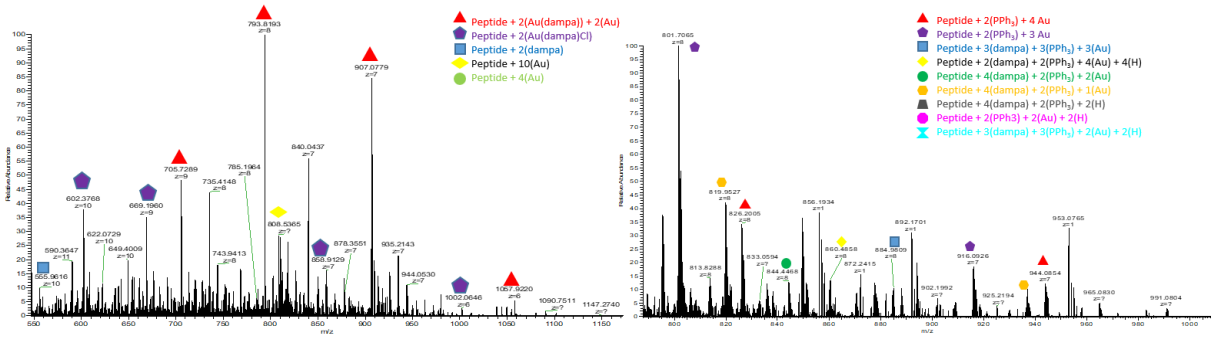

Figure 4.11. Interactions of **A** (left) and **B** (right) with NCp7 after 24 hours. Product configurations shown in the figure legends but not seen in the spectrum are shown in the tables.

Product Identity	Theoretical *m/z*	Observed *m/z*
Peptide + 4(Au) + 2(dampa)	1057.93^{6+}	1057.92^{6+}
	906.94^{7+}	907.08^{7+}
	793.70^{8+}	793.82^{8+}
	705.62^{9+}	705.73^{9+}
Peptide + 2(Au) + 2(dampa) + 2(Cl)	1002.08^{6+}	1002.06^{6+}
	859.07^{7+}	858.91^{7+}
	669.17^{9+}	669.20^{9+}
	602.36^{10+}	602.38^{10+}
Peptide + 2(dampa)	617.52^{9+}	617.51^{9+}
	555.97^{10+}	555.96^{10+}
Peptide + 10(Au)	808.49^{9+}	808.54^{9+}
Peptide + 4(Au)	608.65^{10+}	608.66^{10+}
	677.17^{9+}	677.19^{9+}
	760.30^{8+}	760.29^{8+}

Table 4.3. Products of the reaction between **A** and NCp7 identified by mass spectrometry 24 hours after mixing.

Identity	Theoretical *m/z*	Observed *m/z*
Peptide + 2(PPh_3) + 4(Au)	944.09^{7+}	944.09^{7+}
	826.21^{8+}	826.20^{8+}
Peptide + 2(PPh_3) + 3(Au)	916.10^{7+}	916.09^{7+}
	801.71^{8+}	801.71^{8+}
	712.74^{9+}	712.74^{9+}
Peptide + 3(dampa) + 3(PPh_3) + 3(Au)	885.01^{8+}	884.98^{8+}
Peptide + 2(dampa) + 2(PPh_3) + 4(Au) + 4(H)	860.49^{8+}	860.49^{8+}
Peptide + 4(dampa) + 2(PPh_3) + 2(Au)	844.51^{8+}	844.45^{8+}
Peptide + 4(dampa) + 2(PPh_3) + 1(Au)	937.02^{7+}	937.09^{7+}
	820.02^{8+}	819.95^{8+}
Peptide + 4(dampa) + 2(PPh_3) + 2(H)	795.52^{8+}	795.46^{8+}
Peptide + 2(PPh_3) + 2(Au) + 2(H)	777.22^{8+}	777.21^{8+}
	690.97^{9+}	690.97^{9+}
Peptide + 3(dampa) + 3(PPh_3) + 2(Au) + H	765.01^{9+}	764.99^{9+}

Table 4.4. Products of the reaction between **B** and NCp7 identified by mass spectrometry 24 hours after mixing.

In order to observe the effects of the bulky PPh_3 ligand of the reactivity profile of complexes of this form, one equivalent of **B** per zinc finger was incubated with NCp7. Immediately after mixing, few identifiable products were observed (Figure 4.12). Peaks representing [Peptide-Au_3-$(PPh_3)_2$] (*m/z* = 916.0926 (7+)), [Peptide-Au_3-$(dampa)_3$-$(PPh_3)_3$] (884.6648 (8+)), and [Peptide-Au_2-(dampa)-(PPh_3)-H] (761.2114 (8+)) were observed. Especially at this early timepoint, the product configuration is difficult to predict, as the ligands may remain bound to the gold, or may have been transferred onto the peptide.

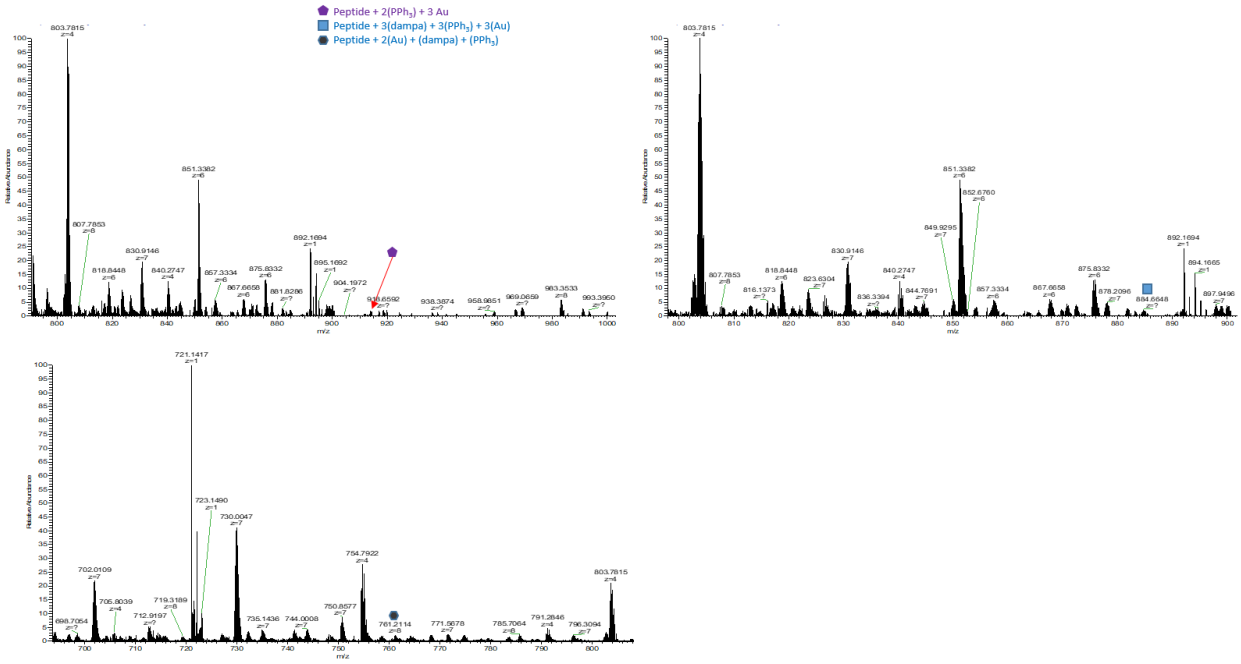

Figure 4.12. Interaction of **B** with NCp7 immediately after mixing.

Product Identity	Theoretical *m/z*	Observed *m/z*
Peptide + 2(PPh_3) + 3(Au)	916.97^{7+}	916.96^{7+}
Peptide + 3(dampa) + 3(PPh_3) + 3(Au)	884.63^{8+}	884.66^{8+}
Peptide + (dampa) + (PPh_3) + 2(Au)	761.21^{8+}	761.21^{8+}

Table 4.5. Products of the reaction between **B** and NCp7 identified by mass spectrometry immediately after mixing.

After 24 hours of incubation, a multitude of products were identified. The most intense signal after 24 hours corresponds to the peptide with two equivalents of triphenylphosphine and three equivalents of gold bound, [Peptide-$(PPh_3)_2$-Au_3] (*m/z* = 916.0926 (7+), 801.7065 (8+), 712.7398 (9+)). The structure [Peptide-$(PPh_3)_2$-Au_4] (*m/z* = 944.0854 (7+), 826.2005 (8+)) was also identified. These structures do not contain the ligand dampa, and show that the triphenylphosphine ligand may contribute to preventing the C-S transfer mechanism. In these products, it is possible that the triphenylphosphine ligand has dissociated from the gold and bound to the protein in an P-

S transfer mechanism analogous to the C-S mechanism previously observed, but it is also possible that the products are bound in a [Peptide-Au-PPh_3] motif, in which the metal center is reduced to gold(I) upon loss of the additional ligands. Some products were identified which retained the ligand dampa. These products include [Peptide-$(dampa)_3$-$(PPh_3)_3$-Au_3] (*m/z* = 884.9809 (8+)), [Peptide-$(dampa)_2$-$(PPh_3)_2$-Au_4] (*m/z* = 860.4858 (8+)), [Peptide-$(dampa)_4$-$(PPh_3)_2$-Au_2] (*m/z* = 844.4468 (8+)), [Peptide-$(dampa)_4$-$(PPh_3)_2$-Au_1] (*m/z* = 936.9445 (7+), 819.9527 (8+)), [Peptide-$(dampa)_4$-$(PPh_3)_2$] (*m/z* = 795.4580 (8+), 690.9666 (9+)), [Peptide-$(PPh_3)_2$-Au_2] (*m/z* = 777.2117 (8+)), and [Peptide-$(dampa)_3$-$(PPh_3)_3$-Au_2] (*m/z* = 764.9870 (9+)). Of particular interest are the signals representing [Peptide-$(dampa)_4$-$(PPh_3)_2$] and [Peptide-$(dampa)_4$-$(PPh_3)_2$-Au], which serve to indicate that the P-S transfer mechanism, analogous to the previously reported C-S transfer mechanism, is possible, as both of these products contain a greater number of equivalents of triphenylphosphine than gold. However, in the studies with the small molecule models NAcCys and GSH this transfer mechanism was not observed, which may indicate that P-S transfer is only favorable if there is a large amount of steric bulk present around the site of reaction. Again, the exact configuration of the products is difficult to predict and warrants further experimentation.

4.4 Conclusions

In conclusion, gold mediated transfer of C-donor and P-donor ligands to sulfur containing biomolecules were observed in the study of complexes **A** and **B** with NCp7. Additionally, the crystal structure of the previously unreported complex **B** is detailed, and shows that the triphenylphosphine ligand is *trans* to the nitrogen of dampa, illustrating "transphobia" in the formation of complexes of this nature. The gold mediated C-S and P-S transfer mechanisms discussed herein offer new and interesting pathways for the targeting of zinc finger protein, allowing for the covalent modification of residues vital to the biological function of the protein,

and show that complexes of this form may provide a platform for the development of agents capable of selectively targeting NCp7. As such, additional investigation into the structure activity relationships of complexes of this form is warranted in order to tune the reactivity with, and therefore selectivity for, zinc finger proteins such as HIV-NCp7.

4.5 Experimental Section

Materials

All reagents were purchased from Sigma Aldrich, and were used without further purification. Complex **A** was synthesized according to previously published methods.[20] The NCp7 zinc finger (SNAIVKCFNCGKEGHIARNCRAPRKKGCWKCGKEGHQMKDCTERQAN, zinc coordinating residues highlighted in red) was a generous gift from Dr. Yangzhong Liu. Solutions of NCp7 were prepared by dissolving NCp7 in water at concentrations of 1 mg/mL (184 μM), and this stock was diluted as necessary.

Synthesis

Synthesis of [AuCl(dampa)(PPh_3)](PF_6) (**B**): Complex **B** was synthesized by an adaptation of previously published methods. Complex **A** was dissolved in acetone. Triphenylphosphine () and potassium hexafluorophosphate were added, and the reaction mixture was stirred for 16 hours. The solvent was evaporated under reduced pressure, and the residue was taken up in dichloromethane. The suspension was filtered, and the filtrate was evaporated to a small volume under reduced pressure. Diethyl ether was added, causing precipitation of the white product (62.3 mg, 62.7% yield). Elemental analysis (experimental(theoretical)) for $C_{27}H_{27}NAuClF_6P_2$: C: 41.61%(41.91%), H: 4.27%(3.52%), N: 1.78%(1.81%). Diffraction quality crystals of **B** were grown by slow evaporation of a solution of **B** in chloroform.

X-Ray Determination of Crystal Structure

Data collection for the single-crystal of **B** was performed at 100 K using a Rigaku MicroMax-007 HF X-ray generator, an EIGER R 4M detector and an Oxford Cobra cryosystem with Cu - K_α (λ = 1.54184 Å) radiation. Data collection, cell refinement and data reduction were performed using *CrysALIS PRO* 1.171.40.4a (Rigaku OD, 2018). The structure was solved with the SHELXT structure solution program using intrinsic phasing and refined as an inversion twin with SHELXL in Olex2.[29–31] All nonhydrogen atoms were refined anisotropically and hydrogen atoms were added to the structure in idealized positions and refined according to the riding model. Molecular graphics were generated using Mercury (v. 1.10).[32] Searches on the Cambridge Structural Database (CSD, v. 5.39) were performed in Conquest (v. 1.22)[33] and Mercury. Crystallographic information of **B** can be found in Table 4.6.

NMR Spectroscopy Studies

^{1}H and ^{31}P NMR studies were recorded on a Bruker AVANCE III 400 MHz spectrometer. ^{1}H NMR samples were referenced to the resonances of the solvent, and ^{31}P NMR samples were referenced to an internal standard of trimethylphosphate.

Mass Spectrometry Studies

Mass spectrometry studies were carried out on a Thermo LTQ-Velos mass spectrometer. Complexes **A** and **B** were incubated with NAcCys and GSH in 1:1 molar ratios, and were incubated with NCp7 at molar ratios of 1 equivalent of complex per zinc finger. Studies involving NCp7 were carried out at 10 µM concentrations in a solution of 10% methanol. Studies involving NAcCys and GSH were carried out at 1 µM concentrations in a solution of 10% methanol. I both cases, the spray voltage was 2.3 kV.

Chemical formula	$C_{27}H_{27}AuClNP{\cdot}F_6P{\cdot}CHCl_3$
Molecular weight ($g{\cdot}mol^{-1}$)	893.22
Crystal system, space group	Monoclinic, *Cc*
Temperature (K)	100
a, *b*, *c* (Å)	25.1639 (3), 8.6579 (1), 17.0485 (2)
β (°)	120.552 (2)
V ($Å^3$)	3198.63 (9)
Z	4
μ (mm^{-1})	13.17
Crystal size (mm)	0.26 × 0.18 × 0.05
T_{min}, T_{max}	0.105, 0.809
No. of measured, independent and observed [$I > 2\sigma(I)$] reflections	53335, 5479, 5462
R_{int}	0.052
$R[F^2 > 2s(F^2)]$, $wR(F^2)$, *S*	0.039, 0.103, 1.04
No. of reflections	5479
No. of parameters	382
No. of restraints	2
$\Delta\rho_{max}$, $\Delta\rho_{min}$ ($e{\cdot}Å^{-3}$)	2.96, −1.29

Table 4.6. Experimental details for crystal structure determination and refinement of **B.**

4.6 References

1. Levin, J. G., Guo, J., Rouzina, I. & Musier-Forsyth, K. Nucleic Acid Chaperone Activity of HIV-1 Nucleocapsid Protein: Critical Role in Reverse Transcription and Molecular Mechanism. *Prog. Nucleic Acid Res. Mol. Biol.* **80,** 217–286, 2005.

2. Darlix, J. L. *et al.* Flexible nature and specific functions of the HIV-1 nucleocapsid protein. *Journal of Molecular Biology* **410,** 565–581, 2011.

3. Sancineto, L., Iraci, N., Tabarrini, O. & Santi, C. NCp7: targeting a multitasking protein for

next-generation anti-HIV drug development part 1: covalent inhibitors. *Drug Discov. Today* **23,** 260–271, 2018.

4. De Guzman, R. N. *et al.* Structure of the HIV-1 nucleocapsid protein bound to the SL3 ψ-RNA recognition element. *Science.* **279,** 384–388, 1998.

5. Anzellotti, A. I., Ma, E. S. & Farrell, N. Platination of nucleobases to enhance noncovalent recognition in protein-DNA/RNA complexes. *Inorg. Chem.* **44,** 483–485, 2005.

6. Anzellotti, A. I., Sabat, M. & Farrell, N. Covalent and Noncovalent Interactions for [Metal(dien)nucleobase] 2+ Complexes with L-Tryptophan Derivatives: Formation of Palladium−Tryptophan Species by Nucleobase Substitution under Biologically Relevant Conditions. **45,** 1638-1645, 2006.

7. Anzellotti, A. I., Liu, Q., Bloemink, M. J., Scarsdale, J. N. & Farrell, N. Targeting Retroviral Zn Finger-DNA Interactions: A Small-Molecule Approach Using the Electrophilic Nature of trans-Platinum-Nucleobase Compounds. *Chem. Biol.* **13,** 539–548, 2006.

8. Anzellotti, A. I., Bayse, C. A. & Farrell, N. P. Effects of nucleobase metalation on frontier molecular orbitals: Potential implications for π-stacking interactions with tryptophan. *Inorg. Chem.* **47,** 10425–10431, 2008.

9. Spell, S. R. & Farrell, N. P. Synthesis and properties of the first [Au(dien)(N-heterocycle)] 3+ compounds. *Inorg. Chem.* **53,** 30–32, 2014.

10. Spell, S. R. & Farrell, N. P. [Au(dien)(N-heterocycle)] 3+ : Reactivity with Biomolecules and Zinc Finger Peptides. *Inorg. Chem* **54,** 79-86, 2015.

11. Spell, S. R. *et al.* Au(iii) compounds as HIV nucleocapsid protein (NCp7)-nucleic acid

antagonists. *Chem. Commun.* **53,** 91–94, 2017.

12. De Paula, Q. A., Tsotsoros, S. D., Qu, Y., Bayse, C. A. & Farrell, N. P. Platinum-nucleobase PtN4 complexes as chemotypes for selective peptide reactions with biomolecules. *Inorganica Chim. Acta* **393,** 222–229, 2012.

13. Tsotsoros, S. D. *et al.* Modulation of the stacking interaction of MN4 (M=Pt, Pd, Au) complexes with tryptophan through N-heterocyclic ligands. *J. Inorg. Biochem.* **132,** 2–5, 2014.

14. Tsotsoros, S. D. *et al.* Enhancement of the physicochemical properties of [Pt(dien)(nucleobase)] 2+ for HIVNCp7 targeting. **8,** 1269-1281, 2017.

15. Quintal, S. M., Depaula, Q. A. & Farrell, N. P. Zinc finger proteins as templates for metal ion exchange and ligand reactivity. Chemical and biological consequences. *Metallomics* **3,** 121–139, 2011.

16. Berners-Price, S. J. & Filipovska, A. Gold compounds as therapeutic agents for human diseases. *Metallomics* **3,** 863, 2011.

17. Kung, K. K. Y. *et al.* Cyclometalated gold(iii) complexes for chemoselective cysteine modification via ligand controlled C—S bond-forming reductive elimination. *Chem. Commun.* **50,** 11899–11902, 2014.

18. Messina, M. S. *et al.* Organometallic Gold(III) Reagents for Cysteine Arylation. *J. Am. Chem. Soc.* **140,** 7065–7069, 2018.

19. de Paiva, R. E. F. *et al.* Au-catalyzed C-S aryl group transfer in Zinc Finger Proteins. *Angew. Chemie Int. Ed.* **57,** 9305–9309, 2018.

20. Price, G. A., Flower, K. R., Pritchard, R. G., Brisdon, A. K. & Quayle, P. First structurally confirmed example of the formation of a gold(iii) carbon bond via transmetallation with a boroxine. *Dalt. Trans.* **40,** 11696–11697, 2011.

21. Vicente, J. *et al.* Some Attempts to Prepare Five-co-ordinated Gold(III) Complexes. Crystal and Molecular Structures of $[Au(C_6H_4CH_2NMe_2\text{-}2)(phen)(PPh_3)][BF_4]_2{\cdot}CH_2C1_2$, $[Au(C_6H_4CH_2NMe_2\text{-}2)(NC_9H_6O)]BF_4$, and $[Au(C_6H_4CH_2NMe_2\text{-}2)(H_2NC_6H_4S)]\text{-}ClO_4$. *J. Chem. Soc. Dalton Trans.* 2361-2366, 1986.

22. Dinger, M. B. & Henderson, W. Organogold(III) metallacyclic chemistry. Part 4. Synthesis, characterisation, and biological activity of gold(III)-thiosalicylate and -salicylate complexes. *J. Organomet. Chem.* **560,** 233–243, 1998.

23. Vicente, J., Bermúdez, M. D., Escribano, J., Carrillo, M. P. & Jones, P. G. Synthesis of intermediates in the C-H activation of acetone with 2-phenylazophenylgold(III) complexes and in the C-C coupling of aryl groups from diarylgold(III) complexes. Crystal and molecular structures of [Au{C6H3(NNC6H4Me-4′)-2-Me-5}(acac-C)Cl](acac = acetylacetonate), cis-[Au(C6H4NNPh-2)Cl2(PPh3)], and [Au(C6H4CH2NMe2-2)(C6F5)Cl]. *Journal of the Chemical Society, Dalton Transactions* **10,** 3083-3089, 1990.

24. Parish, R. V. *et al.* Chemical and Biological Studies of Dichloro(2-((dimethylamino)methyl)phenyl)gold(III). *Inorg. Chem.* **35,** 1659–1666, 1996.

25. Vicente, J., Chicote, M. T., Bermúdez, M. D., Sanchez-Santano, M. J. & Jones, P. G. Synthesis of [2-[(dimethylamino)methyl] phenyl-C1N]-(phenyl) gold(III) complexes. Crystal structure of two modifications of chloro[2-[(dimethylamino)methyl]-phenyl-C1N](phenyl)gold(III). *J. Organomet. Chem.* **354,** 381–390, 1988.

26. Yang, L., Powell, D. R. & Houser, R. P. Structural variation in copper(I) complexes with pyridylmethylamide ligands: Structural analysis with a new four-coordinate geometry index, τ_4. *Dalt. Trans.* **9,** 955–964, 2007.

27. Bernardes, V. H. F. *et al.* Interaction of the HIV NCp7 Protein with Platinum(II) and Gold(III) Complexes Containing Tridentate Ligands. *Inorg. Chem.* **55,** 11396-11407, 2016.

28. Abbehausen, C. *et al.* Gold(I)-Phosphine-N-Heterocycles: Biological Activity and Specific (Ligand) Interactions on the C-Terminal HIVNCp7 Zinc Finger. *Inorg. Chem* **52,** 11280-11287, 2013.

29. Sheldrick, G. M. SHELXT - Integrated space-group and crystal-structure determination. *Acta Crystallogr. Sect. A Found. Crystallogr.* **71,** 3–8, 2015.

30. Sheldrick, G. M. Crystal structure refinement with SHELXL. *Acta Crystallogr. Sect. C Struct. Chem.* **71,** 3–8, 2015.

31. Dolomanov, O. V., Bourhis, L. J., Gildea, R. J., Howard, J. A. K. & Puschmann, H. OLEX2: A complete structure solution, refinement and analysis program. *J. Appl. Crystallogr.* **42,** 339–341, 2009.

32. Macrae, C. F. *et al.* Mercury CSD 2.0 - New features for the visualization and investigation of crystal structures. *J. Appl. Crystallogr.* **41,** 466–470, 2008.

33. Bruno, I. J. *et al.* New software for searching the Cambridge Structural Database and visualizing crystal structures. *Acta Crystallogr. Sect. B Struct. Sci.* **58,** 389–397, 2002.

4.7 Appendix

Supramolecular features of the [AuCl(dampa)(PPh_3)](PF_6) crystal structure

The crystal packing of [AuCl(dampa)(PPh_3)](PF_6) (Figure 4.13(a)) is mainly formed by non-classical hydrogen bonding. Every fluorine atom of the PF_6^- counter ion is involved in hydrogen bonds, some of which are described in Table 4.7 and shown in Figure 4.13(b). Interestingly, two bifurcated hydrogen bonds motifs can be observed in this structure, one in which the chloroform molecule acts as a double donor (C28—H28···F6^{iv} and C28—H28···F1^{iv} in Table 4.7) and the other where F6 is a double acceptor (C7—H7A···F6^{iii} and C8—H8B···F6^{iii} in Table 4.7). The chlorine atoms from the chloroform molecule are also acceptors of H-bonding from either H of the triphenylphosphine ligand or the aryl ring from the dampa ligand (see C5—H5···Cl3^{ii} in Table 4.7 as an example).

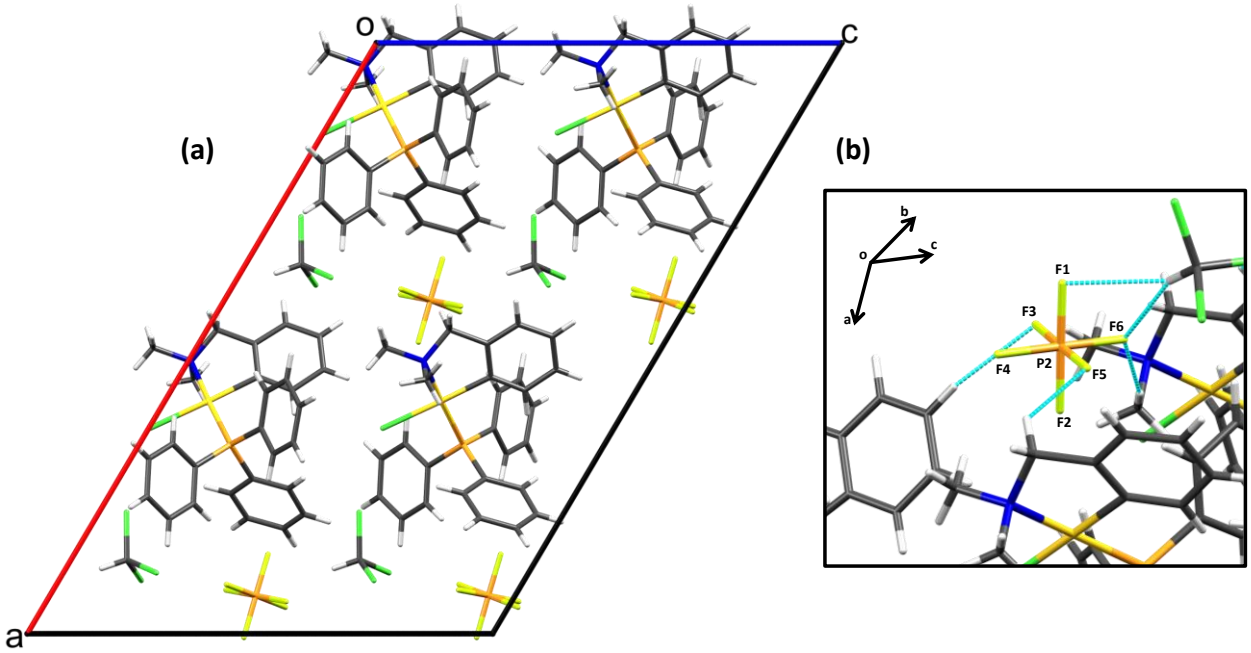

Figure 4.13. (a) Packing of the crystal structure of [AuCl(dampa)(PPh_3)](PF_6), with view along *b* axis and (b) the non-classical hydrogen bonds involving the PF_6^- counter-ion.

D—H···*A*	*D*—H (Å)	H···*A* (Å)	*D*···*A* (Å)	*D*—H···*A* (°)
C4—H4···F3^{i}	0.95	2.53	3.470(14)	170.3
C5—H5···Cl3^{ii}	0.95	2.86	3.493 (14)	125.2
C7—H7A···F6^{iii}	0.99	2.55	3.457(15)	152.2
C7—H7B···F5	0.99	2.45	3.198(16)	132.2
C8—H8B···F6^{iii}	0.98	2.44	3.393(17)	163.2
C28—H28···F6^{iv}	1.00	2.31	3.266(15)	160.1
C28—H28···F1^{iv}	1.00	2.57	3.387(15)	139.1

[Symmetry codes: (i) *x*, −*y*+1, *z*+1/2; (ii) *x*−1/2, *y*−1/2, *z*; (iii) *x*, *y*−1, *z*; (iv) *x*+1/2, *y*−1/2, *z*.]

Table 4.7. Hydrogen bonding geometry of the [AuCl(dampa)(PPh_3)](PF_6) crystal.

Although π···π stacking interactions are absent in this crystal structure, a C—H···π interaction helps the lattice formation along the b axis, as shown in Figure 4.14. The interaction occurs between the C13—H13 donor of one of the phenyl rings of the triphenylhoshine and the phenyl ring of the dampa ligand (C13—H13···Cg1^{v} 2.85Å).

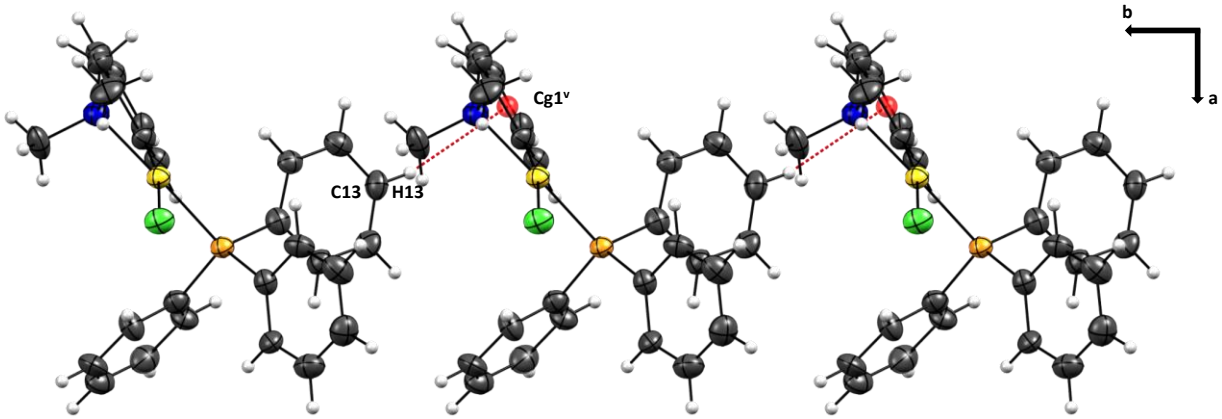

Figure 4.14. The intermolecular C–H···π interaction present in [AuCl(dampa)(PPh_3)](PF_6). Displacement ellipsoids are drawn at the 50% probability level. [Symmetry code: (v) x, -1+y, z.]

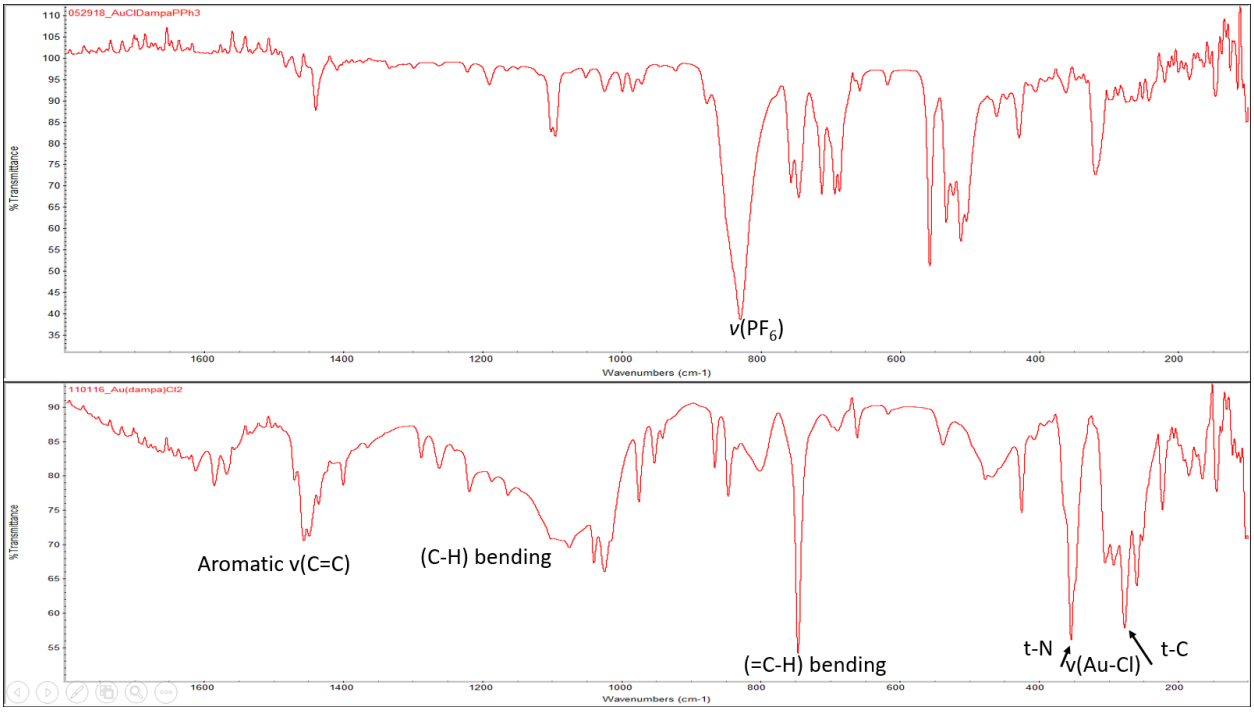

Figure 4.15. Far-IR characterization of **A** (bottom) and **B** (top).

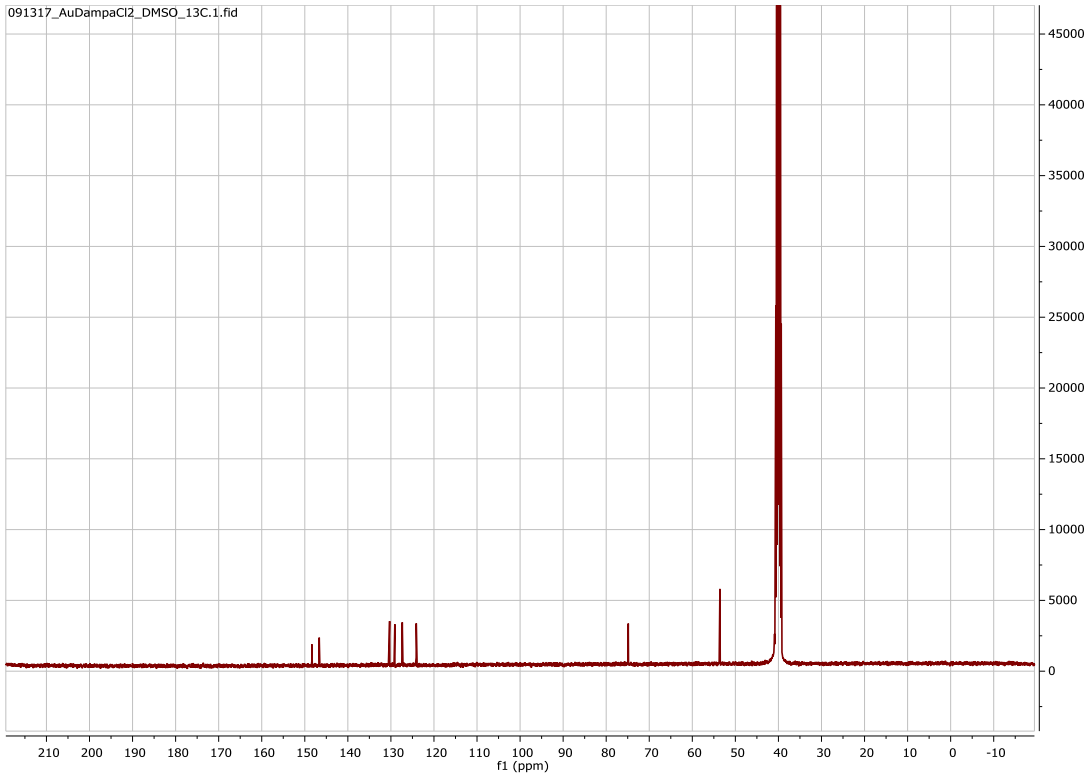

Figure 4.16. ^{13}C-NMR spectrum of **A.**

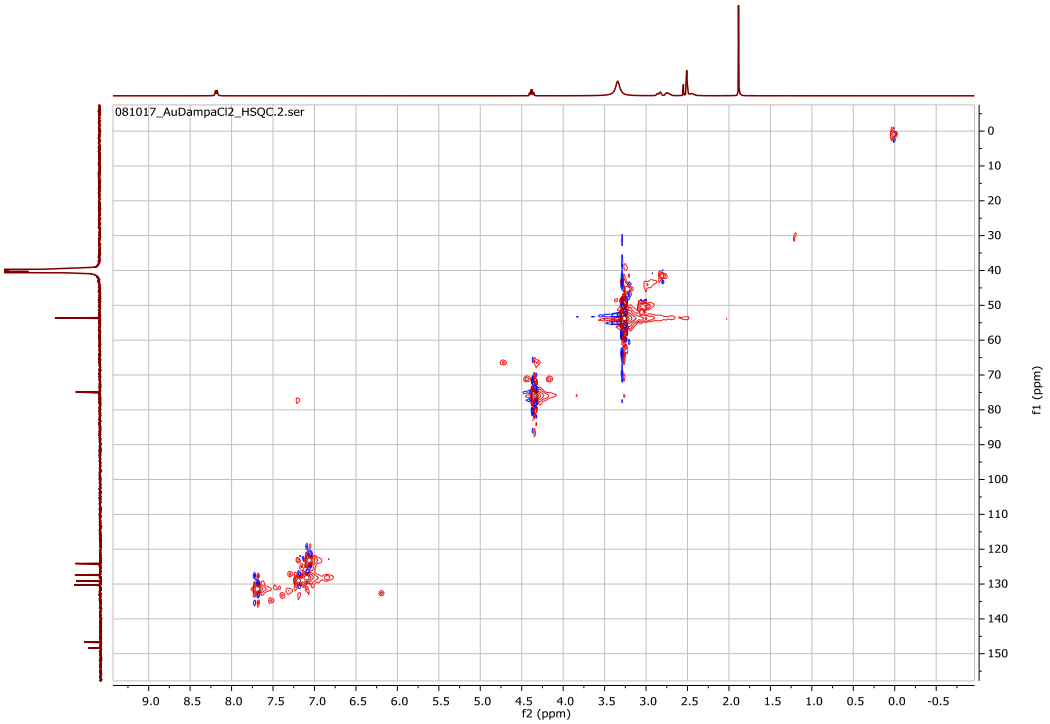

Figure 4.17. $^{1}H/^{13}C$-HSQC spectrum of **A**.

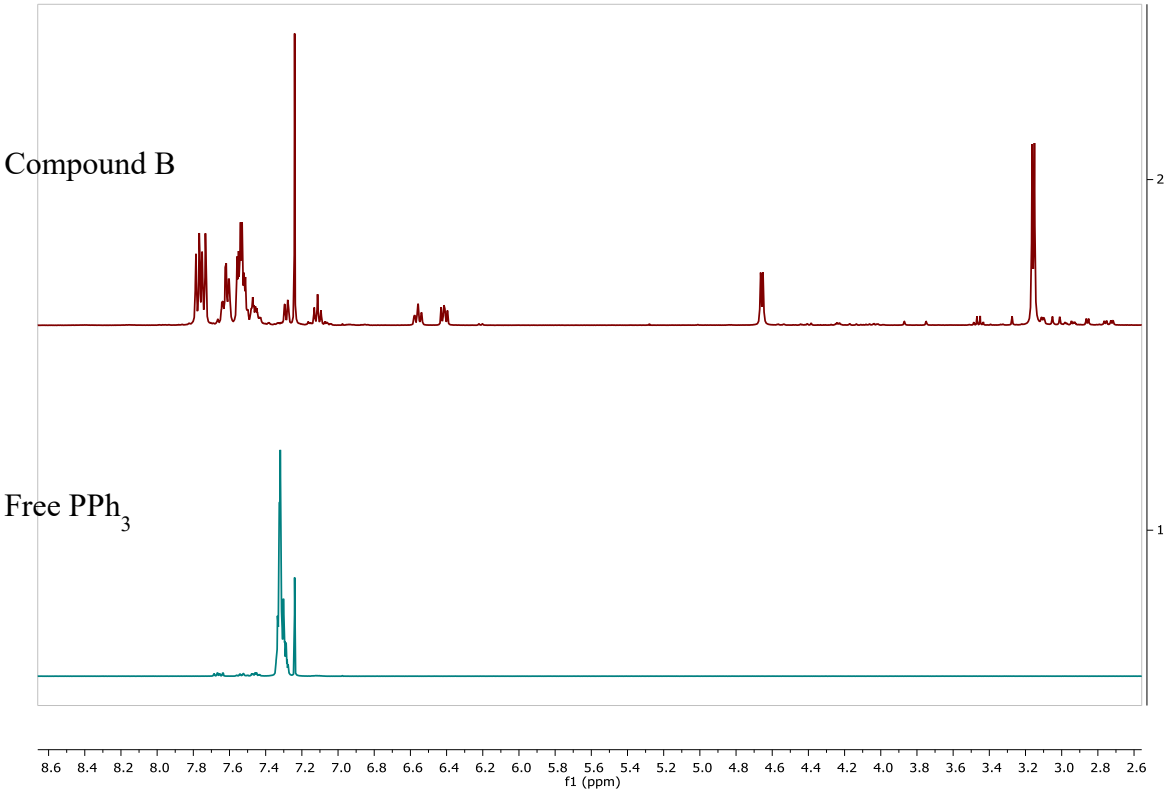

Figure 4.18. ^{1}H-NMR spectrum of **B** (top) and free triphenylphosphine (bottom).

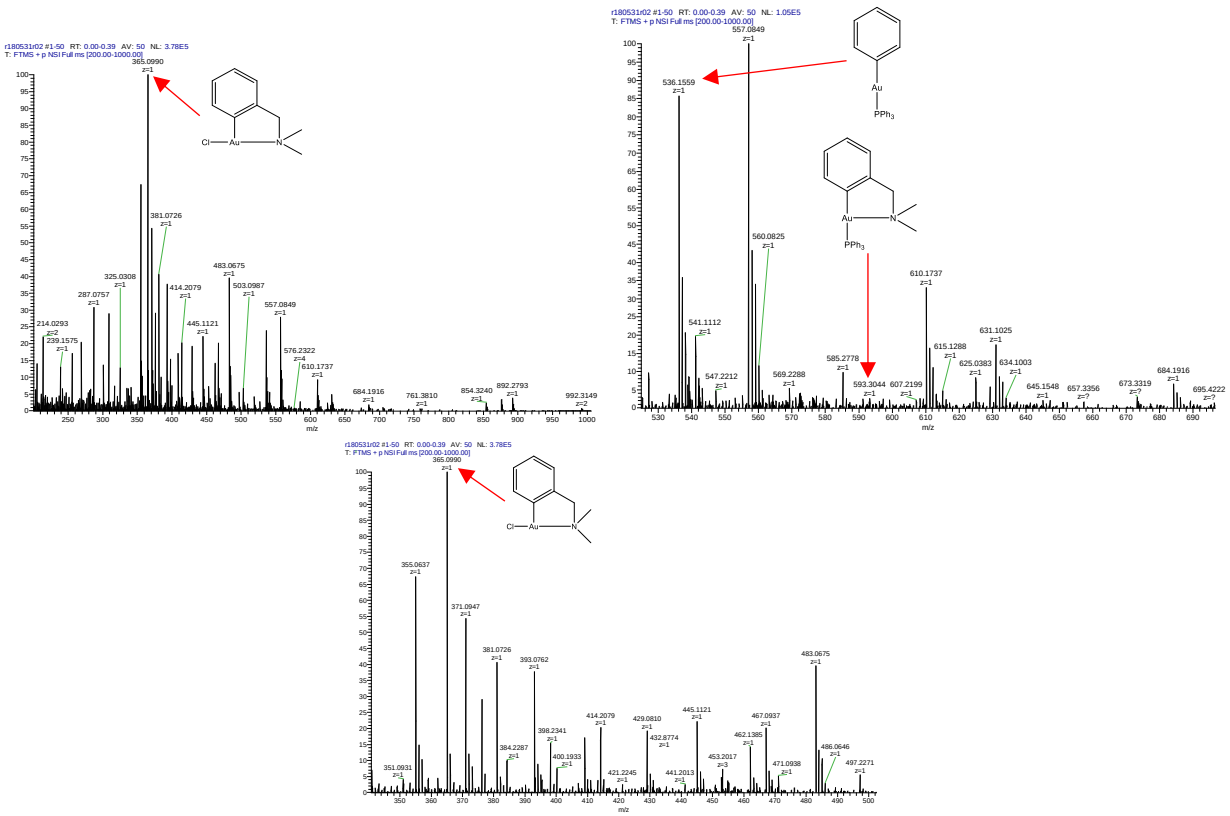

Figure 4.19. Mass spectrum of **B**.

Chapter 5: Differences in the Reaction Products of Gold(I) and Gold(I) Complexes with a Short Peptide Sequence

5.1 Introduction

The short model for the relevant binding sequence of the C-terminal zinc finger from the Sp1 transcription factor, ACPECP, was found to form the unique bridged species {ACPECP-2[Pt(en)]} (en = ethylenediamine) upon a 1:1 interaction between [$PtCl_2$(en)] and ACPECP[1]. Additionally, ion mobility mass spectrometry studies were used to elucidate the site of interaction between the gold(I) complex [(PEt_3)AuCl] and the C-terminal zinc fingers of NCp7 and Sp1[2]. In the case of NCp7, the "gold finger" products formed were gold(I) crosslinks, and the coordinating residues gave the products the forms [Cys^{36}-Au(I)-Cys^{49}] and [Cys^{39}-Au(I)-Cys^{49}]. The experimental data for the interaction with Sp1 confirmed Cys^5 as one of the gold-coordination sites, and either His^{20} or His^{24} as the second binding site, giving the final product the conformation [Cys^5-Au(I)-$His^{20/24}$][2]. This data shows that platinum(II) and gold(III) can coordinate similar peptide sequences with different modes of binding. In order to expand this work to systems with gold(III) metal centers, the interaction of the short peptide sequence ACPECP was interacted with gold(III) complexes containing the tridentate chelating ligand diethylenetriamine, and these interactions were compared to the interaction of ACPECP with the gold(I) complex [(PCy_3)AuCl] (PCy_3 = tricyclohexylphosphine).

5.2 Experimental

Synthesis of Chlorotricyclohexylphosphinegold(I) ([(PCy_3)AuCl]): Chlorotricyclohexylphosphinegold(I) was synthesized by methods adapted from the previously published method[3]. Sodium tetrachloroaurate hyrdate (41.5 mg, 0.115 mmol) was dissolved in 500 µL ethanol. Tricyclohexylphosphine (70.0 mg, 0.250 mmol) was dissolved in 500 µL chloroform, and the solutions were combined, resulting in the immediate precipitation of a white needle-like solid. The reaction mixture was stirred for one hour. The white solid product was collected by vacuum filtration and washed with acetone and diethyl ether. The product was dried under vacuum and characterized by ^{1}H-NMR and ^{31}P-NMR. ^{1}H-NMR ($CDCl_3$, 400 MHz): δ 1.75, m. ^{31}P-NMR: δ 53.9, s. Yield: 25.4 mg, 41.5%.

5.3 Results

The mass spectrum of a 1:1 mixture of $[AuCl(dien)]^{2+}$ and ACPECP showed signals representing both oxidized peptide, indicative of the formation of a disulfide bond across the cysteine residues, and the gold bridged species, in which a single atom of gold is bound between the cysteine residues. The products of the reaction with $[Au(N\text{-}Medien)(1\text{-}MeCyt)]^{3+}$ are the same as the products of the reaction with $[AuCl(dien)]^{2+}$. In both cases, product formation occurs much more rapidly than was observed when ACPECP was interacted with platinum(II) species. In both cases, the signal for the oxidized peptide is significantly stronger than the signal observed for the gold-coordinated species. This may be due to the small number of peptides between the cysteine residues, which could result in a distance too short to easily form the linear coordination geometry that is preferred by gold(I). The signal representing the gold bound species is seen at m/z = 813.15, indicating that the gold(III) metal center is reduced to gold(I) upon coordination, which results in the loss of two protons from the total mass.

The mass spectrum of a 1:1 mixture of [(PCy_3)AuCl] and ACPECP also resulted in the formation of both oxidized peptide and the gold-bridged species. Additionally, signals representing the products of ligand scrambling, as observed in previous studies with gold(I)-trialkylphosphine complexes, were observed[4]. The signal representing the gold bridged species is seen at *m/z* = 815.17, indicating that coordination to the cysteine residues occurs without reduction of the gold(I) metal center.

5.4 Discussion

Interaction of one equivalent of three gold complexes, $[AuCl(dien)]^{2+}$, [Au(N-Medien)(1-MeCyt)]$^{3+}$, and [(PCy_3)AuCl] with one equivalent of the short peptide ACPECP was investigated by mass spectrometry. The binding properties of gold complexes with ACPECP is worthy of investigation, as ACPECP is the polynucleotide binding sequence of the C-terminal zinc finger of Sp1. The investigation of gold complexes as zinc finger proteins has been undertaken, but the differences in the reaction mechanisms between gold(I) and gold(III) complexes have not been thoroughly studied. The oxidation of the peptide sequence, observed at *m/z* = 617.20 (1+), is indicative of disulfide bond formation. Oxidized peptide is observed unilaterally upon interaction of gold complexes with zinc finger proteins[4–6]. In the case of this short model sequence, the oxidation takes the form of disulfide bond formation across the two cysteine residues. In order to maintain oxidation/reduction balance, the oxidation of the cysteine residues is likely coupled to the reduction of the metal center.

The gold bridged oxidized peptide is where differences in the products between the reaction with gold(I) and gold(III) complexes can be observed. Both of the gold(III) complexes that were investigated formed a gold bound product observed as a signal at *m/z* = 813.15 (1+). Conversely, the product of the interaction with the gold(I) complex formed a gold bridged species observed as

a signal at *m/z* = 815.17 (1+). The difference in mass to charge ratio of 2.02 is indicative of two additional protons present on the product of the reaction with gold(I). This difference is caused by the ligand substitution reactions on the gold(I) metal center without reduction. Conversely, the lower observed mass to charge ratio after interaction of the gold(III) complexes is the result of the loss of two protons, which indicates that the metal center was reduced from gold(III) to gold(I) upon binding. The oxidation of the peptide is likely the result of disulfide bond formation. In order for disulfide bond formation to occur, the reduced metal center must bond to a different location on the peptide chain, such as an amine or carboxylate moiety. This result is further evidence that tuning the electronic properties of the metal center can allow for fine-tuning of the reactivity with proteins.

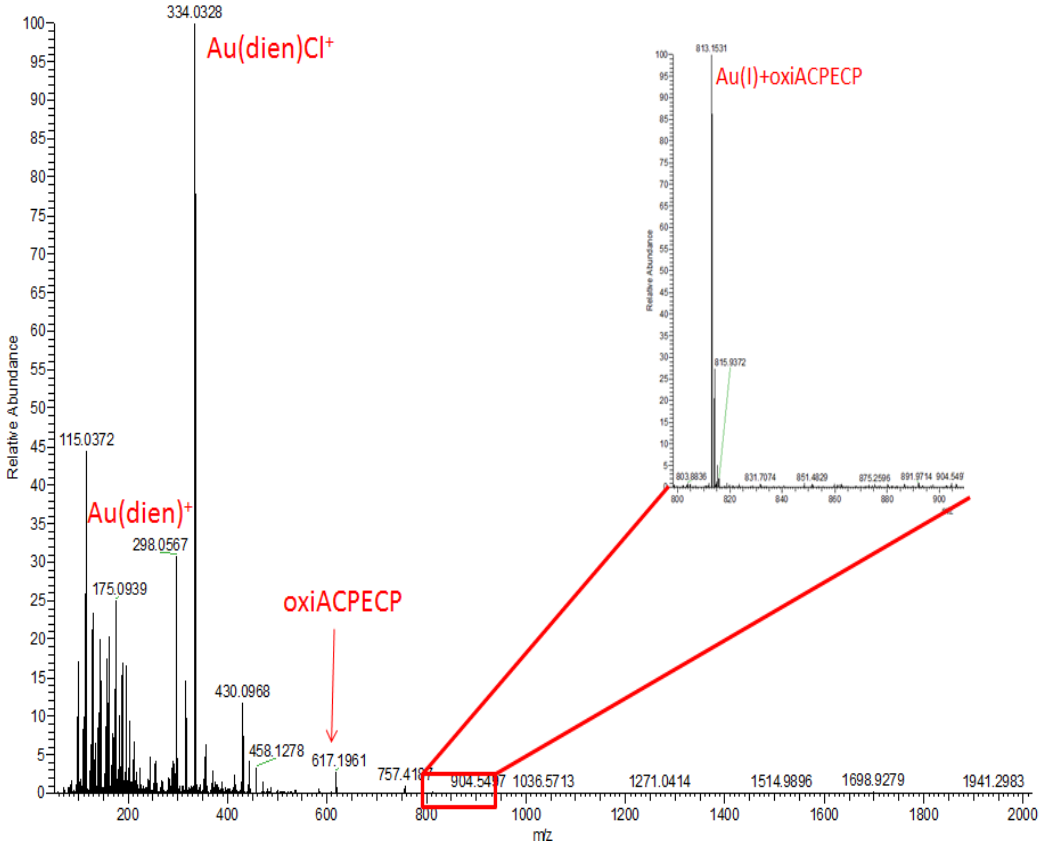

Figure 5.1. Mass spectrum obtained from a 1:1 mixture of $[AuCl(dien)]^{2+}$ and ACPECP.

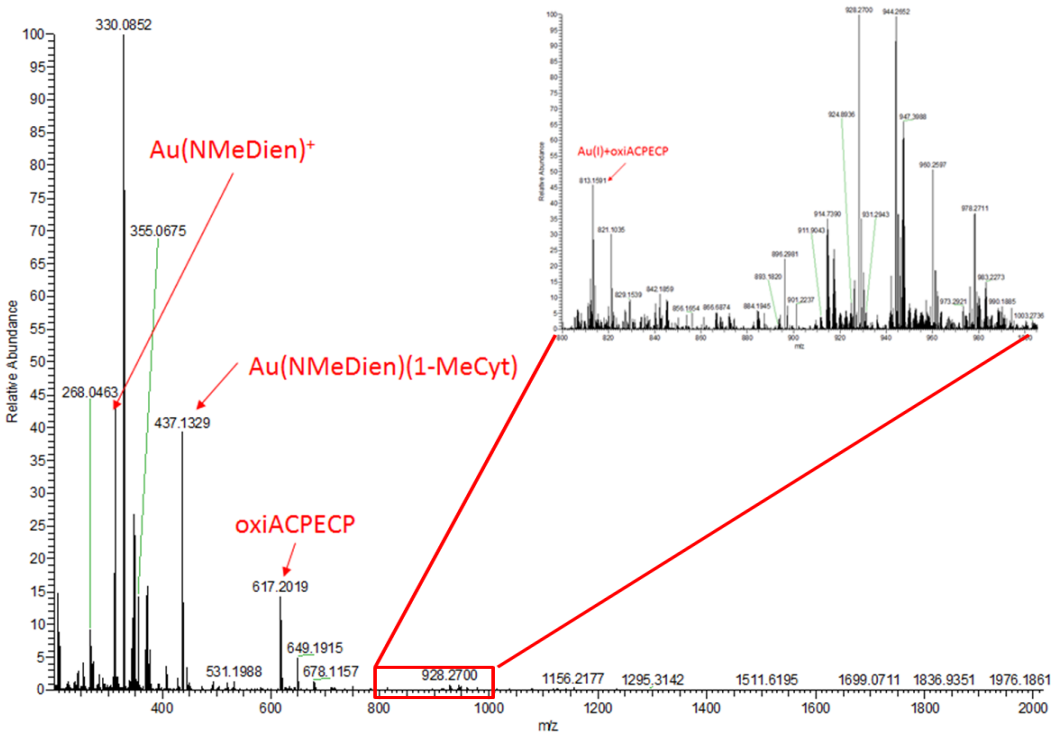

Figure 5.2. Mass spectrum obtained from a 1:1 mixture of [Au(N-Medien)(1-MeCyt)]$^{3+}$ and ACPECP.

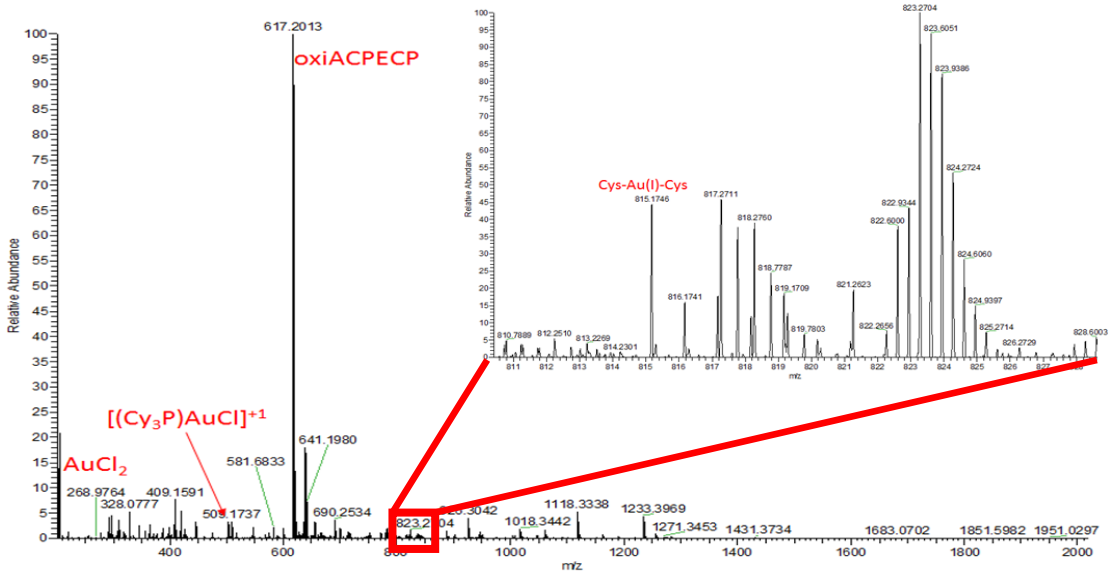

Figure 5.3. Mass spectrum obtained from a 1:1 mixture of [(PCy$_3$)AuCl] and ACPECP.

5.5 References

1. Du, Z., De Paiva, R. E. F., Qu, Y. & Farrell, N. Tuning the reactivity of Sp1 zinc fingers with platinum complexes. *Dalt. Trans.* **45,** 8712, 2016.

2. Du, Z., de Paiva, R. E. F., Nelson, K. & Farrell, N. P. Diversity in Gold Finger Structure Elucidated by Traveling-Wave Ion Mobility Mass Spectrometry. *Angew. Chemie Int. Ed.* **56,** 4464–4467, 2017.

3. Karver, M. R., Krishnamurthy, D., Kulkarni, R. A., Bottini, N. & Barrios, A. M. Identifying potent, selective protein tyrosine phosphatase inhibitors from a library of Au(I) complexes. *J. Med. Chem.* **52,** 6912–6918, 2009.

4. Abbehausen, C. *et al.* Gold(I)-Phosphine-N-Heterocycles: Biological Activity and Specific (Ligand) Interactions on the C-Terminal HIVNCp7 Zinc Finger. *Inorg. Chem* **52,** 11280-11287, 2013.

5. Spell, S. R. & Farrell, N. P. Synthesis and Properties of the First [Au(dien)(N-heterocycle)]$^{3+}$ Compounds. *Inorg. Chem* **53,** 30-32, 2014.

6. Spell, S. R. & Farrell, N. P. [Au(dien)(N-heterocycle)]$^{3+}$: Reactivity with Biomolecules and Zinc Finger Peptides. *Inorg. Chem.* **54,** 79-86, 2015.

Chapter 6: General Conclusions

Up to 10% of the human genome codes for zinc finger proteins. The diverse set of functions of zinc finger proteins makes them an excellent candidate for study, and a number of different zinc fingers have been identified as potential targets for chemical intervention. In the case of NCp7, the development of a selective inhibitor has the potential to make significant progress in the treatment of HIV. This is due to the high conservation of NCp7, as well as the high number of viral life cycle processes in which it is involved. A selective inhibitor of NCp7 would prevent the interaction between NCp7 and its natural polynucleotide substrate. The most promising strategy for preventing this interaction is the modification of the zinc coordination sphere, resulting in the ejection of zinc. Zinc ejection has been shown to inhibit the recognition of NCp7's natural substrate and causes noninfectious virions.

While many examples of complexes, both organic and inorganic, that eject zinc from NCp7 have been described, a complex that achieves zinc ejection with a satisfactory degree of selectivity has not been developed. To this end, inorganic complexes with a "formally substitution-inert" coordination sphere have been investigated. These complexes contain an NCp7 recognition element in the form of a nucleobase or N-heterocycle. In theory, a substitution-inert complex that utilizes a structural element that imparts selectivity for the "essential" tryptophan residue could undergo electrophilic attack at a nearby zinc-coordinating cysteine residue while still being a weak enough electrophile to avoid unwanted side reactions by leveraging the proximity of the cysteine and tryptophan residues.

In order to expand upon the previously studied series of gold(III) complexes of the form $[Au(dien)(N\text{-heterocycle})]^{3+}$, and to complete the series of isoelectronic and isostructural

platinum(II), palladium(II), and gold(III) complexes containing 1-methylcytosine as a ligand, the complex $[Au(dien)(1\text{-}MeCyt)]^{3+}$ was investigated. This previously unreported complex, along with the analogous $[Au(N\text{-}medien)(1\text{-}MeCyt)]^{3+}$ were investigated for their ability to interact with N-acetyltryptophan and the C-terminal zinc finger of NCp7 as models for the full protein. The enhancement of the π-π stacking ability of the aurated complexes over the free N-heterocycle is in agreement with the enhancement observed for the previously studied N-hetercyclic ligands. For the first time, formation of oxidized dimerized peptide was observed by mass spectrometry, indicating that these complexes possessed a reactivity profile distinct from the previously investigated complexes containing other N-heterocyclic ligands. Additionally, a vital feature of the substitution-inert complexes is the stabilization of the gold(III) oxidation state using the AuN_4 coordination sphere. As expected, the stabilization observed for the complex $[Au(dien)(1\text{-}MeCyt)]^{3+}$ follows the trend of ligand basicity, and the reduction potential is intermediate between the previously studied DMAP and 9-EtGua analogs.

In order to further build upon the structure activity relationships of AuN_4 complexes and to investigate the effect of additional steric hindrance on the interactions with NCp7, gold(III) complexes with the chelates BPMA and Me-BPMA were synthesized. These complexes were synthesized alongside the isostructural and isoelectronic platinum(II) complexes in order to make direct comparisons. The upfield ^{1}H-NMR shifts observed metalation of the chelating are more pronounced in the case of the gold(III) than in the platinum(II), highlighting the increased electronegativity of gold(III) relative to platinum(II). Both the gold(III) and platinum(II) complexes possessing the $MClN_3$ coordination sphere are capable of ejecting zinc from the zinc finger structural motif, but the gold(III) analogs eject the central zinc atom much more rapidly than the platinum(II) analogs. Finally, while the PtN_4 complexes, which incorporate an N-heterocycle

creating a "formally substitution-inert" complex, were stable and isolable, the gold(III) analogs were too unstable to be isolated, likely due to the increase of steric hindrance imparted by the chelating ligand. In addition to the steric demands of the BPMA chelate, the electronic demands in going from sp^3 in the case of dien to sp^2/sp^3 may also contribute to the instability of the AuN_4 complexes.

In the future, it would be possible to expand the investigation of AuN_4 complexes as NCp7 inhibitors. The complexes studied in this work have not been able to match the inhibitory ability of the current lead organic compounds such as 4-(Hydroxymethyl)-6-phenyl-2,3-dihydropyridazin-3-one, which act by competing with nucleic acids for binding to NCp7, similarly to the previously studied platinum(II) complexes. The leading platinum(II) candidate for further development is $[Pt(dien)(xanthosine)]^{2+}$. The aurated analog of this complex has not yet been investigated. Therefore, in order to further study gold(III) complexes as inhibitors of NCp7, and to develop a complex capable of rivaling the current organic compounds in NCp7 inhibitory activity, the complex $[Au(dien)(xanthosine)]^{3+}$ should be investigated.

A significant portion of the current investigation into gold coordination-complexes centers around the incorporation of a gold-carbon bond. Organometallic gold complexes possess a reactivity profile distinct from the previously investigated $AuClN_3$ and AuN_4 complexes. In order to extend this observation to the NCp7 system, the complex $[AuCl_2(dampa)]$ and the triphenylphosphine analog $[AuCl(dampa)(PPh_3)]^{1+}$ were investigated. Upon interaction with N-acetylcysteine and glutathione, these complexes showed the ability undergo a C-S transfer, resulting in cysteine arylation. This interaction draws parallels to the mechanism by which N-ada repairs methylated DNA by transferring the methyl group onto a zinc-bound cysteine residue in a zinc finger motif. The triphenylphosphine complex displays "transphobia" and was synthesized

with the intent of blocking the chloride *cis*- to the gold-carbon bond. The ability of the triphenylphosphine complex to undergo cysteine arylation despite lacking the *cis*-chloride disproves the previously published assertion that the *cis*-chloride was essential for the carbon-sulfur transfer to take place. The reactions of the complexes with the dampa chelate highlight the increased flexibility of the dampa chelate relative to the previously investigated benzylpyridine chelate, and it is possible that the reductive elimination mechanism releases the gold(I) complex [(PPh_3)AuCl], which has been previously studied as a zinc ejector.

Additionally, it was found using the short model peptide ACPECP that gold(III) complexes undergo reduction when cysteine residues are oxidized, resulting in disulfide bond formation. This is in contrast to gold(I) complexes, which are not reduced and likely bond so as to bridge the cysteine residues. This coordination motif is likely more favorable in the case of gold(I), as the linear geometry of the metal coordination sphere is maintained.

This work serves to expand the knowledge of how the steric and electronic environment of the gold metal center affects the interactions of gold coordination complexes with NCp7. This work was undertaken with the goal of selectively inhibiting NCp7, and although a complex that did not display reactivity towards sulfur-containing biomolecules such as glutathione was not achieved, the information gained by the investigation of these complexes will aid future investigators to develop a complex that displays the desired reactivity profile. Gold(III) complexes with an organometallic chelate have emerged as prime candidates for development of a selective NCp7 inhibitor. Two approaches to impart selectivity could be: substitution of the labile chloride ligands in order to create a substitution-inert gold coordination sphere and the incorporation of an NCp7 recognition element. This recognition element will likely take the form of a nucleobase or N-heterocycle, which is capable of recognizing the “essential” tryptophan residue of NCp7 through

a π-π stacking interaction. This interaction will bring the metal center into close proximity with the highly nucleophilic zinc-bound cysteine residues, which will allow interaction with a weak electrophile.

In order to continue the investigation of organometallic gold(III) complexes as potential selective inhibitors of NCp7, a library of complexes could be developed. The bidentate organometallic chelating ligands dampa and bnpy offer a well-studied starting point, while tridentate organometallic chelating ligands such as *m*-xylylenediamine offer a lower number of labile chloride ligands which must be replaced in order to impart selectivity. The bnpy analog of the triphenylphosphine complex $[AuCl(dampa)(PPh_3)]^{1+}$ could be investigated to determine if cysteine arylation is possible at the *trans* position in a complex with the less flexible, more sterically hindered bnpy chelate. Additionally, the use of other trialkylphosphine groups could be used to build a library of complexes with the same organometallic chelates, but different steric and electronic environments. Ideally, through careful selection of a combination of a tryptophan recognition element and a steric and electronic environment around the metal center, a selective inhibitor of NCp7 can be developed.

Appendix: Recovery of Platinum and Gold from Laboratory Waste

Introduction

The high cost of platinum makes the recovery of platinum from residual laboratory waste a worthwhile endeavor.

Experimental

Platinum Recovery

Platinum was recovered from residual laboratory waste in the form of $K_2[PtCl_4]$ by methods adapted from the previously published method[1].

Liquid platinum waste was adjusted to a pH of 14 using solid sodium hydroxide. The basic solution was heated to evaporate the solvent. The solid residue was transferred to a porcelain dish, and any solid platinum waste was added. The combined solids were heated with a Meker burner until the color became black/grey and no smoke was observed. During heating, the solid was stirred in order to ensure even burning. In order to remove any residual salts, the solid/ashe mixture was washed with water until the filtrate was colorless and clear. The remaining solid was suspended in aqua regia (30 mL/1 g solid), and gently heated. The solution was filtered, and this process was repeated two additional times (for a total of three extractions). Potassium chloride (1 g/1 g ash) was added to the combined aqua regia filtrate. The volume of the solution was reduced to 1/3 of the original volume by gently heating the solution. The solution was cooled to induce the crystallization of a yellow solid ($K_2[PtCl_6]$). The yellow solid was collected by filtration, washed with cold water, and dried.

The recovered $K_2[PtCl_6]$ was suspended in water (10 mL/g). A solution of hydrazine dihydrochloride (0.1 g/mL) was added dropwise at 60°C until the solution changed from yellow to red. Once the solution was red, addition was stopped and the temperature was increased to 85°C for 30 minutes. The solution as cooled to room temperature, and any remaining $K_2[PtCl_6]$ was removed by filtration. The red filtrate was evaporated under reduced pressure, yielding $K_2[PtCl_4]$ as a red solid.

$K_2[PtCl_4]$ was recrystallized by dissolving the solid in a minimal amount of hot water, removing any residual $K_2[PtCl_6]$ by filtration while the solution was hot, and evaporating the solvent under reduced pressure.

Gold Recovery

Gold recovery was attempted by evaporating liquid gold waste to dryness. The solid was dissolved in aqua regia, and the solution was heated to 70 °C for two hours. The solution was filtered, and the filtrate was concentrated to 1/3 original volume. The solution was extracted with butyl diglyme. 5 wt% oxalic acid was added, and the solution was heated to 75 °C for two hours. The resulting gold(0) was collected by filtration.

Results

40 g of $K_2[PtCl_4]$ was recovered. 1.5 g of gold(0) was recovered.

References

1. Kauffman, G. B., Teter, L. A. & Rhoda, R. N. Recovery of Platinum from Laboratory Residues. 232–236 (Wiley-Blackwell, 2007).

Vitae

Education:

- Virginia Commonwealth University
  - Ph.D. in Chemistry Candidate (Expected Graduation Date: December 8, 2018)
  - Advisor: Dr. Nicholas P. Farrell
  - Dissertation: "Interactions of Gold(III) Complexes with HIV-NCp7 and Models"
  - Chemical Hygiene Safety Officer (Spring 2015 – Present)
  - Head Teaching Assistant – Chemistry 101/102 (Spring 2017 – Present)
  - Nuclear Magnetic Resonance (NMR) Facility Assistant (Spring 2015 – Present)
- University of Virginia
  - B.Sc. in Chemistry with Specialization in Biochemistry (Awarded May 2013)
  - Echols Scholar
  - Chemistry Tutor

Awards and Organizations:

- Virginia Commonwealth University
  - 2018 Outstanding Teaching Assistant Award
  - ACS Virginia Young Chemist Committee Planning Committee (Fall 2017 – Present)
- University of Virginia
  - Sigma Alpha Lambda National Leadership and Honors Organization

Publications:

- Victor H. F. Bernardes, Yun Qu, Zhifeng Du, James Beaton, Maria D. Vargas, and Nicholas P. Farrell. "Interaction of the HIV NCp7 protein with platinum(II) and gold(III) complexes containing tridentate ligands". *Inorganic Chemistry*, **2016**, 55 (21), 11396-11407.
- James Beaton and Nicholas Farrell. "Investigation of 1-Methylcytosine as a Ligand in Gold(III) Complexes: Synthesis and Protein Interactions". *Inorganics*, Submitted.

Publications In Preparation:

- James Beaton, Douglas H. Nakahata, Faik Musayev, Martin K. Safo, and Nicholas P. Farrell. "Synthesis, Crystal Structure, and Protein Interactions of a Triphenylphosphine Au(C^N) Complex – Carbon-Sulfur Transfer Mechanisms on HIV NCp7".

Presentations:

- James Beaton, Thomas Wells, and Nicholas P. Farrell. "Zinc Finger Proteins as Targets for Intervention by Metal Complexes". Poster presented at VirginiaCancerRx 2017, Charlottesville, VA.